

# **Consequences of Xirp2 knockdown in skeletal muscle cells**

**Dissertation**

zur

**Erlangung des Doktorgrades (Dr.rer.nat.)**

der

**Mathematisch-Naturwissenschaftlichen-Fakultät**

der

**Rheinischen Friedrich-Wilhelms-Universität Bonn,**

vorgelegt von

**Venu Kesireddy**

**aus**

**Hyderabad, Indien**

**Bonn (December, 2010)**

**Angefertigt mit Genehmigung der Mathematisch-Naturwissenschaftlichen-  
Fakultät der Rheinischen Friedrich-Wilhelms-Universität Bonn**

**1. Gutachter: Prof. Dr. Dieter O. Fürst**

**2. Gutachter: PD Dr. Gregor Kirfel**

Tag der Promotion: (17/05/2011)

Erscheinungsjahr: 2011

**List of publications**

1. **Venu Kesireddy**, Peter FM Van der Ven, Dieter O Fürst, Multipurpose modular lentiviral vectors for RNA interference and transgene expression, *Molecular Biology Reports* 2010, 37:2863-2870; DOI 10.1007/s11033-009-9840-8.
2. Expression and function of Xin and Xirp2 in skeletal muscle and satellite cells. (Manuscript in preparation)

## Acknowledgements

---

I would like to thank Prof. Dr. Dieter O. Fürst for his supervision, support, helpful criticism and for giving me the opportunity to work in his laboratory on this project which enabled me to learn several valuable techniques and allowed me to conduct research in the field of molecular cell biology of the muscle.

I am thankful especially to PD Dr. Gregor Kirfel for his interest and time he applied for the assessment of this work. I would like to extend my gratitude to Prof. Dr. Walter Witke and Prof. Dr. Gerd Bendas for their time, as part of my thesis committee.

I would like to give my special thanks to Dr. Peter FM Van der Ven for his valuable suggestions to help me in my project and for teaching me the essentials of molecular cloning and cell culture. I am greatly thankful to all TAs in our group especially Frau Beate Schröder and Frau Cäcilia Hennes, for their understanding and great technical and non-technical support during my work. Words are not enough to give my heartily thanks to my colleagues Anja Linnemann, Stefan Eulitz, Julia Otten, Rudi Kley, Dirk Anhuf, Yvonne Matuschek, Silvia Lommel and Katharina Stranzenbach for providing always friendly and scientific environment throughout my PhD studies starting from Potsdam till now. In addition, I wish to thank all past and present members of the group and my friends who supported me throughout this study. It was a real pleasure to work and share this time with you all.

I wish to thank Prof. A. Pfeifer and Dr. A. Hoffmann, University of Bonn for providing HEK293T cells, allowing us to use their infrastructure for Real time PCR and for helpful discussions and valuable support in setting up the lentiviral system. I would like to extend my thanks to Prof. John J. Rossi for plasmid pTZU6+1, Prof. Dr. Jennifer E. Morgan, Imperial College, London for the H-2K<sup>b</sup>-tsA58 cells, Dr. Christian Therion, Universitätsklinikum, München, for early guidance in RNAi and viral vectors. I would like to thank Dr. Torsten Becker, Universitätsklinikum Bonn, for help with isolation of satellite cells and lentiviral transductions. I would like to acknowledge the assistance of the Flow Cytometry Core Facility at the Institute of Molecular Medicine and Experimental Immunology, University of Bonn, supported in part by grant HBFEG-109-517." for assistance with FACS analysis and sorting of the cells.

Finally, I would like to thank my family back home in India, for their unwavering support even during hard times.

## Abbreviations

---

XIRP2 or Xirp2 – Xin repeat protein 2  
GAPDH or *Gapdh* - Glyceraldehyde-3-phosphate dehydrogenase  
cDNA- Complementary deoxyribonucleic acid  
mRNA- Messenger ribonucleic acid  
RNAi- RNA interference  
siRNA- Small interfering RNA  
shRNA- Short hairpin RNA  
miRNA- MicroRNA  
shRNAmir- MicroRNA 30 based short hairpins  
Pol II- RNA polymerase II promoter  
Pol III- RNA polymerase III promoter  
Dox- Doxycycline  
tetO- Tetracycline operator  
5' LTR - 5' Long terminal repeat  
3' LTR-SIN - 3' Long terminal repeat-self inactivating unit  
psi - Packaging signal  
RRE - Reverse response element  
mir5' and mir3' - 5' and 3' context sequences of miR30  
WPRES - Woodchuck hepatitis virus post-transcriptional regulatory element  
AmpR- Ampicillin resistance  
pBR322\_ori- pBR322 origin of replication  
SV40 - Simian virus 40 polyadenylation signal  
EF 1 alpha - Elongation factor 1 alpha promoter  
CAG- A composite cytomegalovirus immediate early gene (CMV-IE) enhancer-chicken  $\beta$ -actin promoter  
cPPT - Central polypurine tract  
VSVG- Vesicular stomatitis virus glycoprotein  
GFP - Green fluorescence protein  
GOI-GFP - a GFP fusion protein of gene of interest  
IRES - Internal ribosomal entry site  
tTRKRAB - A fusion protein of tetracycline repressor (tetR) and Krüppel-associated box (KRAB) domain  
HSKM- Human skeletal muscle cells  
SIN- Self inactivating vectors  
HIV1- Human Immunodeficiency virus 1  
FACS- Fluorescence activated cell sorting  
HEK293T- Human Embryonic Kidney 293 cells stably transduced with large T-antigen  
q-RT-PCR- Quantitative real time polymerase chain reaction

RT-PCR- Reverse transcription polymerase chain reaction  
FCS- Fetal calf serum  
DMEM- Dulbecco's modified eagle medium  
IMDM- Iscove's Modified Dulbecco's Medium  
MOI- Multiplicity of infection  
CCD - Cooled charge-coupled device  
DMSO –Dimethyl sulphoxide  
DNase- Deoxyribonuclease  
ECL- Enzymatic chemiluminescence  
EST - Expressed sequence tag  
GST- Glutathione S-transferase  
HEPES- N-[2-Hydroxyethyl] piperazine-N-2-ethanesulphonic acid  
HRP- Horse radish peroxidase  
IPTG- Isopropyl--D-thiogalactopyranoside  
KDa- Kilo Dalton  
MOPS- Morpholinopropanesulphonic acid  
PAGE- Polyacrylamide gel electrophoresis  
TBS- Tris buffered saline  
TBST- Tris buffered saline with 0.05% tween-20  
PBS -Phosphate-buffered saline  
ABPs- Actin binding proteins  
ATP- Adenosine tri phosphate  
ADP- Adenosine di phosphate  
F-actin-Filamentous actin  
G-actin- Globular actin (monomer)

---

## LIST OF FIGURES

Figure 1.1. Functions of actin binding proteins determined from in vitro experiments.....	3
Figure 1.2. Structure of a skeletal muscle fiber.....	5
Figure 1.3. Schematic representation of the sarcomere.....	6
Figure 1.4. Protein structure of filamin C.....	10
Figure 1.5. Schematic diagram of the HIV 1 genome.....	14
Figure 1.6. Schematic representation of a lentivirus life cycle.....	16
Figure 1.7. Typical self inactivating (SIN) lentiviral vector showing modified U3 and U5 regions in 3' and 5' LTRs.....	17
Figure 1.8. Schematic diagram of HIV-1 based third generation lentiviral vector system.....	18
Figure 1.9. The miRNA biogenesis pathway in vertebrate cells.....	24
Figure 1.10. The silencing triggers of RNAi.....	26
Figure 1.11. siRNA and target mRNA structures.....	29
Figure 1.12. Generation of knockdown mice by various transgenic approaches.....	32
Figure 3.1. Semi quantitative RT-PCR reaction setup.....	51
Figure 4.1. Expression pattern of <i>Xirp1</i> and <i>Xirp2</i> at mRNA level in differentiating H-2K <sup>b</sup> -tsA58 mouse immortal cells.....	64
Figure 4.2. Localization of Xin in proliferating and differentiating H-2K <sup>b</sup> -tsA58 cells.....	65
Figure 4.3. Localization of human <i>Xirp2</i> protein in cultured human skeletal muscle (HSKM) cells undergoing differentiation.....	67
Figure 4.4. <i>Xirp2</i> doublet band flanking the Z-disk in differentiating HSKM cells.....	68
Figure 4.5. Localization of Xin and <i>Xirp2</i> in adult human skeletal muscle tissues.....	69
Figure 4.6. Schematic representation of the cloning steps performed to construct the vector, pLVmir from pLVCT-tTRKRAB and pGIPZ.....	72
Figure 4.7. Vector map of pLVmir with its unique restriction sites emphasizing its modular design.....	73
Figure 4.8. Schematic diagram showing the designing and cloning of shRNAmirs.....	74
Figure 4.9. Schematic diagram showing all modules that may be combined to achieve transgene expression and/or knockdown.....	79
Figure 4.10. Cloning of hairpins (shRNAmirs) into the modular vectors and confirmation of the presence of hairpins.....	83
Figure 4.11. FACS-based validation of the combination of modules IB and IIB in conditional lentiviral vector.....	84
Figure 4.12. Expression of MyoD-GFP in HEK293 cells.....	86

Figure 4.13. Analysis of expression of FLNCD18-21-GFP fusion protein and GFP control protein in HEK293 cells by Western blotting.....	86
Figure 4.14. Selection of siRNAs targeting <i>Xirp2</i> gene.....	87
Figure 4.15. FACS-based testing of promoter switch off in the absence of tetracycline in C2C12 cells transduced with a conditional version of shRNAmir targeting <i>Xirp2</i> .....	89
Figure 4.16. Knockdown levels obtained with different shRNAmir sequences targeting the endogenous <i>Xirp2</i> mRNA in HSKM, H-2K <sup>b</sup> -tsA58 and C2C12 cells.....	90
Figure 4.17. Xin expression is unchanged in <i>Xirp2</i> knockdown cells both at RNA and protein level.....	91
Figure 4.18. Phenotype in HSKM- <i>Xirp2</i> knockdown cells.....	93
Figure 4.19. Localization of myofibrillar proteins in untransduced and H-2K <sup>b</sup> -tsA58- <i>Xirp2</i> knockdown cells .....	94
Figure 4.20. Localization of myofibrillar proteins in mock transduced C2C12 and C2C12- <i>Xirp2</i> knockdown cells. ....	95
Figure 4.21. Myoblast cultures established from single myofibers of diaphragm muscles of wild type and <i>Xin</i> <sup>-/-</sup> mice.....	96
Figure 4.22. Transduction efficiencies and myofibrillar structures in differentiating wild type and <i>Xin</i> <sup>-/-</sup> myotubes .....	98
Figure 4.23. Effect of <i>Xirp2</i> knockdown in wild- type myotubes.....	99
Figure 4.24. Overview images of myotube cultures from <i>Xin</i> <sup>-/-</sup> mice: <i>Xin</i> <sup>-/-</sup> control and <i>Xin</i> <sup>-/-</sup> - <i>Xirp2</i> knockdown cells.....	100
Figure 4.25. Confocal microscopy images of myofibrillar markers in wild type and double gene depleted myotubes .....	101
Figure 5.1. The possible role of Xin in satellite cell differentiation.....	110
Figure 5.2. Schematic representation of the double-copy design showing the duplication of 3' LTR during viral replication of pLVTHM.....	116
Figure 5.3. Design and mode of action of the tTRKRAB based reversible, tetracycline controlled systems for conditional knockdown.....	116

## **LIST OF TABLES**

Table 3.1. Apparatus.....	36
Table 3.2. Bacterial strains.....	38
Table 3.3. Plasmids.....	39
Table 3.4. Primary antibodies.....	40
Table 3.5. Secondary antibodies.....	41
Table 3.6. Media for Molecular Biology.....	41
Table 3.7. Antibiotics for Molecular Biology.....	42
Table 3.8. Established Cell lines and Primary cultures.....	43
Table 3.9. Transient transfection method for production of lentiviruses.....	44
Table 3.10. Semi quantitative RT-PCR reaction setup.....	50
Table 3.11. Semi qRT-PCR conditions for amplification of <i>Xin</i> , <i>Xirp2</i> and <i>Gapdh</i> .....	50
Table 3.12. Reaction setup in a 96 well plate on iCycler <sup>®</sup> instrument.....	52
Table 3.13. PCR conditions for Real time PCR with QuantiFast SYBR green PCR kit.....	53
Table 3.14. Thermo cycler setting.....	53
Table 3.15. SDS-PAGE Resolving gel composition.....	58
Table 3.16. SDS-PAGE Stacking gel composition.....	58
Table 3.17. Buffer composition.....	58
Table 3.18. Composition of ECL solutions.....	60
Table 4.1. Compatible vectors for cloning into Pol III modular vectors.....	77
Table 4.2. Comparison of the vectors generated in this work with currently available vectors for RNAi.....	80
Table 4.3. List of combinations of modules, the resulting vectors and their potential use.....	81

## **CONTENTS OF APPENDIX**

Appendix Figure 1: pLVCT-tTRKRAB vector map.....	120
Appendix Figure 2.1: Schematic diagram of vector pGIPZ .....	121
Appendix Figure 2: pGIPZ vector map.....	122
Appendix Figure 3: pLVTHM vector map.....	123
Appendix Figure 4: pLVET-tTRKRAB vector map.....	124
Appendix Figure 5: pLVCT-rtTRKRAB-2SM2 vector map.....	125
Validation of sensitivity of SYBR Green based Real Time PCR method-Melting Curve analysis of primer sets.....	126
Figure A1: Melting curve, Primer set 1, Xin.....	126
Appendix Table 1: Primers used SYBR Green based Real Time PCR.....	126
Figure A2: Melting curve, Primer set 2, Xirp2.....	127
Figure A3: Melting curve, Primer set 3, Gapdh .....	127
Figure A4: C <sub>T</sub> Values- first detection in H2k-ts A58 mouse muscle (control) cells.....	128
$\Delta\Delta C_t$ Method for calculation of percentage of remaining mRNA after normalization to GAPDH levels.....	128

# Table of Contents

1. Introduction.....	1
1.1. The Muscle.....	1
1.1.1. The cytoskeleton.....	1
1.1.1.1. Microtubules.....	1
1.1.1.2. Intermediate filaments.....	2
1.1.1.3. The actin filament system.....	2
1.1.1.4. The actin binding proteins.....	2
1.1.2. Structure and function of cross striated muscle.....	4
1.1.3. Ultrastructure and components of adult skeletal muscle tissue.....	5
1.1.3.1. Thin filaments.....	6
1.1.3.2 Thick filaments.....	7
1.1.3.2.1. Myosin.....	7
1.1.3.3. Z-disk.....	7
1.1.3.3.1. Titin.....	8
1.1.4. Myofibrillogenesis and myodifferentiation.....	8
1.1.4.1. Filamins.....	10
1.1.4.2. Xin family of proteins.....	11
1.1.4.2.1 Regulation of Xin family of genes by muscle-specific transcription factors.....	11
1.1.4.2.2. Binding properties of Xirp proteins.....	12
1.2. Lentivirus as a tool for gene expression and gene knockdown in skeletal muscle cells ...	12
1.2.1. Introduction to Lentivirus.....	13
1.2. 2. The general biology and life cycle of Lentivirus (HIV 1).....	13
1.2.2.1. The genes and elements of HIV 1 genome.....	13
1.2.2.2. The life cycle of the lentivirus.....	14
1.2.3. HIV1 based lentiviral systems- three generations of lentiviral vectors.....	15
1.2.3.1. Self inactivating (SIN) lentivectors.....	16
1.2.3.2. Envelope plasmid and pseudotyping.....	19
1.2.3.3. Promoters and inducible systems based on lentiviral vectors.....	19
1.2.4. Biosafety issues related to lentiviral usage.....	20
1.3. RNA interference.....	21
1.3.1. RNAi in mammalian systems compared to plants flies and worms.....	21

1.3.2. RNAi pathway and endogenous miRNAs .....	22
1.3.3. Approaches to RNAi-mediated gene knockdown in mammalian cells .....	23
1.3.3.1. Small interfering RNAs (siRNAs).....	23
1.3.3.2. Short hairpin RNAs (shRNAs) .....	25
1.3.3.3. shRNAmirs.....	25
1.3.4. Designing effective and specific siRNAs .....	26
1.3.4.1. Target accessibility.....	28
1.3.4.2. Sequence characteristics .....	28
1.3.4.3. Specificity .....	29
1.3.5. In vivo RNAi and generation of transgenic animals.....	30
1.3.6. Conditional systems for RNAi.....	31
1.3.6.1. Reversible knockdown systems based on Pol III promoter .....	32
1.3.6.1.1. Steric hindrance .....	33
1.3.6.1.2. Transactivation.....	33
1.3.6.1.3. Epigenetic repression.....	33
2. Aim of the thesis .....	35
3. Materials & Methods .....	36
3.1. Materials .....	36
3.2. Apparatus .....	36
3.3. Bacterial strains.....	38
3.4. Plasmids .....	39
3.5. Antibodies .....	40
3.5.1. Primary antibodies .....	40
3.5.2. Secondary antibodies .....	41
3.6. Molecular Biology Methods .....	41
3.6.1. Culture media.....	41
3.6.2. Antibiotics for molecular biology.....	42
3.6.3. Preparation of chemical competent cells .....	42
3.7. Established Cell lines and Primary cultures.....	43
3.8. Lentivirus methods.....	43
3.8.1. Transient transfection method for production of lentiviruses.....	43
3.8.2. Lentiviral titer determination .....	44
3.8.3. Lentiviral transductions .....	45

3.8.3.1. Immortalized mouse myoblast culture- H-2K <sup>b</sup> -tsA58 cells .....	45
3.8.3.2. C2C12 and human skeletal muscle (HSKM) cells .....	45
3.8.3.4. FACS-based sorting and establishment of stable cell lines .....	46
3.8.3.5. Satellite cell isolation from wild type (strain SV129) and Xin knockout mice .....	46
3.9. RNA isolation .....	47
3.9.1. RNeasy mini kit protocol .....	47
3.9.2. Total RNA isolation with TRIzol <sup>®</sup> reagent.....	47
3.9.2.1. DNase I treatment of RNA to remove traces of genomic DNA.....	48
3.9.2.2. Measuring RNA quality, integrity, purity and concentration.....	48
3.10. Reverse Transcription-PCR .....	49
3.10.1. Semi quantitative RT-PCR .....	49
3.10.2. Quantitative Real time PCR (q-RTPCR) .....	52
3.11. Polymerase chain reaction .....	53
3.12. Standard molecular cloning techniques .....	54
3.12.1. Blunting of DNA fragments.....	54
3.12.2. Dephosphorylation of vector DNA.....	54
3.12.3. Ligation.....	54
3.12.4. Transformation of E. coli by heat shock.....	54
3.12.5. Bacterial mini overnight cultures.....	55
3.12.6. Plasmid DNA preparation.....	55
3.12.6.1. Mini preparation of plasmid DNA (mini preps).....	55
3.12.6.2. Transfection quality plasmid DNA preparation: Midi preps and Maxi preps .....	55
3.12.7. Restriction enzyme digests .....	56
3.12.8. Agarose gel electrophoresis of DNA .....	56
3.12.9. DNA fragment recovery from agarose gels .....	56
3.13. Biochemical Methods .....	56
3.13.1. Protein expression.....	56
3.13.2. Expression and purification of recombinant proteins .....	57
3.13.5. Protein Transfer .....	59
3.13.5.1. Semidry blot.....	59
3.13.5.2. Tank blot .....	59
3.13.6. Immunodetection of membrane bound proteins .....	59
3.13.6.1. ECL method.....	59

3.13.6.2. Odyssey infrared scanning method .....	60
3.13.6.3. Western blot overlay .....	60
3.13.6.4. Dot blot overlay .....	61
3.14. Fixation and Permeabilization of cells.....	61
3.14.1. Paraformaldehyde fixation.....	61
3.14.2. Methanol- acetone fixation .....	61
3.15. Immunohistochemical staining of tissue sections.....	61
3.16. Microscopy .....	62
3.16.1. Confocal and epifluorescence microscopy .....	62
4. Results.....	63
4.1. Expression patterns of <i>Xin</i> and <i>Xirp2</i> in skeletal muscle cells .....	63
4.1.1. Comparative expression levels of <i>Xirp1</i> and <i>Xirp2</i> by semi-quantitative RT-PCR ...	63
4.1.2. Localization of <i>Xin</i> protein in proliferating and differentiating cells.....	64
4.1.3. Expression of <i>Xirp2</i> in various muscle cells, primary cells and tissue samples.....	66
4.2. Knockdown of <i>Xirp2</i> expression in muscle cells .....	70
4.2.1. Construction of multipurpose modular lentiviral vectors .....	70
4.2.1.1. Construction of the plasmid- pLVmir.....	71
4.2.1.2. Designing and cloning of shRNAmirs into modular lentivectors .....	73
4.2.1.3. Construction of modular vectors based on pLVmir.....	75
4.2.1.3.1. Construction of pLVTHM-mir.....	76
4.2.1.3.2. Construction of pLVTU6+1.....	76
4.2.1.3.3. Construction of pLVTU6-mir .....	76
4.2.1.4. Construction of constitutive and conditional transgene modules .....	76
4.2.1.5. Compatible vectors for cloning into Pol III modular vectors .....	77
4.2.1.6. The modular nature of the vectors.....	78
4.2.2. Validation of the modular vectors.....	82
4.2.2.1. Confirmation of hairpins after cloning into modular vectors.....	82
4.2.2.2. FACS based validation of cloned vectors demonstrates functionality of the modular design.....	82
4.2.2.3. Validation of constitutive transgene modules by the analysis of protein expression and localization .....	85
4.2.2.3.1. Expression of MyoD in HEK293 cells.....	85
4.2.2.3.2. Expression of filamin C d 18-21 in HEK 293 cells .....	86

4.2.3.1 Selection of siRNAs .....	87
4.2.3.2. Lentiviral transduction and establishment of stable cell lines from mouse and human skeletal muscle cell lines .....	87
4.2.3.2.1. Significance of fixation methods in Xin and Xirp2 antibody staining in Xirp2 knockdown cells.....	88
4.2.3.3. Confirmation of Xirp2 knockdown .....	89
4. 3. Consequences of Xirp2 knockdown in muscle cell lines.....	91
4.3.1. Xin expression level is unchanged upon knockdown of Xirp2 in H-2K <sup>b</sup> -tsA58 cells	91
4.3.2. Effects of Xirp2 knockdown on muscle cell differentiation .....	92
4.3.2.1 Knockdown of Xirp2 in human skeletal muscle (HSKM) cells .....	92
4.3.2.2 Knockdown of Xirp2 in H-2Kb-ts A58 cells .....	93
4.3.2.3. Knockdown of Xirp2 in C2C12 mouse myoblasts.....	95
4.3.2.4. Establishment and transduction of primary muscle cells derived from wild type and Xin knockout mice.....	96
4.3.2.4.1. Transduction efficiencies in wild type and Xin <sup>-/-</sup> primary muscle cells .....	97
4.3.2.5. Knockdown of Xirp2 in wild type mouse primary myoblasts .....	98
4.3.2.6. Knockdown of Xirp2 in Xin <sup>-/-</sup> mouse primary muscle cells.....	100
4.3.2.6.1 Consequences of Xirp2 knockdown in Xin <sup>-/-</sup> primary muscle cells.....	100
4.3.2.6.2 Comparison of myotubes developed from wild type and double gene depleted satellite cells.....	101
5. Discussion .....	102
5.1. Expression patterns of Xin and Xirp2 in skeletal muscle cells.....	102
5.1.1. Localization of Xin and Xirp2 in skeletal muscle cells .....	103
5.2. The role of Xirp proteins in muscle cells.....	104
5.3. Xin expression levels are unchanged in Xirp2 knockdown cells – H-2Kb-tsA58 cells ..	107
5.4. Possible role of Xin in satellite cells and their commitment to differentiation .....	107
5.5. The rationale behind the design of the modular vectors .....	110
5.6. Advantages of the modular vectors.....	112
5.6.1. Advantages of miRNA design over shRNA design.....	113
5.6.2. Proposed uses of the modular lentivectors.....	115
5.6.3. Double copy design and the Cre-Lox strategy with modular vectors.....	115
6. Summary .....	118
7. Appendix.....	120
8. References.....	129

Erklärung/Declaration..... 141

# 1. Introduction

---

## 1.1. The Muscle

Muscle is the contractile tissue of the body that is derived from the mesodermal layer of embryonic germ cells. Its main function is to produce force and cause motion. Muscles are responsible for locomotion of the organism itself and movement of internal organs. There are three basic types of muscles (a) cross-striated skeletal muscles, which are necessary for voluntary movement and breathing (diaphragm) (b) cross-striated cardiac muscles, which are involuntary, and necessary to circulate the blood and (c) smooth muscles, which are involuntary muscles that line the blood vessels, digestive tract, uterus and several internal organs. There are two broad types of voluntary muscle fibers: slow twitch and fast twitch. Slow twitch fibers (e.g. Soleus muscle) contract for long periods of time but with little force while fast twitch fibers (e.g. Tibialis Anterior muscle) contract quickly and powerfully but fatigue very rapidly.

### 1.1.1. The cytoskeleton

The cytoskeleton is a multi-protein framework. The fundamental aspects of cell division, fusion, intracellular transport, polarity, shape and organization depend on this multi-protein supporting structure. However, the cytoskeleton is at the same time a highly dynamic structure (Carballido-Lopez et al., 2003) which undergoes constant restructuring and modifications. This physical property of the cytoskeleton is a manifestation of the biochemical properties of various proteins, which form three major filamentous systems. This dynamic system consists of the microtubules, the intermediate filament proteins and the actin containing microfilaments.

#### 1.1.1.1. Microtubules

The microtubules are one of the components of the cytoskeleton. They have a diameter of 25 nm and length varying from 200 nanometers to 25 micrometers. Microtubules serve as structural components within cells and are involved in many cellular processes including mitosis, cytokinesis and vesicular transport.

### 1.1.1.2. Intermediate filaments

Intermediate filaments are one of the three main components (along with thin filaments and microtubules) of cytoskeleton. Intermediate filaments have an average diameter of 8-10 nanometers, (intermediate in size compared to thin filaments (actin) and microtubules. There are five different types of intermediate filaments. Type I (acidic keratin) and Type II (basic keratin) are produced by different types of epithelial cells (eg. bladder, skin etc). Type III intermediate filaments are distributed in a number of cell types (eg. vimentin in fibroblasts, endothelial cells and leukocytes; desmin in muscle). Type IV (eg. neurofilament proteins) and Type V (eg. lamins). Most types of intermediate filaments (Types I-IV) are cytoplasmic, but type V, the lamins, are nuclear ([http://www.cytochemistry.net/cell-biology/intermediate\\_filaments.htm](http://www.cytochemistry.net/cell-biology/intermediate_filaments.htm)).

### 1.1.1.3. The actin filament system

Actin is among the most abundant proteins within any eukaryotic cell and it has been highly conserved across divergent phyla. Cellular movement is primarily based on the interaction of actin filaments with myosin motors that lead to a sliding motion of the filaments. Actins are globular proteins of 42 kDa with four sub-domains. Above a critical concentration and in the presence of ATP,  $Mg^{2+}$  and  $K^+$  ions, these monomers associate to form polarized filaments or the F-actin. Under physiological conditions, actin filaments are maintained in a dynamic equilibrium with monomeric, ATP-bound G-actin. The growth of actin filaments at the barbed ends and the simultaneous disassembly at the pointed end are parts of a process known as tread milling (Bindschadler et al., 2004).

### 1.1.1.4. The actin binding proteins

The dynamical property of the actin cytoskeleton is mainly regulated by a plethora of participating actin binding proteins (ABPs). These are classified into several main groups, according to their mode of binding to and modification of actin and their function in the cell (Figure 1.1). The G-actin binding proteins predominantly serve to function as helper proteins for exchanging ATP/ADP during the assembly and disassembly of filamentous actin, but also in severing and in promoting new actin polymerization. Varying the mechanical properties of F-actin is essential for maintaining the structural integrity of the cell, cell motility and adhesion. During this, the actin filaments may be organized into stress fibers (Wang et al., 1984), dorsal

arcs (Heath et al., 1981), concave or convex bundles (White et al., 1984), geodesic arrays (Mochizuki et al., 1988), or a loose meshwork (Trotter et al., 1978).

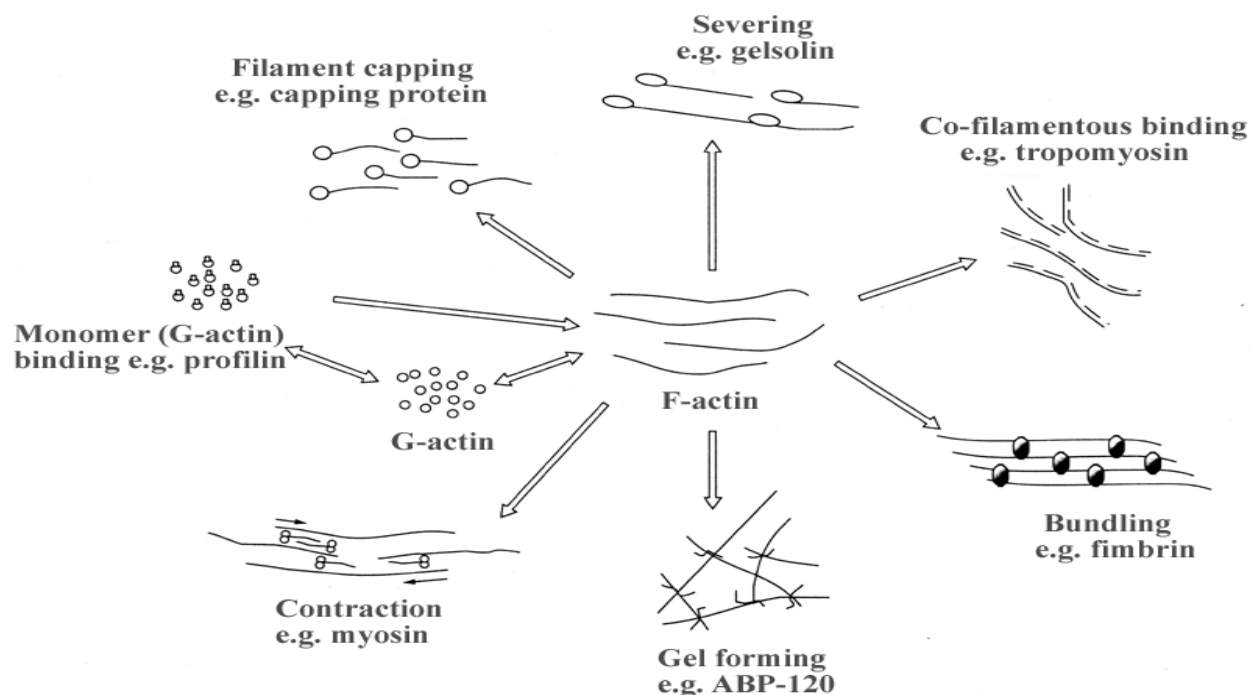


**Figure 1.1. Functions of actin binding proteins determined from *in vitro* experiments.** Each actin binding protein has a unique role and in a very significant manner modulates the nature of F-actin from a simple meshwork structure to highly cross-linked, tight thick bundles. Such a complex sub-cellular scaffold is brought about by the participating actin binding proteins. Figure adapted from reference (Ayscough et al., 1998).

Formation of such complexes and the cytoarchitecture in general, depend predominantly on one or more actin-binding proteins. Several proteins are known to contain more than one actin binding site, these proteins typically bundle actin filaments e.g.  $\alpha$ -actinin. Other parameters which govern the formation of complex structures are binding stoichiometry, kinetics of actin polymerization, and regulation of cross-linking activity. The expression profile and spatio-temporal distribution of the ABPs also helps us in understanding a cell and in turn understand the function of the ABPs. The actin binding regulatory proteins cross-talk with components of intracellular signaling pathways and can act either as down-stream targets or as up-stream regulators in these cascades. Identification of novel components of the cytoskeleton and understanding their biological functions may help to design strategies to cure various diseases. Numerous diseases are associated with the cytoskeletal systems of the cytoplasm, the nuclear envelope or the nucleus. Among them are inherited skeletal muscle disorders, cardio myopathies,

diseases of the central nervous system, liver cirrhosis, viral and fungal infections, and inflammation, blistering skin disease, tumors and fibrotic disorders.

### 1.1.2. Structure and function of cross striated muscle

Cross striated muscles are highly complex structures formed by precise organization of macromolecular complexes regulated by functional interactions of its individual components. Skeletal muscle fibers are long, multinucleated cells connected to nerve terminals, blood vessels, and connective tissue. Each muscle fiber is built up from contractile organelles called **myofibrils** (Figure 1.2A). The individual myofibril in both skeletal and cardiac muscle forms the contractile apparatus and it is composed of repetitive units called '**sarcomeres**'. The length of the fiber is determined by the number of sarcomeres that is lined up in series, one next to the other and the thickness depends on the number of myofibrils that are aligned in parallel. The regular arrangement of the sarcomere gives the characteristic striated appearance of myofibrils and can readily be seen by the light microscopy as alternating light and dark bands (Figure 1.2 A, B). The light band is termed the **I-band** because it is isotropic in polarized light. The dark band is known as **A-band** because it is anisotropic. The principle components of striated muscle sarcomeres are parallel arrays of actin-containing thin filaments and myosin-containing thick filaments. Thin filaments span the I-band and overlap with thick filaments in the A-band. The tail part of myosin binds to several proteins and approximately 300 myosin molecules are assembled in a tail to tail fashion to build the thick filaments. The head parts (which can bind actin filaments and hydrolyze ATP) project out from the thick filament overlapping and interacting with thin filaments. Several myosin binding proteins, such as myomesin, reside at the center of the **M-band**. A third filament system that integrates both compartments is composed of the giant protein titin (also called connectin) and its associated proteins. Individual titin molecules span half sarcomere length and connect the Z-disk to the M-line. In addition, titin is thought to function as a molecular spring (Li et al., 2002; Linke et al., 1996; Linke et al., 1998). Another gigantic protein, called nebulin, spans the entire length of the actin filaments and is supposed to determine the length of the actin filaments. **Z-disks** represent the lateral boundaries of the sarcomere, where the actin filaments, titin, and nebulin are anchored (Huxley et al., 1954).

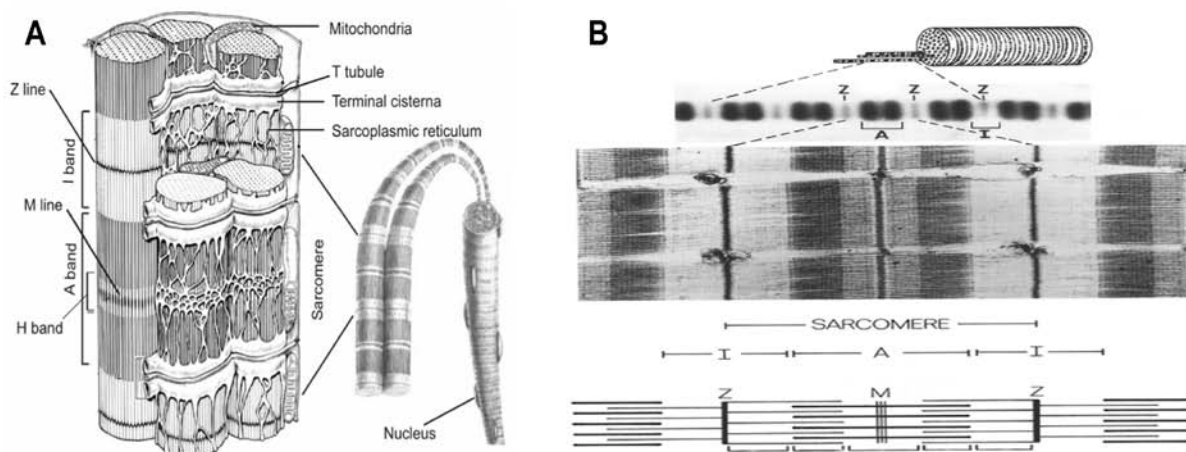


**Figure 1.2. Structure of a skeletal muscle fiber.** (A) Myofibrils, which are composed of sarcomeres, are surrounded by the sarcoplasmic reticulum (SR) and plasma membrane (sarcolemma). Near the A/I junctions, terminal cisternae and T tubules form triads, which regulate the  $\text{Ca}^{2+}$  transport and release. (B) Electron micrograph of human skeletal muscle. The A-band is the thick filament region of the sarcomere, whereas the I-band is composed of thin filaments. The Z-line anchors thin filaments from opposing sarcomeres and myomesin connects thick filaments to titin in the M-line. Adapted from (Stryer et al., 1981; Van Der Ven et al., 1996).

Contraction and relaxation occurs when the myosin heads of the thick filament slide past the actin thin filaments (Huxley et al., 1954). Thereby the thick filaments penetrate into the thin filament region. The contractile apparatus is regulated by the thin filament-associated protein complex troponin, that consists of troponin T, C and I and tropomyosin, which is wound over the actin filament. Muscle contraction begins with a depolarization signal from the nerve terminals and subsequent release of  $\text{Ca}^{2+}$  ions from the sarcoplasmic reticulum. The free  $\text{Ca}^{2+}$  binds to troponin C, which causes troponin I to shift and pull tropomyosin to which it is attached. The movement of tropomyosin from its position allows myosin heads to interact with the thin filaments by undergoing a conformational change (Cooke et al., 1986; Rayment et al., 1993b). This interaction of myosin heads with the actin-containing thin filaments is coupled to the ATP-ADP hydrolysis cycle (Lyman et al., 1971; Rayment et al., 1993a; Rayment et al., 1993b). Force generated by the interaction of myosin and actin is transduced across the plasma membrane by sub-sarcolemmal and transmembrane proteins to the extracellular matrix and neighboring cells.

### 1.1.3. Ultrastructure and components of adult skeletal muscle tissue

Skeletal muscle tissue is a precisely ordered structure. This order in the contractile machinery is essential for efficient function and it can only be achieved by other molecules that contribute to structural integrity. These are numerous actin- and myosin-associated proteins, as well as titin and

its associated proteins. All these components are essential for maintaining this complex architecture and regulation during differentiation (Figure 1.3).

### 1.1.3.1. Thin filaments

In striated muscle cells, the thin filament system consists of actin microfilaments. The striated muscle specific isoforms, cardiac actin (ACTC1) is expressed solely in cardiac tissue, while skeletal muscle actin (ACTA1) is found only in skeletal muscles. Both variants are products of individual genes. In striated muscle cells the thin filaments of the myofibrils measure approximately 1  $\mu\text{M}$  in length on the either side of the Z-disk. The polymerized actin forms a polar structure with barbed ends and pointed ends. The capping protein CapZ binds to barbed ends and the tropomodulin binds to pointed ends. In cross striated muscle cells several other proteins bind to actin filaments; these include tropomyosin (66 kDa) and the troponin complex (TnT, TnC and TnI), which are bound along the length of the actin filament and regulate myosin binding. The giant protein nebulin also binds to F-actin and is thought to regulate the length of the filaments. At the Z- line,  $\alpha$ -actinin binds to the barbed ends of the actin filaments, and tethers them into the characteristic tetragonal lattice. In addition to this structural role, recent data suggest an involvement of actin in transcriptional regulation and an activity as a scaffold for the transcriptional machinery (Franke et al., 2004).

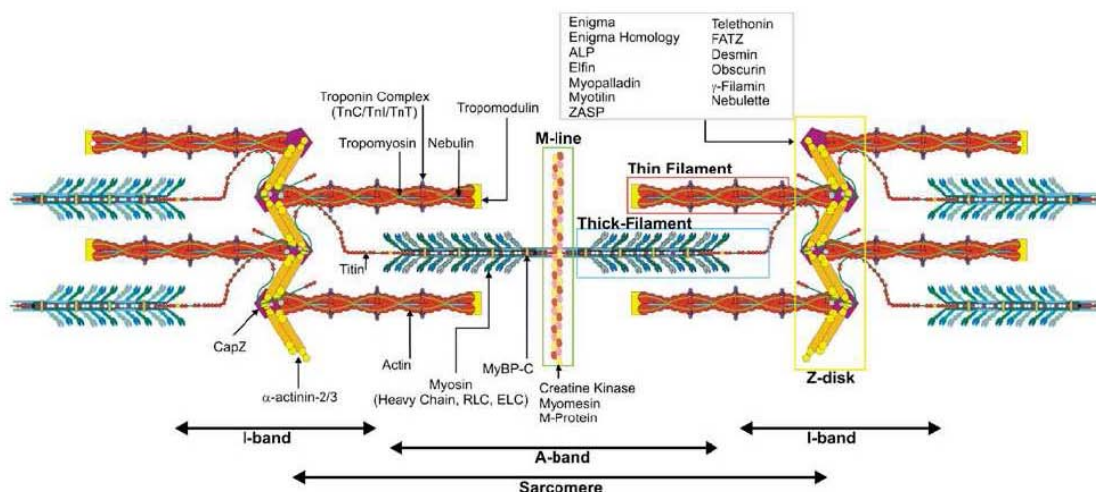


**Figure 1.3. Schematic representation of the sarcomere.** The sarcomere is composed of thin filaments (red), thick filaments (blue) and associated structures like the M-line (green box) and the Z-disk (yellow

box). The proteins that are found at the Z-disk are listed in the adjacent box above. Adapted from (Au et., 2004).

---

### 1.1.3.2 Thick filaments

#### 1.1.3.2.1. Myosin

Myosins are a huge superfamily of genes whose protein products share the basic properties of actin binding, ATP hydrolysis (ATPase enzyme activity), and force transduction. Virtually all eukaryotic cells contain myosin isoforms. Some isoforms have specialized functions in certain cell types (eg. Myosin II in muscle) while other isoforms are ubiquitous. Myosin II is responsible for producing the contractile force in muscle cells. Most myosin molecules are composed of a head, neck, and tail domain.

- The head domain binds the filamentous actin, and uses ATP hydrolysis to generate force and to "walk" along the filament towards the barbed (+) end.
- The neck domain acts as a linker and as a lever arm for transducing force generated by the catalytic motor domain. The neck domain can also serve as a binding site for myosin *light chains* which are distinct proteins that form part of a macromolecular complex and generally have regulatory functions.
- The tail domain generally mediates interaction with cargo molecules and/or other myosin subunits. In some cases, the tail domain may play a role in regulating motor activity (<http://en.wikipedia.org/wiki/Myosin>).

In muscle cells, the long coiled-coil tails of the individual myosin molecules join together, forming the thick filaments of the sarcomere. A single thick filament consists of most likely 296 myosin molecules bundled at the stalk in the M-line, which has a similar function to the Z-disk forming a bipolar thick filament (Figure 1.3, myosin filaments are colored in blue).

#### 1.1.3.3. Z-disk

Electron microscopic images of striated muscles show alternating dark and light bands (Figure 1.2B). The center of the light band, also known as the I-band, contains a narrow electron-dense zone, the Z-disk. Here, the barbed ends of the thin filaments from the neighboring sarcomeres are tethered together in a bipolar fashion. Proteins found at this location are termed Z-disk proteins. The major component of the Z-disk is  $\alpha$ -actinin. The complete composition of Z-disk is still not

clear. Each Z-disk is aligned to the neighboring ones by making molecular connections, at least in part utilizing the intermediate filament system including desmin. Z-disks located beneath the sarcolemma are linked to the costamere, mainly with the help of specific sub-sarcolemmal proteins, such as vinculin. Sarcomeric integrity is maintained mainly by two major cross-linking proteins the  $\alpha$ -actinin and the filamin. Several other molecules that associate at the Z-disk have been discovered relatively recently. Many of these make an interesting link to signaling mechanisms such as myotilin, myopalladin, PDZ/LIM proteins, ZASP/Cypher/Oracle, enigma, ENM (Enigma like LIM domain protein), CLP36/CLIM1, the FHL protein family, zyxin, MLP, T-cap/telethonin, calsarcins (myozenin /FATZ), calcineurin/protein phosphatase 2B, myopodin, PKC, phosphodiesterase 5A, Arg-binding protein 2 and p21-activated kinase-1. Most of these proteins associate with  $\alpha$ -actinin and/or filamin (Frank et al., 2006; Lange et al., 2006). However, a complete understanding of the structure and function of the Z-disk has not been possible, due to the great number of proteins that have been identified in the recent past.

#### 1.1.3.3.1. Titin

The thin and thick filament systems are sufficient to produce force by the sliding mechanism. However, both for the assembly of this complex structure and for the proper functioning in particular during relaxation, the giant protein titin is necessary to integrate the two filament systems. Titin (from the Greek 'titan': giant, of great size) is the largest known monomeric protein. It connects thin and thick filaments and spans half the sarcomere. Titin is anchored to the Z-disk with its amino-terminal portion, while its carboxy-terminus binds to the M-line. A striking and unique feature of titin is its serine/threonine kinase domain, known as 'the titin kinase domain' (Labeit et al., 1992). Titin binds to several sarcomeric proteins, including  $\alpha$ -actinin, actin, telethonin/T-cap, myosin, C-protein, myomesin, calpain, the potassium channel minK, obscurin, MURF-1, MLP, nebulin, calsarcin and myopalladin. The interaction partners of titin suggest that it acts as a scaffolding protein that is primarily involved in establishing and maintaining sarcomeric integrity.

#### 1.1.4. Myofibrillogenesis and myodifferentiation

Skeletal muscle development is a multistep pathway, in which mesodermal precursor cells are selected to form myoblasts that later are withdrawn from normal cell cycle and subsequently differentiate. Two families of transcription factors, MyoD and myocyte enhancer factor-2

(MEF2) play an essential role in this cascade by binding specific target motifs (CANNTG and an A/T rich sequence, respectively) in the promoters of skeletal muscle specific genes. The interaction of these transcription factors with each other, leads to a unique complex that regulates muscle specific gene activation (Black et al., 1998). Both MyoD and MEF2 are targets for diverse intracellular signaling pathways, that control myogenesis by modulating the function and expression of these factors (Naya et al., 1999). Myocyte differentiation and myofibril formation can be studied *in vitro* using cultured myocytes, although the individual events are much slower than *in vivo* differentiation (Gregorio et al., 2000). Differentiation in culture is initiated by serum withdrawal and the progression to mature myocytes takes about seven days (Auerbach et al., 1997; Ehler et al., 1999; Fürst et al., 1989; Gregorio et al., 2000). Expression of desmin is the first sign of muscle differentiation. Subsequently, other proteins taking part in myofibrillogenesis appear in a precise order and timing of expression (Gregorio et al., 2000). Three distinct forms of myofibrils can be distinguished during the differentiation progress. In the beginning of myofibrillogenesis, titin and  $\alpha$ -actinin appear in a punctate pattern along stress fiber-like structures, forming premyofibrils (Ehler et al., 1999; Fürst et al., 1989; van der Loop et al., 1996). These fibrils are composed of "mini-sarcomeres", where non-muscle myosin interdigitates the bipolar actin filaments, which are linked by  $\alpha$ -actinin in Z-disk primordia, called Z-bodies (Rhee et al., 1994). A N-terminal Z-disc region and a C-terminal M-line region bind to the Z-line and M-line of the sarcomere respectively so that a single titin molecule spans half the length of a sarcomere. Titin also contains binding sites for muscle associated proteins so it serves as an adhesion template for the assembly of contractile machinery in muscle cells. This structure seems to form a template for thick filament integration into the sarcomeres and the premyofibrils turn into nascent myofibrils. Other thin filament proteins like tropomodulin, T-cap, nebulin and filamin C (Almenar-Queralt et al., 1999; Ojima et al., 1999; van der Ven et al., 2000) are also expressed at early stages of differentiation and they incorporate into premyofibrils (Dabiri et al., 1997). Like premyofibrils, nascent myofibrils have punctate Z-bodies, that are spaced closer (0.3  $\mu\text{m}$ ) together than Z-disks of mature myofibrils (1.4  $\mu\text{m}$ ). Thus the growth in sarcomere length and alignment of nascent myofibrils leads to formation of cross-striated, mature myofibrils (Rhee et al., 1994).

### 1.1.4.1. Filamins

Filamins are a small family of large actin-binding proteins that stabilize delicate three-dimensional actin webs and link them to cellular membranes. In this way, they integrate functions in establishing cell architecture and signaling (Revenu et al., 2004). Primarily, they link actin filaments into a network, but they also anchor plasma membrane receptors and other transmembrane proteins to the cytoskeleton and are thought to act as scaffolding proteins. The important functions of filamins are exemplified by their essential roles in fetal development (Stossel et al., 2001). The three filamin isoforms (filamin A, B, and C), are each encoded by a unique gene (Feng et al., 2004). Whereas filamin A and B are ubiquitously expressed, filamin C is the striated muscle specific isoform.



**Figure 1.4. Protein structure of filamin C.** Filamins are rod shaped molecules, composed of an N-terminal actin binding domain harboring two calponin homology domains followed by twenty four C2-type Ig- domains, separated by one or two hinge regions. The 24<sup>th</sup> Ig domain dimerizes, which brings about the ability of the filamins to cross link actin polymers. Filamin C harbors a unique insertion in Ig-like domain 20 and is expressed only in striated muscle cells. Figure adapted from (van der Ven et al., 2006).

In adult skeletal muscles and cultured cells, filamin C localizes to the Z-disk and to sites where myofibrils are attached to the membrane (myotendinous junctions). In the heart, the protein is localized mainly in the intercalated disks and in Z-disks. A minor fraction of filamin C is associated with plasma membrane (Lee et al., 2004). During *in vitro* muscle cell morphogenesis Filamin C shows a striking colocalization with  $\alpha$ -actinin, initially in adherens junctions and in the Z-bodies of immature myofibrils, and later during development in Z-disks. Previous work in our laboratory focused on Filamin C and its interaction partners. While large parts of the molecule are homologous to the non-muscle variants A and B, one of the immunoglobulin-like domains of filamin C (domain 20) contains a unique 78 amino acid insertion. Since domains 19-21 of filamin C targeted to Z-disks upon transient transfections in muscle cells, this region was predicted to harbor one or more protein-protein interaction motifs. Subsequent yeast two hybrid screens with filamin C domains 19-21 as bait identified myotilin, myopodin and Xin as interacting partners (van der Ven et al., 2006). The latter protein was found to specifically interact with domain 20.

Filamin C has several other binding partners ( $\beta$  and  $\gamma$ -sarcoglycan, calsarcin-3, nephrocystin, calsarcin-2, MAP2K4, KCND2, Calpain-3 and SHIP2).

#### 1.1.4.2. Xin family of proteins

The Xin family of proteins is expressed exclusively in striated muscles. The first member of the family, cXin was discovered in chicks based on its robust expression in developing chick hearts (Wang et al., 1999). The human orthologue of cXin was first named CMYA1, since it was found to be coexpressed with cardiomyopathy associated genes. A second member of the family XIRP2 (Xin Repeat protein 2) was discovered in silico first in humans. The gene *XIRP2* is also known as *CMYA3*. Since their first discovery in chick, mouse and humans, extensive database searches have further revealed that the Xin protein family is expressed across the species but only in vertebrates (Grosskurth et al., 2008). The family is characterized by the presence of 16 amino acid repeat regions, the so called Xin repeats (Wang et al., 1999). The biochemical role of these Xin repeats was established in this laboratory by demonstrating that they define a novel actin binding motif (Pacholsky et al., 2004). Xin (Xirp1 or CMYA1) was found to localize along actin stress fibers and the cell membrane in cultured muscle cells (C2C12 myotubes), at the ICD in the heart and at the MTJ in skeletal muscle (Sinn et al. 2002). In contrast, Xirp2 (myomaxin, CMYA3) was found at Z-discs in the heart and skeletal muscle, at the ICD, as well as in proliferating C2C12 myoblasts (Huang et al., 2006; Gustafson-Wagner et al., 2007).

##### 1.1.4.2.1 Regulation of Xin family of genes by muscle-specific transcription factors

Promoter analyses revealed the presence of several muscle-specific transcription factor binding sites in the promoter of *xirp1*, such as Mef2, Nkx2 and MyoD binding sites (Wang et al., 1999). Luciferase assays showed that MyoD, Myf5, and Mef2 could activate *xirp1* expression, probably in complementary or partially overlapping temporal and spatial patterns (Gustafson-Wagner et al., 2005). The heart-specific transcription factor Nkx2.5 was also found to activate the expression of *xirp1* (Wang et al. , 1999) and consequently, Nkx2.5 knock-out mice express less Xin (Jung-Ching Lin et al. , 2005). *Xirp2* expression was found to be regulated by Mef2c and Mef2a (Huang et al., 2006).

#### 1.1.4.2.2. Binding properties of Xirp proteins

The Xin repeats have been extensively analyzed biochemically to determine their physical properties. Three Xin repeats were shown to be sufficient to crosslink and stabilize actin filaments and to inhibit the binding of tropomyosin to actin filaments (Pacholsky et al., 2004). It was also shown that Xin repeats and nebulin repeats bind to actin filaments in a similar manner, although nebulin repeats bundle actin filaments, whereas Xin repeats crosslink actin filaments (Cherepanova et al., 2006). Indeed, two studies found that Xin repeats do not bundle actin filaments (Cherepanova et al., 2006; Pacholsky et al., 2004). In contrast, the full-length protein does show actin bundling activity that is enhanced in the presence of  $\beta$ -catenin (Choi et al., 2007). Xin is found at the ICD and the MTJ, where it colocalizes with  $\beta$ -catenin, N-cadherin and vinculin (Sinn et al., 2002; Wang et al., 1999). In contrast, Xirp2 additionally colocalizes with  $\alpha$ -actinin at the Z-disc (Gustafson-Wagner et al., 2007; Huang et al., 2006). Both Xin and Xirp2 always colocalize with filamin C at various stages of development and in various muscle tissues, in structures such as the ICD, Z-discs and premyofibrils in neonate cardiomyocytes (van der Ven et al., 2006). Moreover, in neonate cardiomyocytes, Xin colocalizes with Mena, filamin C,  $\beta$ -catenin and  $\alpha$ -actinin (van der Ven et al., 2006)

## 1.2. Lentivirus as a tool for gene expression and gene knockdown in skeletal muscle cells

Skeletal muscle cells are generally considered as difficult to transfect with transfection efficiencies ranging from as low as 1 % and rarely reaching 30 %. Studying the expression of a gene which might play an important role in skeletal muscle differentiation requires studying the cells from a myoblast (mononuclear cell) to a fully differentiated mature myotube (multi-nucleated cell). Knocking down the gene of interest in myoblasts and subsequent monitoring of differentiation of the knockdown cells requires a high transfection efficiency to nullify the effect of high background due to non-transfected cells. Ideally a virus based system is the method of choice. Both adenoviruses and lentiviruses (LVs) are capable of transducing dividing and non-dividing cells. However LVs offer the advantage that they stably integrate in the host genome and hence stable cell lines can be generated, which are more convenient to study. Stable integration into the host genome obviates the need for repeated vector administration. LVs also offer other advantages such as animal transgenesis and the possibility of gene therapy.

## 1.2.1. Introduction to Lentivirus

Lentiviruses belong to the large family of retroviruses. The genus *lentiviridae* includes the human immunodeficiency viruses HIV 1 and HIV 2, the simian immunodeficiency virus (SIV) and non-primate lentiviruses, such as the visna virus, the equine infectious anemia virus (EIAV) and the feline and the bovine immunodeficiency viruses (FIV and BIV). Among all LVs, the HIV 1 is the most widely studied and used virus. Lentiviral based systems have attracted vast interest primarily due to their ability to transduce terminally differentiated cells including primary cells, neurons, macrophages, hematopoietic stem cells, retinal photoreceptor cells, muscle and liver cells etc. LVs integrate with a very high frequency into the host genome which provides an efficient tool for creation of stable cell lines and transmission of integrated transgenic cassettes to the progeny (vertical transmission). Because of integration into the host genome LVs provide long term expression of the cassettes they carry within the vector. Unlike adenoviral based expression systems they do not induce immunological responses and unlike other retroviral based systems they have the capability to transduce non-mitotic cells. LVs largely escape epigenetic silencing in embryonic stem cells and early embryos and thus can be used to generate transgenic animals (Pfeifer et al., 2002). LVs can infect both dividing and non-dividing cells because their preintegration complex (virus “shell”) can cross the intact membrane of the nucleus of the target cell (Bukrinsky et al., 1993). Lentiviruses cannot efficiently transduce truly quiescent cells (cells in the G<sub>0</sub> state) owing to a block at the reverse transcription step (when the RNA viral genome is transcribed into DNA) (Zack et al., 1990), and they require progression through at least the G<sub>1b</sub> stage of the cell cycle (during which active RNA synthesis takes place) (Korin et al., 1998).

## 1.2. 2. The general biology and life cycle of Lentivirus (HIV 1)

### 1.2.2.1. The genes and elements of HIV 1 genome

Like all retroviruses, HIV 1 is an RNA virus. Its genome contains three main genes encoding the polyproteins *Gag*, *Pol* and *Env*. The polyproteins are post-translationally and proteolytically cleaved to form structural proteins and enzymes. *Gag*, the precursor of the virus core, is cleaved into MA (matrix), CA (capsid), NC (nucleocapsid) and P6, *Env* into the proteins which form the outer membrane envelop SU (surface or gp120) and TM (transmembrane or gp 41), and *Pol* into the three main enzymatic components-PR (protease), RT (reverse transcriptase), and IN (integrase).

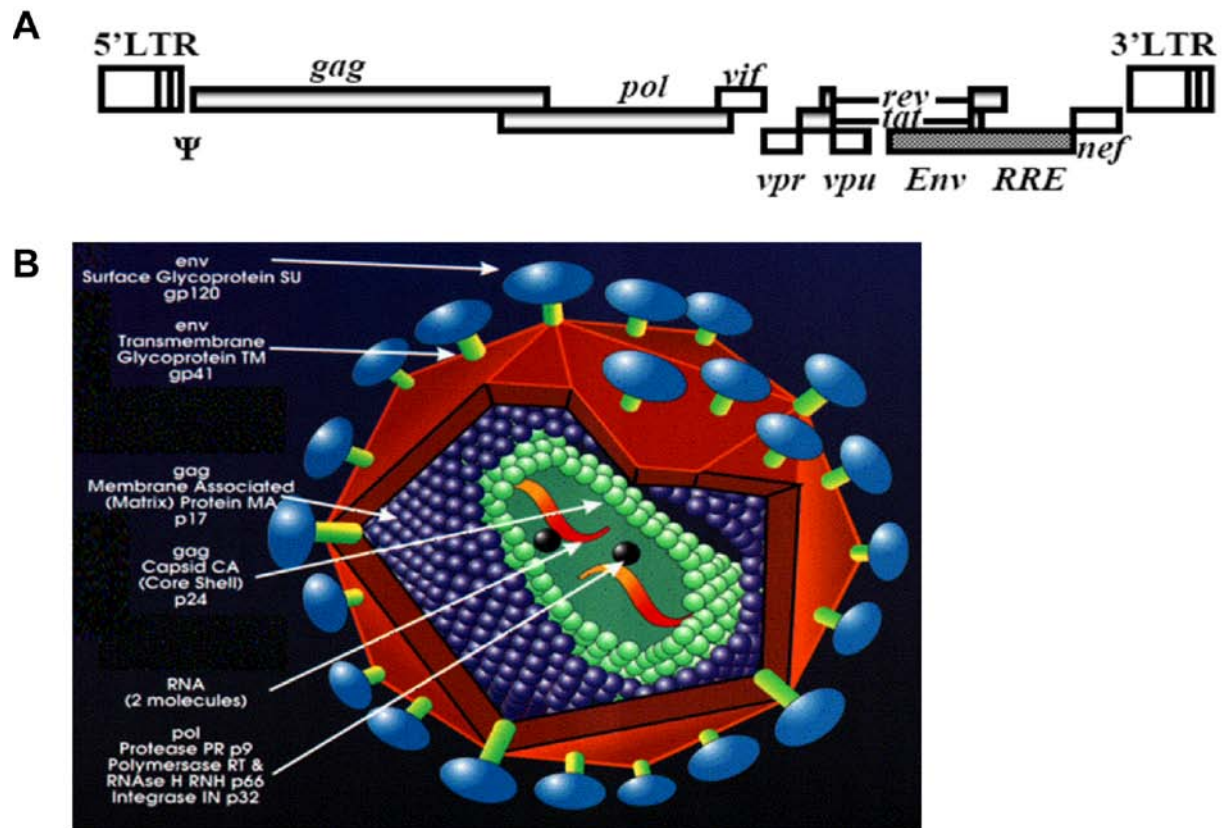


**Figure 1.5. Schematic diagram of the HIV 1 genome.** The 5' and 3' Long terminal repeats (LTRs) serve to integrate the dsDNA copy of the virus into host genome. The packaging signal ( $\psi$ ) acts as a signal sequence and is necessary for packaging RNA with the reporter or therapeutic gene in virions. The three structural genes (*gag*, *pol* and *env*), the two regulatory genes (*tat* and *rev*) and the four accessory genes (*vif*, *vpr*, *vpu* and *nef*) and the Rev-response element (RRE) that is located in the intron of *rev* and *tat* are also shown. B. Shows the structural proteins encoded by various genes of the HIV 1 genome (Figure adapted from <http://biology.kenyon.edu>).

Apart from the three genes mentioned above and unlike simple retroviruses, the HIV genome encodes additionally two regulatory genes, *tat* and *rev* and four accessory genes, *vif*, *vpu*, *vpr* and *nef*, all of which are involved in viral pathogenesis. Figure 1.5 gives an overview of the genes and elements of the HIV1 genome.

### 1.2.2.2. The life cycle of the lentivirus

The life cycle of lentiviruses is common to all members of the *Retroviridae* family and can be described by the following steps (schematically represented in Figure 1.6).

1- Attachment and entry: The interaction between the virus and the target cell occurs via specific receptors. Once bound to the surface, the viral and cellular membranes fuse and the viral

nucleoprotein is delivered to the cytoplasm where reverse transcription begins. For example, HIV 1 infects human CD4+ T cells and macrophages by utilizing CD4 as its receptor and a variety of chemokine receptors as its co-receptor. The two most important chemokine receptors, CXCR4 and CCR5, not only provide a crucial function for viral entry into cells, but also determine the tropism (ability to infect) of virus.

2- Reverse transcription: After HIV entry into cells, its RNA is converted into double stranded DNA by the viral reverse transcriptase using cellular tRNA as a primer in a large nucleoprotein complex called preintegration complex (PIC). The PIC of HIV 1 contains matrix proteins, integrase and vpr. The viral cDNA is actively transported into the nucleus, a process that is facilitated by the PIC.

3- Integration: Once in the nucleus, the viral integrase processes the 3'ends of the viral cDNA and then mediates its integration into the host genome.

4-Transcription and viral protein synthesis: To complete the life cycle, HIV needs other regulatory proteins and accessory proteins either to facilitate the viral replication or to overcome the cellular constraints to the virus (Figure 1.6). One of the regulatory proteins, Rev, competes with the cellular splicing machinery and exports intact or partially spliced viral RNA out of the nucleus, a process that is crucial for Gag-Pol expression and new viral genome packaging. The four accessory proteins have various other functions such as augmentation of viral release, downregulation of MHC class I molecules and modulation of host cell cycles, all of which are involved in viral pathogenesis but not necessary for lentiviral vector packaging, transduction and expression (Emerman et al., 1998).

5-Virion assembly and release: Viral genome and structural proteins are packaged into the viral particles and released at the plasma membrane.

### 1.2.3. HIV1 based lentiviral systems- three generations of lentiviral vectors

The discovery that HIV-type1 can infect both mitotic and non-mitotic cells brought a new perspective to the field of gene therapy and led to the development of lentiviral vectors as a gene delivery tool. For reasons of biological safety and efficiency, lentiviral gene transfer vectors

based on the HIV1 genome were created by deleting and altering native sequences in HIV1( reviewed in (Sinn et al., 2005). The major goal was to prevent generation of replication competent viruses which might occur due to homologous recombination of wild type sequences present on different vectors. The first generation of lentiviral vectors, were not intended for use in gene delivery but for the study of HIV-1 pathogenicity. These vectors generally contained the entire viral genome with the exception of the *env* gene. A reporter gene was expressed in place of *env* and the envelope protein was expressed by another construct making it a two vector system, a situation that implied a high risk of generating wild type virus.

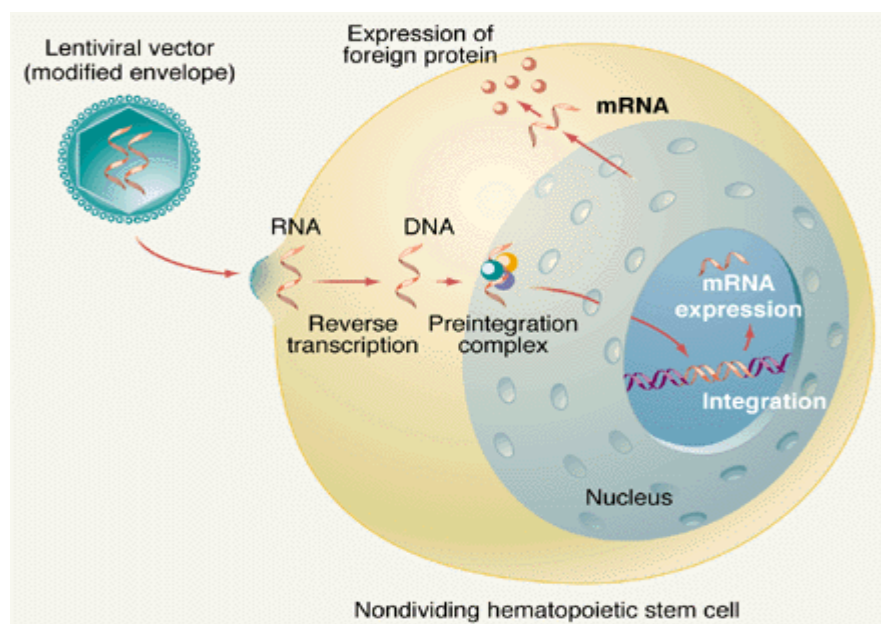


**Figure 1.6. Schematic representation of a lentivirus life cycle.** The life cycle can be described in five steps starting from attachment of the virus to the host cell till the new virion assembly and release. For a complete description see above (Figure adapted from (Amado et al., 1999)).

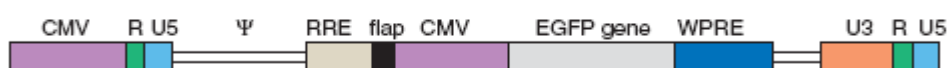
In the second generation of lentiviral vectors, this safety issue was dealt with by splitting packaging helper elements (*gag-pol*) and transgene expression cassette into two separate plasmids and by deleting all accessory genes of HIV1 from the vectors to minimize the possibility of homologous recombination.

### 1.2.3.1. Self inactivating (SIN) lentivectors

To further improve the safety, a chimeric LTR was made by using constitutive promoters such as human CMV intermediate-early enhancer/promoter to replace the U3 region at the 5'LTR (Figure 1.7). In this case, the transcription of transfer vector became *tat*-independent and *tat* could be

removed from the vectors (Dull et al., 1998). Additionally most of the U3 region, except for the integrase attachment sites in the 3'LTR was also deleted, thus the U3 of the 5' LTR of provirus no longer exists after the viral RNA undergoes reverse transcription and integrates into the host genome (Miyoshi et al., 1998).

### Packaging Construct



### Integrated vector



**Figure 1.7. Typical self inactivating (SIN) lentiviral vector showing modified U3 and U5 regions in 3' and 5' LTRs.** The U3 region of the 5' LTR was replaced with a chimeric 5' LTR using a constitutive promoters such as human CMV intermediate-early enhancer/promoter. Most of the 3' LTR was also deleted except for the integrase attachment sites to generate a SIN vector.

It is virtually impossible that SIN vectors are mobilized once introduced into cells, even if the target cells are infected with wild-type replication competent viruses (Bukovsky et al., 1999). Additionally, U3 deletion abolishes LTR promoter activity, which minimizes the possibility to activate oncogenes downstream of the provirus integration site in the host genome. However, the deletion of U3 region at the 3' LTR has also been found to compromise the polyadenylation signal of the 3' LTR that increases the transcriptional read-through (Zaiss et al., 2002). Thus the transgenes of SIN lentiviral vectors are designed to be driven by a heterologous internal promoter and terminated by a heterologous polyadenylation signal that replace the wild type 5' LTR and 3' LTR respectively. Since the efficient transportation of full-length and partially spliced RNA out of the nucleus is required for the gag-pol polyprotein production, the RRE element is designed into the packaging helper vector for the full-length RNA transportation through Rev-RRE interaction (Naldini et al., 2000). A minimal transgene expression cassette contains the LTRs (usually the chimeric LTRs and thus generating SIN vector), the packaging signal ( $\psi$ ) and a heterologous promoter that drives the transgene of interest. However, to increase gene transfer efficiency, additional cis-acting regulatory sequences are routinely incorporated into lentiviral vector backbones. One such element is the central polypurine tract (cPPT), which enhances HIV vector efficiency by facilitating nuclear translocation of preintegration complexes. The viral transduction efficiency was further enhanced by the posttranscriptional regulatory element of

woodchuck hepatitis virus (WPRE). Insertion of the WPRE in the 3' untranslated region of lentiviral vectors enhances transgene expression 5- to 8 fold in a promoter and transgene-independent manner (Zufferey et al., 1999). Thus wild type cis elements are minimized, additional cis elements are added within the transfer vector and necessary trans-elements are supplied from packaging and envelope helper constructs to increase viral titer and thus gene transfer efficiency (reviewed in (Sinn et al., 2005)). Thus the second generation lentiviral vector systems are made up of three different plasmids namely a transfer vector, a packaging vector and an envelope plasmid.

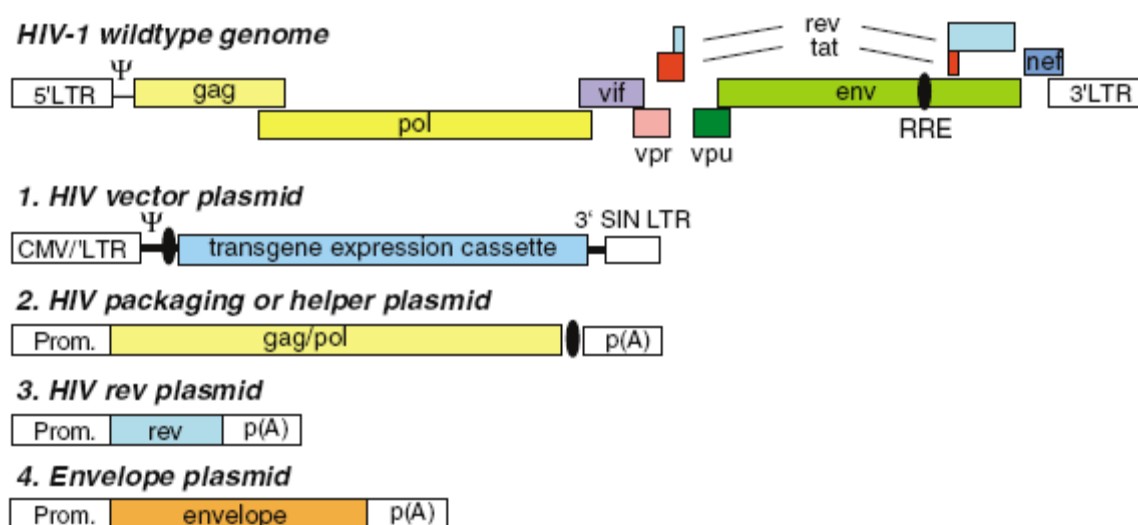


**Figure 1.8. Schematic diagram of HIV-1 based third generation lentiviral vector system.** Panel A shows the overview of genes in HIV 1 genome. In panel B, 1 shows the minimal HIV vector plasmid consisting of the CMV/HIV LTR hybrid promoter followed by the packaging signal ( $\psi$ ), the rev-binding element (RRE) for cytoplasmic export of the RNA, the transgene expression cassette consisting of internal promoter (s) and transgene (s), and the 3' self-inactivating (SIN) LTR. All genes coding for enzymatic or structural HIV proteins have been removed. Together with the HIV vector plasmid (1), the HIV packaging plasmid (2), HIV rev (3), and an envelope protein expressing plasmid (4) are needed for HIV vector production.

The lentiviral vectors used in this work belong to the second generation and are produced by co-transfecting the three plasmids mentioned above into human packaging cells such as human embryonic kidney cells transformed with SV40 large T antigen also known as, HEK293T. The SV40 large T antigen facilitates replication of plasmids containing the SV40 origin of replication, which is present on the transfer vector used. In the third generation of lentiviral vectors gag-pol and rev are supplied from different plasmids thus four plasmids need to be transfected into HEK 293T cells to produce the lentivirus. To obtain a lentiviral gene vector, a reporter gene or a

therapeutic gene is cloned into a vector sequence that is flanked by LTRs and the  $\psi$  -sequence of HIV. The LTRs are required to integrate the therapeutic gene into the genome of the target cell, just as the LTRs in HIV integrate the dsDNA copy of the virus into its host genome. The  $\psi$  -sequence is necessary for packaging viral RNA with the reporter or therapeutic gene into virions or viral particles. The packaging and envelope plasmids code for viral proteins, which make virus shells, however, they are not in context of LTRs and  $\psi$  -sequences (which are located on the transfer vector) therefore are not packaged into virions. Thus, the lentiviral particles produced are replication deficient, competent for initial infection but incompetent to spread from one cell to another cell.

### 1.2.3.2. Envelope plasmid and pseudotyping

Pseudotyped lentiviral vectors consist of vector particles bearing glycoproteins (GPs) derived from other enveloped viruses. Such particles possess the tropism (ability to infect) of the virus from which the GP was derived. Vesicular stomatitis virus G envelope glycoprotein (VSV-G) is a membrane fusion protein that utilizes a ubiquitous phospholipid as its cellular receptor. Lentiviral vectors pseudotyped with VSV-G envelope have a greatly extended host range (broad tropism). The pseudotyping of viral particles with the VSV-G protein allows for great stability compared to pseudotyping with other viral glycoproteins. VSV-G pseudotyped particles may be stored at 4° C for 2-3 days, can tolerate a freeze and thaw cycle and may be concentrated 100-fold by ultracentrifugation, all without a significant loss in viral titer (Burns et al., 1993). The only disadvantage of using VSV-G pseudotyped virus is its inactivation upon contact with human serum, limiting its experimental use (DePolo et al., 2000). While VSV-G has broad tropism and is the most frequently used GP for pseudotyping, other pseudotypes have also been applied for special applications. For example, to exploit the natural neural tropism of rabies virus and mokoala virus, vectors designed to target the central nervous system have been pseudotyped with GPs derived from these viruses. GPs derived from Ebola virus were used for pseudotyping lentiviruses for infecting respiratory and lung tissues (Cronin et al., 2005).

### 1.2.3.3. Promoters and inducible systems based on lentiviral vectors

Lentiviral vectors often contain ubiquitously expressing promoters that allow broad transgene expression in almost all organs. Such promoters are the human cytomegalovirus immediate early promoter (CMV), the promoter of the human phosphoglycerate kinase gene (PGK), the human

Ubiquitin-C promoter and the CAG promoter (a chicken beta-actin/CMV compound promoter). By introduction of inducible transcriptional elements, spatial and temporal regulation of the lentiviral transgene expression can be achieved. The most frequently used regulatable systems are Tet-ON, Tet-OFF system (reversible) and Cre-lox based system (irreversible). LVs have relatively large cloning capacity (up to 10kb) between the 3' and 5' LTRs for cloning transgene cassettes. However the packaging ability and the viral titers decrease with increasing size of the expression cassettes.

#### 1.2.4. Biosafety issues related to lentiviral usage

As discussed above, the second and third generations of lentiviral systems have adequate safety for laboratory use. The remote possibility to generate replication competent virus and their possible spread through liquids and aerosols is minimized by confining all the work related to lentivirus production and transduction to specific areas designed for this work (Biosafety level 2 laboratory). According to the decision of the Institutional Biological Committee, which was approved by the Institutional Safety Committee, lentivirus work is done locally, within the facilities of each department and is under the responsibility of the principle investigator. Since lentiviruses produced in the laboratory are pseudotyped with VSV-G coat, which has broad tropism and could infect many cell types including human cells, accidental exposure to lentivirus is to be avoided. The separation of cis and trans-acting regions of the viral genome onto separate vectors and decreasing the level of homogeneity between these vectors has enabled the use of this system in scientific and clinical research. However, the presence of some sequences is required on more than one vector, e.g. approximately 300bp of gag is required on both the packaging and transfer vectors, thus the possibility of recombination, albeit very small, must still be considered. If such an event were to occur, infected cells could not express viral proteins due the SIN property of the system. In the third generation of lentiviral vectors the transport of transcripts to the cytoplasm could not occur in the absence of Rev, which is delivered to packaging cells on its own expression vector. Thus the third generation of lentiviral vectors offers highest bio-safety although they require four plasmids for production of lentiviruses. Another concern in clinical research is the possibility of recombination events between an engineered virus and a wild type virus in patients already infected with HIV-1. Studies suggest that if such an event were to occur, the possibility of recombination between the genomes of both viruses is quite likely, resulting in the emergence of a new viral species. The development of SIN LVs has also decreased the risk of

aberrant expression of genes endogenous to the transduced cells and induction of proto-oncogenes from viral LTRs, a matter of major concern in clinical gene therapy trials (Marshall et al., 2003).

## 1.3. RNA interference

RNA interference (RNAi) is a post-transcriptional gene silencing mechanism that is evolutionarily conserved across many species. It is a process whereby small double stranded RNAs suppress the expression of target genes in a sequence specific manner (Fire et al., 1998). It is widely believed that RNAi has originally evolved as a defense mechanism against invading viruses or active transposable elements. Many foreign RNAs differ from endogenous transcripts in that they are not single stranded but consist of two anti-parallel strands. In case dsRNAs appear in the cell, they are recognized by a cytoplasmic ribonuclease called 'Dicer' and cut to RNA duplexes of about 21 nucleotides with characteristic 2-nucleotide 3'-overhangs also known as siRNAs. The next stage of cellular RNAi mediated degradation involves a multi-protein complex called RNA induced silencing complex (RISC). Functional RISC is believed to contain at least four different subunits including a helicase, an endonuclease, an exonuclease and a homology searching component. Upon binding of siRNA to RISC the helicase unwinds the double stranded siRNA molecule resulting in two short single strands. In doing so activated RISC is poised for 'homology searching'. One single strand of siRNA (usually the antisense strand also called 'guide strand' is used as bait for searching and binding a complementary mRNA strand. Finally the RISC bound target mRNA is degraded through action of the exo- and endonuclease subunits of RISC (Prawitt et al., 2004).

### 1.3.1. RNAi in mammalian systems compared to plants flies and worms

Long dsRNAs (400-700 base pairs) can induce efficient and highly specific gene silencing when introduced into worms, flies or plants. However in mammalian cells molecules of the same length are recognized by the RNA dependent protein kinase (PKR). Activation of PKR and 2', 5'-oligoadenylate synthetase elicits an interferon response, which results in general inhibition of protein synthesis and mRNA degradation in a sequence independent manner. The only exceptions where long dsRNAs do not produce interferon response are restricted to oocytes and early

embryos. Plants, flies and worms have developed additional defense mechanisms to effectively defeat double stranded RNAs. They use RNA dependent RNA polymerase (RdRp) and amplify the silencing triggers (siRNAs). In contrast such amplification does not occur in mammalian systems, which necessitates continuous supply of silencing triggers (Prawitt et al., 2004). A major breakthrough was made in 2001, when it was discovered that small dsRNAs (< 30 base pairs) produce sequence specific mRNA degradation in mammalian cells (Elbashir et al., 2001a). This breakthrough together with a better understanding of the RNAi pathway and the discovery of several endogenous miRNAs lead to an explosion in the field and to the development of RNAi as a powerful and widespread reverse genetics tool for functional annotation of mammalian genes (Hannon and Rossi, 2004) to genome wide phenotypic screens in cell culture (Paddison et al., 2004b) and creation of knockdown mice (Rubinson et al., 2003; Tiscornia et al., 2003). RNAi continues to make a huge impact on rapid functional annotation of genomes and has made enough promises for clinical use for a number of diseases (Kim et al., 2007; Lee et al., 2002) and is rightly recognized by awarding the discoverers of RNAi with Nobel Prize in medicine for 2006.

### 1.3.2. RNAi pathway and endogenous miRNAs

Micro RNAs (miRNAs) are highly related to siRNAs. They are endogenous small RNAs that repress the expression of their target genes. Micro RNAs differ from siRNAs in their biogenesis, however not in their function. Hundreds of miRNA genes have been found in animals, plants and viruses (Bartel et al., 2004; Murchison et al., 2004; Pfeffer et al., 2004) making them one of the largest gene families. Micro RNAs are defined as single-stranded RNAs of 19–25 nt in length generated from endogenous transcripts that can form hairpin structures (Ambros et al., 2003). Micro RNAs act as guide molecules, by base-pairing with their target mRNAs leading to translational repression (when the sequence is partially complementary) and/or mRNA cleavage (when the sequence is fully complementary). Several studies revealed the key roles of miRNAs in diverse regulatory pathways, including development timing control, hematopoietic cell differentiation, apoptosis, cell proliferation and organ development (Bartel et al., 2004). A single miRNA can bind to and regulate many different mRNA targets and, conversely, several different miRNAs can bind to and cooperatively control a single mRNA target (Lewis et al., 2003). The majority of miRNA genes are located in intergenic regions or in antisense orientation to annotated genes (Lagos-Quintana et al., 2001; Lee et al., 2001) indicating that they form

independent transcription units (Lee et al., 2001). Most of the other miRNA genes are found in intronic regions, which may be transcribed as part of the annotated genes.

Micro RNAs are initially transcribed by RNA polymerase II (Pol II) as part of a long primary miRNA (pri-miRNA) precursor (Figure 1.9). Mature miRNAs form part of one arm of a ~ 85-nt RNA stem-loop in the pri-miRNA. The first step in miRNA processing is mediated by the RNase III enzyme Droscha, which cleaves the stem ~ 22 nt away from the terminal loop to generate an ~65-nt pre-miRNA hairpin intermediate. Droscha cleavage defines one end of the mature miRNA and leaves a characteristic 2-nt 3' overhang. The pre-miRNA is transported to the cytoplasm by the nuclear export factor, Exportin-5 (Exp 5), where it interacts with a second RNase III enzyme called Dicer (Figure 1.10.). Dicer binds the 2-nt 3' overhang found at the base of the pre-miRNA hairpin and cleaves ~ 22 nt away from the base, removing the terminal loop and leaving another 2-nt 3' overhang. The resultant duplex intermediate interacts with RISC components, including Argonaute-2 (Ago2), which selectively incorporate the RNA strand whose 5' end is less tightly base-paired. Once programmed, RISC can downregulate the expression of homologous mRNAs.

### 1.3.3. Approaches to RNAi-mediated gene knockdown in mammalian cells

Three types of small RNAs ( siRNAs, shRNAs and shRNAmirs) can be used to silence gene function by RNA interference (RNAi) in mammalian cells (Moffat and Sabatini, 2006) and they correspond to the three intermediate stages of miRNA biogenesis pathway (Figure 1.9.). The siRNAs correspond to miRNA duplexes, the shRNAs to the pre-miRNA hairpin and shRNAmir to the initial pri-miRNA transcript. So the endogenous miRNA pathway can be entered at all three points with different types of small RNAs to ultimately guide mRNA degradation via RISC.

#### 1.3.3.1. Small interfering RNAs (siRNAs)

siRNAs are short double-stranded RNAs (dsRNAs) that are typically 19–22 bp in length with 2-nucleotide 3'overhangs on either end, including a 5' - phosphate group and a 3' - hydroxyl group (Figure 1.10 a). siRNAs can be made by chemical synthesis, in vitro transcription, RNase III digestion of dsRNAs or by PCR expression cassettes. siRNAs can be introduced into target cells by transfection to achieve transient silencing of a target gene.

Transfection of chemically synthesized siRNAs is a relatively quick method. But siRNAs are not amplified in mammalian systems unlike in plants and worms so siRNAs must be continuously supplied to get long-term knockdown. Without continuous supply the effective siRNA concentration goes down and knockdown efficiency decreases rapidly. Since there are no selection markers and reporters (unless siRNAs themselves are labeled) it is impossible to select transfected cells from untransfected cells and hence stable knockdown cell lines cannot be established.

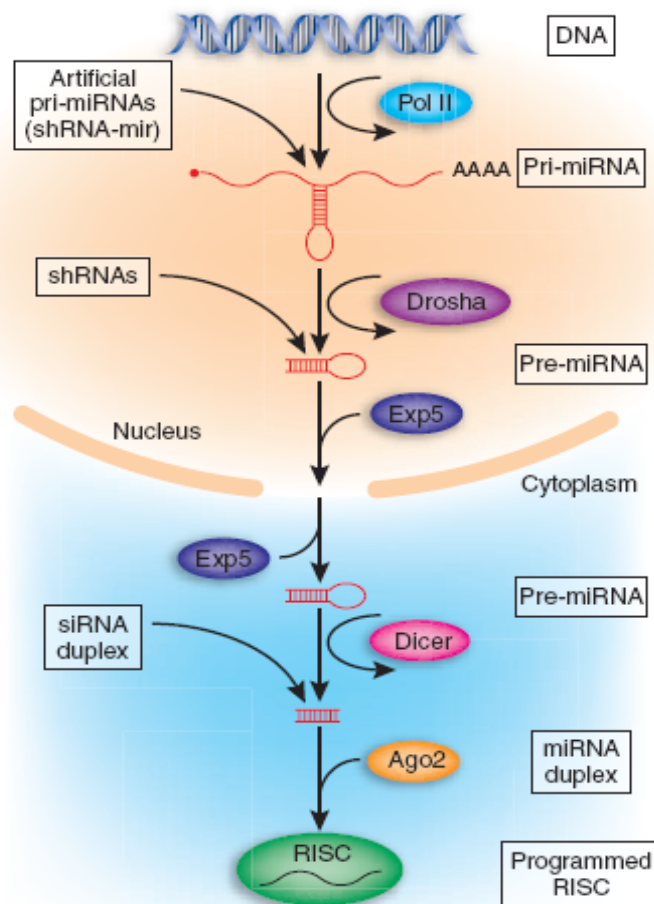


**Figure 1.9. The miRNA biogenesis pathway in vertebrate cells.** Artificial siRNAs can enter this pathway as synthetic siRNA duplexes, as shRNAs transcribed by Pol III or as artificial pri-miRNAs (shRNAmir). shRNAmirs enter the pathway upstream of shRNAs which in turn enter the pathway upstream of siRNAs. For simplicity, not all factors involved in miRNA biogenesis are shown. Figure adapted from (Cullen et al., 2005).

### 1.3.3.2. Short hairpin RNAs (shRNAs)

shRNAs are transcribed from plasmid DNA under the control of a RNA pol III promoter as single-stranded RNA molecules of 50–70 nucleotides in length and form a stem–loop structure in vivo. A 5–10-nucleotide loop keeps the complementary 19–21 nucleotide stem sequences in close proximity to allow base pairing to occur (Figure 1.10 b). shRNAs exit the nucleus and are recognized and cleaved at the loop by the nuclease Dicer and enter the RNA-induced silencing complex (RISC) as siRNAs ( Figures 1.10 b & 1.9.).

Expression of shRNAs from plasmids ensures a continuous supply of siRNAs. Since selection markers and reporters can be added in plasmids it is possible to select transfected cells from non-transfected cells and to create stable cell lines. shRNAs are expressed from pol III promoters and require a precise transcription start site as well as a 3' termination signal (TTTTT). shRNAs also lack the polyadenylation signal and the 5'-cap (Brummelkamp et al., 2002). The main disadvantage of shRNAs is that Pol III-based expression systems that are used to express shRNAs cannot be applied in a tissue-specific manner due to the lack of tissue-specific Pol III promoters. The only alternative is to use a lox P system producing a functional Pol III promoter in a tissue-specific manner. shRNAs can be ineffective inhibitors of target mRNA when expressed from single copy vector hence multiple copies of a vector should be present in cells to get reliable knockdown.

### 1.3.3.3. shRNAmirs

shRNAmirs are actually shRNAs in a micro RNA context. These artificial pri-miRNAs (i.e. shRNAmirs) and endogenous pri-miRNAs undergo the same processing steps but result in the production of siRNAs and miRNAs respectively (Figure 1.9 & 1.10c). shRNAmirs are expressed from a RNA pol III promoter or a RNA pol II promoter. The shRNAmirs transcribed from either a Pol II or a Pol III promoter fold back to form a dsRNA hairpin molecule that is referred to as the primary polyadenylated miRNA structure (pri-miRNA). Drosha, a nuclear enzyme, cleaves the base of the hairpin to form the miRNA precursor pre-miRNA of ~70–90 nucleotides with a 2-nucleotide 3' overhang. This pre-miRNA molecule is actively transported from the nucleus to the cytoplasm by Exportin-5, a carrier protein. The Dicer enzyme then cuts 20–25 nucleotides from the base of the hairpin to release the mature miRNA. The artificial target sequence in the shRNAmir is incorporated into the RISC as a siRNA to cause target knockdown. shRNAmirs or artificial

pri-miRNAs not only induce an exceptionally potent RNAi response but also allow regulated RNAi when using Pol II–dependent promoters to drive pri-miRNA expression (Silva et al. , 2005, Dickins et al. , 2005). Both shRNAs and shRNAmirs are designed in a plasmid backbone and can be transfected or packaged into a virus and transduced into target cells. Retroviral or lentiviral transduction results in the stable integration and expression of shRNA or shRNA-mir in the target cell.

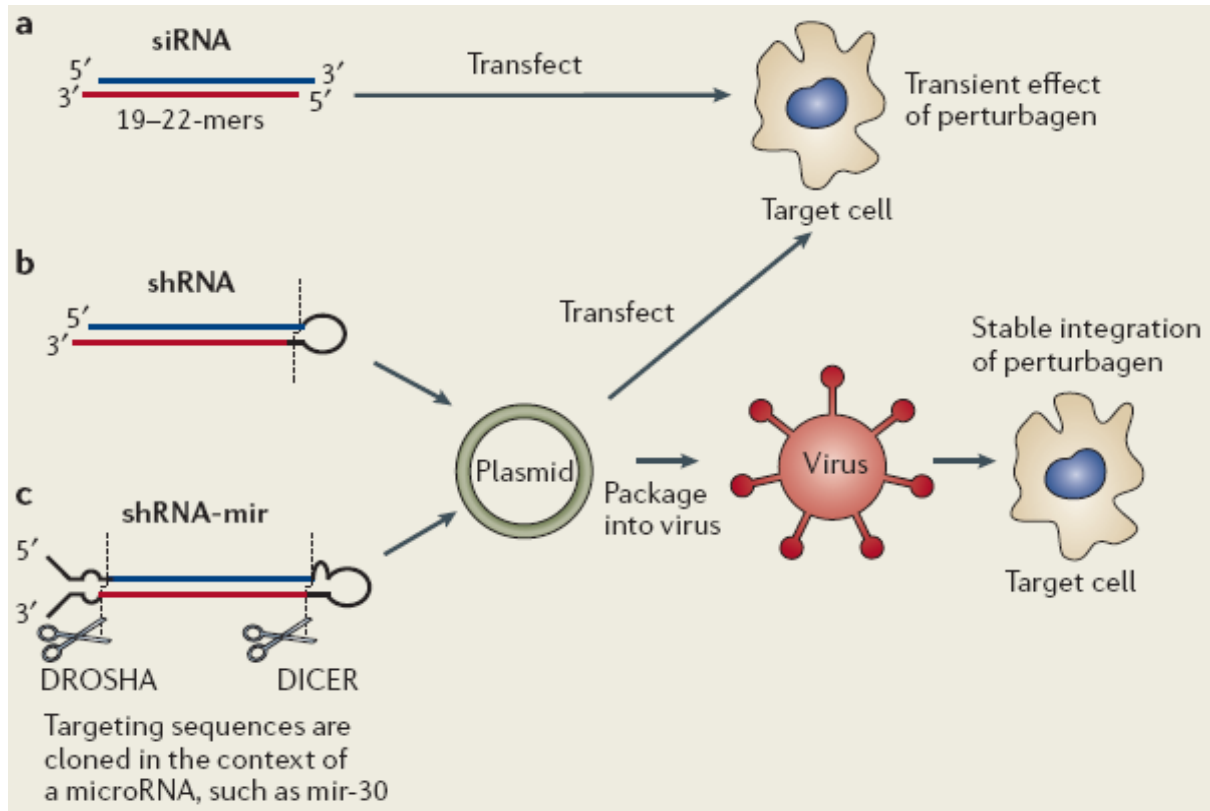


**Figure 1.10. The silencing triggers of RNAi.** (a) siRNAs 19-22 bp dsRNAs are transfected to get a transient effect (phenotype) in target cells. (b) shRNAs which are transcribed from plasmid DNA under the control of a Pol III promoter as single strand RNA molecules and fold back in vivo to give shRNAs which are recognized and cleaved by Dicer to give functional siRNAs. (c) shRNAmirs, which are shRNAs expressed in the context of miRNAs are cleaved first by Drosha and then by Dicer to give functional siRNAs. Both shRNAs and shRNAmirs are expressed from plasmids and can be transfected or packaged into viruses and transduced to target cells, in later case producing stable knockdown. Figure adapted from (Moffat et al., 2006).

### 1.3.4. Designing effective and specific siRNAs

Not all siRNAs complementary to a cognate mRNA are functional. They usually show a spectrum of potency, and only a fraction of them are highly effective. Small positional shifts along the length of target mRNA, were shown to be sufficient to alter siRNA function in an

unpredictable manner (Reynolds et al., 2004). Moreover siRNAs may nonspecifically target unrelated genes with only partial sequence-complementarity (off-target effects) (Birmingham et al., 2006; Jackson et al., 2006; Anderson et al., 2008). Hence it is critical to identify effective and specific siRNA sequences to perform reliable gene-knockdown experiments. Initially empirical rules had been proposed for siRNA selection based on some of the first identified functional siRNAs (Elbashir et al., 2001a). However these rules did not ensure that each selected siRNA will be functional. The evolving understanding of RNAi biochemistry and endogenous miRNA function coupled with statistical analyses of libraries of siRNAs with experimentally determined efficiency, lead to computer based approaches that increased likelihood of identifying effective and specific siRNAs (Pei et al., 2006). However these rules are not perfect, firstly not every selected siRNA meets the desired thresholds of potency and specificity, so experimental proof of down-regulation and evaluation of potential off-target effects is necessary. A second important point is that a substantial fraction of functional siRNAs might have been dismissed based on the parameters chosen by the algorithm for selecting siRNAs (Pei et al., 2006).

Several siRNA sequence selection algorithms have been developed in recent years that rely on the intrinsic sequence and stability features of functional siRNAs also known as 'Rational design principles'. The crucial observation that RISC contains only one of the two strands of siRNA duplex and the antisense strand must be preferentially loaded into RISC to target the sense mRNA meant functional siRNAs and miRNAs exhibit strand bias (Khvorova et al., 2003). The same finding emerges from sequence analysis of miRNA precursors and largely explains the asymmetric accumulation of the majority of miRNAs. The asymmetry is determined by the different sequence composition, and the consequent differences in thermodynamic stability and molecular dynamic behavior of the two base-paired ends of an siRNA duplex: the strand with the less stable 5' end, owing to either weaker base-pairing or introduction of mismatches, is favorably or exclusively loaded into RISC (Khvorova et al., 2003)The asymmetry rule has been implemented in many siRNA design algorithms by computing either the A+U base pair content or local free energy at both ends of an siRNA, followed by selection of the duplexes with less stable, (A+U)-enriched 5' end on the guide strand.

Most of the functional siRNAs had a low-to-medium G+C content ranging between 30% and 52% (Reynolds et al., 2004). It has been argued that too low G+C content may destabilize siRNA duplexes and reduce the affinity for target mRNA binding, whereas too high G+C content may

impede RISC loading and/or cleavage-product release (Pei et al., 2006). Additionally, surveys of functional siRNAs revealed that stable duplexes devoid of internal repeats or palindromes (which might form intra-strand secondary structures) were better silencers (Patzel et al., 2005; Reynolds et al., 2004). Although the overall duplex stability is important, the center of the duplex (positions 9–14 on the guide strand) appears to preferentially have low internal stability (Khvorova et al., 2003). It has recently been noticed that miRNAs and siRNAs assemble into RISC by different mechanisms; siRNAs require cleavage of the passenger strand for effective RISC assembly, whereas a mismatched RNase III–processed miRNA duplex does not require passenger strand cleavage (Matranga et al., 2005).

#### 1.3.4.1. Target accessibility

The local secondary structures (short stem-loops) in target mRNAs might restrict the accessibility of RISC, and attenuate or abolish siRNA efficacy. A major obstacle in assessing target-accessibility is the lack of tools that reliably predict mRNA secondary structure (Pei et al., 2006). Several algorithms that filter the siRNAs based on local secondary structure of target mRNA have shown improved selection of functional siRNAs (Heale et al., 2005).

#### 1.3.4.2. Sequence characteristics

Several sequence analyses of siRNAs have independently identified single nucleotide positional preferences, which are summarized using the guide strand as reference (Reynolds et al., 2004) (Figure 1.11): (i) U or A at position 1; (ii) C or G (C is more common) at position 19; (iii) A+U richness between positions 1 and 7; (iv) A or U (A is more common) at position 10; The first three sequence features correlate with the rule of thermodynamic asymmetry, and the preferred nucleotides on indicated positions may contribute to the bias for selection of the antisense strand. The A or U at position 10 is at the cleavage site and may promote catalytic RISC-mediated passenger strand and substrate cleavage. Other sequence determinants may be involved in steps along the RNAi pathway, such as RISC loading (Pei et al., 2006).

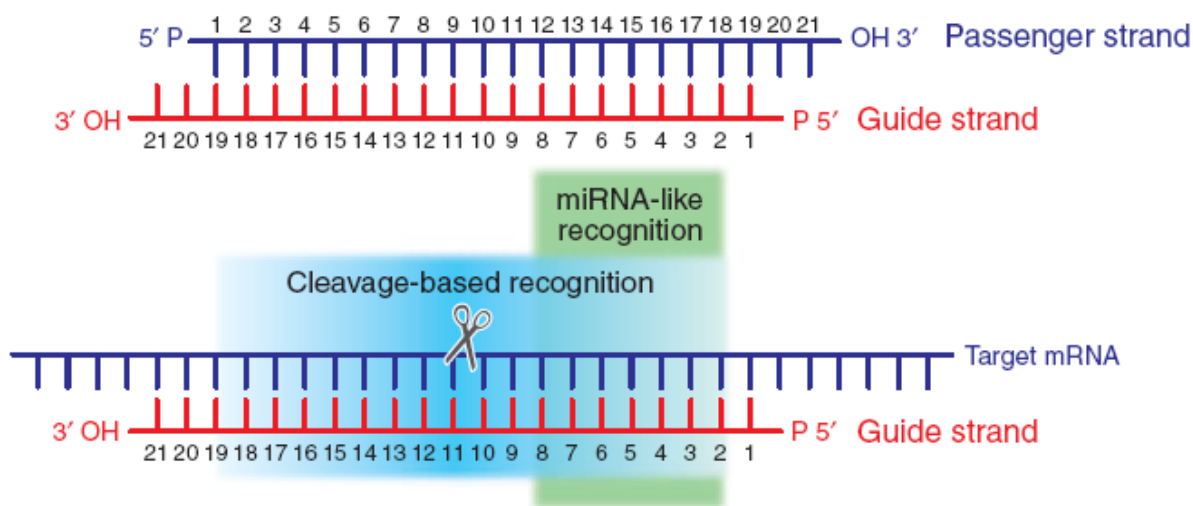


**Figure 1.11. siRNA and target mRNA structures.** (a) Standard siRNA duplex. (b) Target mRNA specificity. The cleavage site is indicated by scissors in the target mRNA. Target recognition and off-target activity can occur in two modes, the catalytic siRNA-guided cleavage reaction requiring extensive complementarity in the region surrounding the cleavage site (blue) and the miRNA-like destabilization of mRNAs requiring pairing of the siRNA 5' end (green). Figure adapted from (Pei et al., 2006).

### 1.3.4.3. Specificity

Each strand of a siRNA duplex, once assembled into RISC, can guide recognition of fully and partially complementary target mRNAs, referred to as on- and off-targets, respectively. Off-target effects arising due to sense strand loading in RISC can be avoided by following asymmetry rules and biasing antisense strand to load in RISC complex. Off-target effects arising from anti sense strand loading in RISC can be mainly classified into two classes, (i) those that share contiguous and centrally located sequence complementarity over more than half of the siRNA sequence somewhere within the mRNA sequence, and (ii) those that show solely 6 or 7 nucleotides of perfect match preferentially in the 3' UTRs with positions 2–7 or 2–8 (seed region) of the guide siRNA (Anderson et al., 2008; Birmingham et al., 2006; Jackson et al., 2006b). The latter interaction is the major driving force behind endogenous miRNA–target mRNA recognition. Although the off-targets of the latter class are predominant, their actual number identified in microarray analyses was significantly smaller than the number of computationally predicted targets with sequence complementary to the seed region of the guide strand, suggesting that additional specificity determinants remain to be identified (Birmingham et al., 2006; Jackson et al., 2006b). Furthermore, structural and biochemical studies showed that guide-strand position 1

and the nucleotides at the 3' overhang (positions 20 and 21) have little, if any, contribution to the specificity of target recognition, and that mismatches near the 5' and 3' ends can be tolerated for RISC-guided cleavage if the remaining pairing to the target was unperturbed. To enforce specificity, the current strategy is to select siRNAs in which the strand(s) entering RISC has some mismatches to all undesired target mRNAs, especially their 3'UTRs. Typically at least three mismatches are recommended between positions 2 and 19 and the mismatches near the 5' end and in the center of the examined strand should be assigned higher significance (Elbashir et al., 2001b; Holen et al., 2005; Jackson et al., 2003; Lin et al., 2005).

### 1.3.5. In vivo RNAi and generation of transgenic animals

RNAi has also been successfully used to create animal models of gene inactivation in mice (Singer et al., 2006; Tiscornia et al., 2003). In many cases knockdown mice generated by RNAi have displayed phenotypes similar to a conventional knockout mice (Xia et al., 2006). RNAi has also demonstrated its utility in many species where a conventional knock out is not feasible, for example knockdown in the rat model was achieved whereas a conventional knock out in rats was not possible due to the non-availability of suitable ES cells. Furthermore knockdown mice could be created even in situations where a conventional knockout produced embryonic lethality thereby allowing the researchers to study those essential genes and their role in development. The ability of RNAi to create graded hypomorphic alleles combined with the conditional knockdown systems allows greater flexibility in deciphering gene function (Dickins et al., 2005; Dickins et al., 2007; Szulc et al., 2006; Ventura et al., 2004).

In vivo RNAi can be achieved in many ways. Systemic RNAi is usually achieved by hydrodynamic tail vein injection, in which a saline solution containing siRNA or the shRNA vector is rapidly introduced into the blood stream of the animal. This method is particularly suitable to target highly perfused organs such as liver. The main disadvantage however, is the physiological shock and cardiac arrest associated with injecting large volumes of solutions rapidly. In recent years, it has been shown that intravenously administered, cholesterol-conjugated siRNAs targeting apolipoprotein B, a protein implicated in the metabolism of cholesterol, significantly reduced serum lipoprotein levels. These findings and other on-going phase I clinical trials demonstrate that RNAi may soon become a relevant therapeutic tool in humans (Sandy et al., 2005).

Mouse embryonic stem cells (mES) can be electroporated with the appropriate transgene or transduced with a lentivirus-based vector (Figure 1.12.). In both cases, the resulting clones can be assayed for transgene copy number, shRNA expression, and degree of knockdown (if the gene is expressed in ES cells) before proceeding further. Selected clones are then injected into diploid blastocysts that are subsequently transferred to pseudopregnant females. The resulting chimeric mice are then bred further to obtain germ line transmission of the shRNA vector. To bypass the chimeric stage, it is possible to generate entirely ES cell-derived mice by injecting the ES cells into tetraploid blastocysts (Ventura et al., 2004) or by the tetraploid aggregation method. Standard transgenesis can also be used for introducing shRNA vectors into the germ line (Figure 1.12). In this case, a linearized DNA fragment containing the shRNA expression cassette is injected into the pronucleus of fertilized eggs that are subsequently transferred to pseudopregnant females. Finally, lentiviruses carrying shRNA expression cassettes can be directly injected into the perivitelline space of single-cell mouse embryos that are then transferred into female recipient mice (Rubinson et al., 2003; Tiscornia et al., 2003).

### 1.3.6. Conditional systems for RNAi

Conditional or inducible RNAi refers to RNAi that can be controlled externally. External control can be temporal (at specific time points) or/and spatial (in specific tissues). Conditional RNAi can also be classified into reversible and irreversible types. Reversible gene knockdown generally relies on drug controlled expression of interfering RNAs. The most popular systems are doxycycline- and ecdysone-controlled units, which take advantage of regulating molecules (drugs) that can easily be added to cells in culture or administered to animals (Wiznerowicz et al., 2006).

Irreversible gene-knockdown systems, in contrast, make use of recombinases such as Cre or Flp, which allow one-time excision of an inactivating sequence that otherwise, prevents the expression of an interfering RNA. Alternatively, the RNAi-producing unit itself can be excised to stop its activity. In both cases, once excision is completed, the system cannot be switched back to its original state; hence the knockdown is permanently established or abrogated. The main field of application of this technique is the generation of conditional-knockdown animals (Wiznerowicz et al., 2006). External control of down-regulation of a gene is a desirable feature in many situations. It allows parallel analysis of the 'off' and 'on' states of a gene. Inducible knockdown

also allows researchers to examine the function of genes essential during development in differentiated tissues of transgenic animals. Conditional knockdown is also useful for modeling human pathologies *in vivo* i.e. to induce and revert at will the shutoff of a disease-influencing gene, for example an oncogene or a tumor suppressor gene (Wiznerowicz et al., 2006).

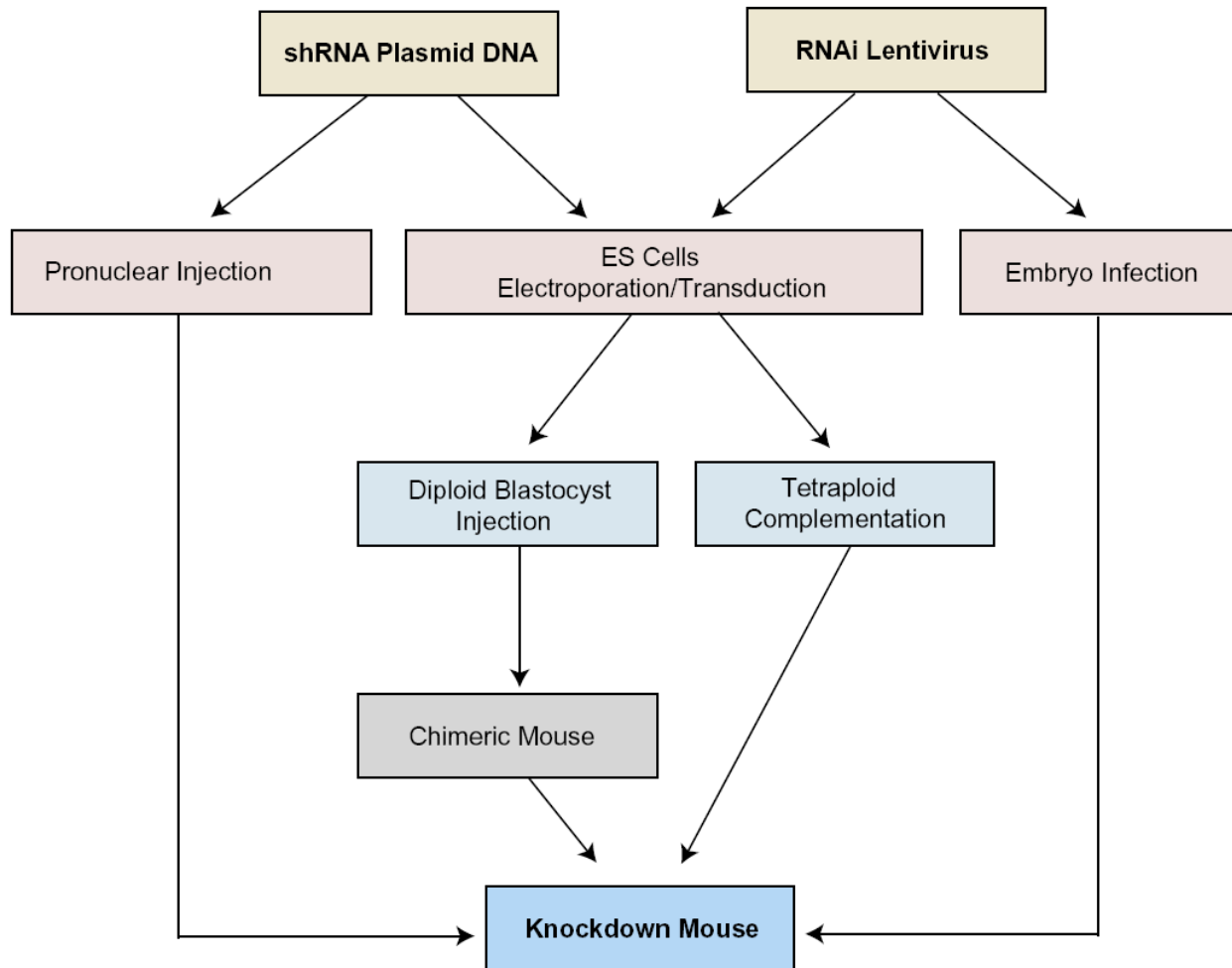


**Figure 1.12. Generation of knockdown mice by various transgenic approaches.** The fastest method is infection of single-cell embryos with high-titer lentiviruses. The advantage of using embryonic stem (ES) cells is that copy number and expression of the integrated short hairpin RNA (shRNA) can be monitored before blastocyst injection. Figure adapted from (Sandy et al., 2005).

### 1.3.6.1. Reversible knockdown systems based on Pol III promoter

The drug mediated control of Pol III promoters has been achieved by (i) steric hindrance, (ii) transactivation and (iii) epigenetic repression.

#### 1.3.6.1.1. Steric hindrance

Repression of a shRNA driven by a Pol III promoter can be achieved by placing an *Escherichia coli* Tet operator (TetO) sequence just upstream of the transcription start site to interfere with the function of the TATA box through recruitment of the tetracycline repressor (tetR). In the absence of a drug, tetR binds to TetO, and production of shRNA is suppressed (Chen et al., 2003; Hoeflich et al., 2006; Ohkawa et al., 2000; van de Wetering et al., 2003). Upon addition of tetracycline or doxycycline, repression is relieved by sequestration of tetR.

One major pitfall of this system is the weakening of the pol III promoter strength after TetO insertion, which leads to suboptimal levels of shRNA production and hence of target-gene knockdown (Berns et al., 2004). Moreover, steric hindrance does not guarantee complete repression, and this usually results in leaky shRNA repression in the non-induced state (Ohkawa et al., 2000).

#### 1.3.6.1.2. Transactivation

An ecdysone-inducible, retroviral vector-based system for transactivation of pol III promoters has been described (Gupta et al., 2004). It relies on the conditional expression of an engineered pol III transactivator, which in turn induces transcription of a shRNA from a modified U6 promoter. Using this system, tight and reversible regulation of *TP53* was achieved in tissue culture. But such multi-component design is prohibitively complex for broad applications.

#### 1.3.6.1.3. Epigenetic repression

The Krüppel-associated box (KRAB) domain found in many zinc-finger proteins can silence both pol II and pol III promoters by triggering heterochromatin formation. When tethered to specific DNA regions within the context of chimeric proteins, KRAB can induce a general silencing of transcription within up to 3 kilo bases (kb) from its binding site. When KRAB is fused to the tetR DNA binding domain, the resulting tTRKRAB chimeric protein allows for the doxycycline-mediated control of any promoter placed nearby tetO sequences, in either 'tet-on' or 'tet-off' configurations depending on the tetR version used. The researchers at Ecole Polytechnique, Lausanne, Switzerland had used tTRKRAB based system to regulate the expression of a shRNA delivered via a lentiviral vector first in a multi vector system (Wiznerowicz et al., 2003) and later

in a single vector system (Szulc et al., 2006) to achieve reversible knockdown of a gene both in vitro and in vivo with a high degree of efficiency and without substantial leakiness.

## 2. Aim of the thesis

---

Previous work in our laboratory has identified Xin as a specific interaction partner of filamin C domain 20. Since filamin C domains 19-21 (including the domain 20) localized to Z-disks upon transient transfections in muscle cells, our group became interested in elucidating the role of Xin in striated muscles. Xin was initially described by the group of Jim Lin at the University of Iowa, as a protein that plays a major role in cardiac morphogenesis in chick embryos (Wang et al., 1999). Based on these observations, the ablation of the *Xin* in mice was predicted to have similar effects on heart development. Instead, mice lacking Xin were found to be fully viable and displayed only mild hypertrophic response (Gustafson-Wagner et al., 2007; Otten et al., 2010) and changes in the localization of the ICDs (Otten et al., 2010).

In contrast to the Xin knockout mice developed in our laboratory, the one from Jim Lin group was observed to upregulate *Xirp2*, the homologous gene of Xin. (Gustafson-Wagner et al., 2007). Accordingly the authors mooted a hypothesis that, the milder phenotype observed in mice is due to an upregulation of *Xirp2* which is argued to be complementing the function of Xin.

In two recent reports of *Xirp2* knockouts (*Xirp2* hypomorphic mice of Mc Calmon et al and *mXinβ* knockout of Qinchuan Wang et al) varying degree of severity in cardiac phenotype was displayed. These reports did not describe the skeletal muscle phenotype.

In the light of these observations, this work aimed at the characterization of the expression of *Xirp2* and Xin during muscle cell differentiation at the RNA and protein level and their localization in differentiating skeletal muscle cells. To fully understand the role of *Xirp2*, a functional knockdown of the gene via lentiviral mediated RNA interference (RNAi) strategy was attempted in various cell models including primary *Xin*<sup>-/-</sup> myoblasts. A further goal was the development of a novel versatile lentiviral vector system with different modules that would enable simultaneous and / or controlled expression of shRNAs and transgene components. Phenotypes resulting from the depletion of Xin and *Xirp2* were also studied in various cell models. Possible compensatory mechanisms in the absence of either of the proteins were also tested.

## 3. Materials & Methods

---

### 3.1. Materials

Laboratory chemicals and materials used in this work were purchased from standard suppliers like Carl Roth (Karlsruhe, Germany), Bio-Rad (Munich, Germany), and Sigma (Taufkirchen, Germany) unless stated otherwise. All the restriction enzymes, DNA modifying enzymes and polymerases etc. were obtained from Fermentas (St. Leon-Roth). Primers and oligo-nucleotides were ordered from TIB-Mol bio (Berlin). Cell culture media and fetal calf serum (FCS) were purchased from Gibco (Invitrogen). Lentiviral plasmids were obtained from Addgene (Cambridge, MA, USA) and Open Bio systems and their distributor Bio cat GmbH in Germany. For plasmid DNA isolation, endogen free plasmid DNA purification (Maxi, Midi, Mini) kits from Qiagen (Hilden) or Machery Nagel were used. Gel extraction kits were either from Promega or Qiagen. For RNA isolation, RNeasy mini kits and QIAshredder from Qiagen and for total RNA isolation TRIZOL reagent from Invitrogen were used. All the solutions and buffers were prepared with Milli Q (Millipore) quality water and where necessary solutions were autoclaved or sterile filtered before use. Whatman blotting paper was from 3M Corporation. Nitrocellulose blotting membranes were from Schleicher-Schuell. Cell culture consumables like Petri dishes, tissue culture flasks and multi-well plates were purchased from TPP or Nunc.

### 3.2. Apparatus

**Table 3.1. Apparatus**

<b>Apparatus</b>	<b>Name</b>	<b>Company</b>
PCR Thermo cycler	T 3000 Thermo cycler	Biometra
Table top centrifuge	Biofuge pico	Heraeus
Table top cool centrifuge	Biofuge fresco	Heraeus
Centrifuge I	Allegra X-15R, Rotor SX4750A	Beckman Coulter
Centrifuge II	Avanti J-25, Rotor JA 10	Beckman Coulter
Ultracentrifuge	Optima L-80XP	Beckman Coulter
Swinging bucket rotor	SW 40 rotor	Beckman Coulter

Centrifuge tubes for SW40 rotor	Ultra Clear tubes 14x95mm	Beckman Coulter
Falcon centrifuge	-	Heraeus
Protein electrophoresis	Mini-Protean II System	Bio-Rad
Protein transfer	Trans-Blot Transfer Cell Trans-Blot SD Semi-Dry Transfer Cell	Bio-Rad Bio-Rad
Agarose electrophoresis	-	PEQLAB
Bacterial culture shaker	Certomat BS-I	Sartorius
UV Trans illuminator	-	Schütt Labortechnik
UV-Vis spectrophotometer	Cary 50 scan	Varian
ELISA plate reader	-	Biotek
Microtome	Leica CM3050S	Leica
Confocal laser scanning microscope	LSM 510	Zeiss
Live cell imaging	Nikon Eclipse TE 2000E	Nikon
Fluorescence microscope	Axiophot	Zeiss
Cell culture microscope (Inverted)	Nikon Eclipse TS 100	Nikon
Autoclave	Systec 5075 ELVC	Systec
FACS	FACSDiva	BD biosciences
Cell strainers 40µm	-	BD biosciences
Dark room photographic film developer	Curix 60	AGFA
Infrared Imager	Odyssey Infra red imager	LI-COR
See-Saw Rocker	-	Stuart
Millipore water	Milli-Q UF plus	Millipore
Pipettes	-	Abimed
CO <sub>2</sub> Incubator		Thermo Fischer Scientific

<ul style="list-style-type: none"> <li>• Software</li> </ul>	<ul style="list-style-type: none"> <li>• ImageJ</li> <li>• LSM Image browser 4.0</li> <li>• Adobe Photoshop CS3</li> <li>• Adobe Illustrator CS3</li> <li>• NISElements 2.0</li> <li>• EndNote 6.0</li> <li>• BLAST</li> <li>• BioEdit</li> <li>• Vector NTI 10.0</li> <li>• Quantity One for GelDoc</li> </ul>	<ul style="list-style-type: none"> <li>• Public domain free software</li> <li>• Carl Zeiss</li> <li>• Adobe Systems</li> <li>• Adobe Systems</li> <li>• Nikon</li> <li>• EndNote</li> <li>• PubMed</li> <li>• BioEdit</li> <li>• Invitrogen</li> <li>• Bio-Rad</li> </ul>
--	---	---

### 3.3. Bacterial strains

**Table 3.2. Bacterial strains**

<b>Strain</b>	<b>Genotype</b>	<b>Purpose</b>
E. coli JM 109	e14-(McrA-) recA1 endA1 gyrA96 thi-1 hsdR17(r-k m+k) supE44 relA1(lacproAB) [F' traD36 proAB lacIqZ M15]	DNA cloning and plasmid propagation
E. coli DH5 $\alpha$	F- endA1 hsdR17(rK-mK+) supE44 thi-1 recA1 gyrA (NalR) relA1 D(lacIZYA-argF)U169 deoR (F80dlacD(lacZ)M15)	DNA cloning and plasmid propagation especially for lentiviral plasmids
E. coli SCS 110	rpsL (Strr) thr leu endA thi-1 lacY galK galT aratonA tsx dam dcm supE44D (lac-proAB) [F' traD36 proAB lacIqZ $\Delta$ M15]	Dam <sup>-</sup> host
BL21(DE3) Codon Plus (DE3)-RP, Stratagene (Heidelberg)	B F- ompT hsdS(r-B m-B) dcm+ Tetr gal (DE3) endA Hte [argU proL Camr]	Protein expression

### 3.4. Plasmids

**Table 3.3. Plasmids**

<b>Plasmid</b>	<b>Purpose</b>	<b>Remarks</b>
pETW2	Vector for protein expression	Contains both T7 and His tags
pETW1	Vector for protein expression	Contains both EEF and His tags
pMypG	Eukaryotic expression Myomesin promoter, EGFP tag	modified pCAT3-Enhancer (Promega) (Pacholsky et al., 2004)
pMypG $\Delta$ XhoI	Used as an intermediate plasmid for transferring miRNA to lentivector mpLVTHM	Deleted XhoI site from pMypG (Made in this work)
pLVTHM	Lentivector, EF 1 $\alpha$ promoter (Pol II) drives GFP and H1 promoter (Pol III) drives shRNA expression	(Szulc et al., 2006) and Addgene website
pLVTHM-mir	For shRNAmir expression from H1 promoter	Constructed from pLVTHM backbone (made in this work)
pLVTU6+1	For shRNA expression from U6 promoter	Constructed from pLVTHM backbone (made in this work)
pLVTU6-mir	For shRNAmir expression from U6 promoter.	Constructed from pLVTHM backbone (made in this work)
pLVmir	An intermediate plasmid for shRNAmir expression from a Pol II promoter like CAG or EF1 $\alpha$ .	Constructed from pLVCT-tTRKRAB and pGIPZ (made in this work)
pLVET- tTRKRAB	EF1 $\alpha$ promoter drives GFP, used for conditional expression	(Szulc et al., 2006) and Addgene website
pLVCT- tTRKRAB	CAG promoter drives GFP, used for conditional expression	(Szulc et al., 2006) and Addgene website
pLVET-mir	Constitutive knockdown from EF1 $\alpha$ (Pol II) promoter	Obtained by adding module I from pLVTHM to pLVmir
pLVET- tTRKRABmir	Conditional knockdown from EF1 $\alpha$ (Pol II) promoter	Obtained by adding module I from pLVET-tTRKRAB to pLVmir
pLVET-GOI-	Conditional gene expression	Obtained by cloning GOI-GFP in place

GFP-tTRKRAB		of GFP in pLVET-tTRKRAB
pLVET-GOI-GFP (GOI = Gene of interest)	Constitutive gene expression	Obtained by and deleting the tTRKRAB module from the above vector (by digesting with EcoRI and self-ligating larger fragment)

## 3.5. Antibodies

### 3.5.1. Primary antibodies

**Table 3.4. Primary antibodies**

Name	Epitope	Classification	Purpose	Reference
a653	$\alpha$ -actinin	Rabbit polyclonal	WB,IF	(van der Ven et al., 2000)
T12	Titin	Mouse IgG1	IF	(Fürst et al., 1988)
BB78	Myomesin	Mouse IgG 2a	IF	
RR90	Filamin A+C	Mouse IgA	IF	(van der Ven et al., 2000)
XR1B	Xin	Mouse IgG1	WB,IF	(van der Ven et al., 2006)
mAbXIRP2	hXIRP2	Mouse IgG1	WB,IF	
antiPR2-6	hXIRP2	Rabbit polyclonal	WB,IF	
antiX2HN	hXIRP2	Rabbit polyclonal	WB,IF	
antiZF20a	Zf XIRP2	Rabbit polyclonal	WB,IF	
antiGFP	GFP	Mouse monoclonal	WB,IF	Roche, Mannheim, Germany
antiGAPDH	GAPDH	Mouse monoclonal	WB	Calbiochem, Darmstadt, Germany
antiActin	Actin	Rabbit polyclonal	WB,IF	

### 3.5.2. Secondary antibodies

**Table 3.5. Secondary antibodies**

Name	Donor	Against	Conjugate	Supplier
GAMPO	Goat	Mouse	HRPO	Dianova
GARPO	Goat	Rabbit	HRPO	Dianova
GAM IRDye 800	Goat	Mouse	IR Dye 800	Rockland Immunochemicals, Gilbertsville, USA
GAR IRDye 800	Goat	Rabbit	IR Dye 800	Rockland Immunochemicals, Gilbertsville, USA
GAM IgG1-TXR	Goat	Mouse	TXR	Southern Biotech
GAM IgG2a-FITC	Goat	Mouse	FITC	Southern Biotech
GAM IgA-TXR	Goat	Mouse	TXR	Southern Biotech
GAM Cy3	Goat	Mouse	Cy3	Dianova
GAM Cy5	Goat	Mouse	Cy5	Dianova
GAR Cy2	Goat	Rabbit	Cy2	Dianova
GAR Cy5	Goat	Rabbit	Cy5	Dianova

## 3.6. Molecular Biology Methods

### 3.6.1. Culture media

All media and buffers were prepared essentially as described in Sambrook et al., 1989. The media were prepared with de-ionized water that was filtered through an ion-exchange unit (Millipore). Culture media were sterilized by autoclaving at 121°C. For making agar plates, 15g agar (1.5 % w/v) was added to 1 liter of LB medium before autoclaving.

**Table 3.6. Media for Molecular Biology**

Medium	Composition
LB medium	10 g Tryptone, 5 g yeast extract, 10 g NaCl per Liter, pH 7.5
SOB medium	20.g Tryptone, 5g yeast extract, 0.59g NaCl, 0.19g KCl per Liter, pH 7.0
SOC medium	5 mM MgCl <sub>2</sub> , 5 mM MgSO <sub>4</sub> , 20 mM Glucose in SOB- Medium
PBS	0.14 M NaCl, 3 mM KCl, 2 mM K <sub>2</sub> HPO <sub>4</sub> , 10 mM Na <sub>2</sub> HPO <sub>4</sub> , pH 7.4

TBS	50 mM Tris/HCl, 150 mM NaCl, 0.05 %, pH 7.9
TBST (Tween-20)	50 mM Tris/HCl, 150 mM NaCl, 0.05 % Tween-20, pH 7.9
TBST (Triton X-100)	300.µl of 20% Triton X-100 in 1 liter of TBS (Odyssey washing buffer)

---

### 3.6.2. Antibiotics for molecular biology

The following antibiotics were used in indicated concentrations for all bacterial cultures meant for plasmid propagation and bacterial expression of proteins. LB-agar antibiotic selection plates meant for transformation purposes were prepared by adding antibiotics at indicated concentrations after cooling LB-agar media to 45°C.

**Table 3.7. Antibiotics for Molecular Biology**

Antibiotic	End concentration
Carbenicillin	100µg/ml
Chloramphenicol	34µg/ml
Kanamycin	50µg/ml

### 3.6.3. Preparation of chemical competent cells

Glycerol stocks of E. coli strains JM109 and DH5α containing 30 % glycerol (v/v) were stored -80°C. For each type of competent cells to be prepared 3 ml of LB medium is freshly inoculated with desired bacteria from glycerol stocks. Cultures were shaken continuously (250rpm, 37°C) overnight. 5 µl of this culture were subsequently used to inoculate 50 ml of fresh LB medium and grown at 18° C for 3-4 days until an OD of 0.9 was reached. This culture was pelleted and washed with ice cold water and subsequently incubated on ice cold HD buffer (shown below). The final suspension was snap frozen in 200 µl portions in liquid nitrogen and stored at -80°C.

K-MES buffer: 0.5 M MES pH 6.3 adjusted with KOH and autoclaved/ filtered sterile.

HD buffer: (10 %) glycerol 49.0 ml, 1.0 ml K-MES (0.5 M; pH 6.3), CaCl<sub>2</sub> and MnCl<sub>2</sub>

## 3.7. Established Cell lines and Primary cultures

**Table 3.8. Established Cell lines and Primary cultures**

Name	Cell type	From	Reference
HSKM,	Human skeletal muscle cell line	Human skeletal muscle	(van der Ven et al., 1993)
C2 C12	Myoblast cell line	Established cell line of satellite cells from the thigh muscle of C3H mouse	(Yaffe and Saxel, 1977)
H-2K <sup>b</sup> -tsA58	Mouse skeletal muscle cells	Cells derived from H-2Kb-ts A58b-tsA58 mice	(Morgan et al., 1994)
Primary cells	Satellite cells	Mouse diaphragm	protocol Ulrich Becher
PtK2	Epithelial cells	Male Rat Kangaroo kidney	ECACC# CB2059
HEK 293 (AD293)	Epithelial cells	Human embryonic kidney	Stratagene
HEK293T	HEK293 stably expressing a large T antigen	Transformed human embryonic kidney 293 cells	ATCC CRL-11268
3T3	Fibroblast cells	Albino Swiss mouse embryo	(Todaro et al., 1963)

## 3.8. Lentivirus methods

### 3.8.1. Transient transfection method for production of lentiviruses

All the recombinant lentiviruses used in this work were generated using transient transfection of HEK293T cells (kindly provided by Prof. A. Pfeifer; University of Bonn) as previously described (Szulc et al., 2006). The human embryonic kidney 293T (ATCC CRL-11268) cells were cultured in 10 cm and 15cm tissue culture dishes with proliferation medium containing DMEM plus Glutamax, supplemented with 10% fetal calf serum (FCS) and 2 mM sodium pyruvate (all from Invitrogen, Germany) at 37°C and 5% CO<sub>2</sub>. Cells were regularly split before reaching confluence,

usually at 1: 6 to 1:10 ratio. For transfection, either  $2 \times 10^6$  cells per a 10 cm plate or  $5 \times 10^6$  cells per a 15 cm plate were plated a day before transfection. Next day, the cells were transfected with 20 $\mu$ g of the transfer vector, 15 $\mu$ g of the packaging vector (psPAX2) and 6 $\mu$ g of the envelope plasmid vector (pMD2G) per one 10 cm plate using calcium phosphate transfection. For transfection of cells in a 15 cm plate double the amounts of the respective vectors were used. A typical lentivirus production consisted of two to six 15 cm plates.

**Table 3.9. Transient transfection method for production of lentiviruses**

	10 cm plate	15 cm plate
Cell number	$2 \times 10^6$	$5 \times 10^6$
Transfer plasmid	20 $\mu$ g	40 $\mu$ g
Packaging plasmid, psPAX2	15 $\mu$ g	30 $\mu$ g
Envelope plasmid, pMD2G	6 $\mu$ g	12 $\mu$ g
Sterile water	500 $\mu$ l	1000 $\mu$ l
2.5M CaCl <sub>2</sub> solution	50 $\mu$ l	100 $\mu$ l
Added drop-wise		
2X HBSS (HEPES buffered saline solution)	500 $\mu$ l	1000 $\mu$ l

The CaPO<sub>4</sub> mixture was mixed thoroughly and immediately dispensed into the tissue culture dishes drop-wise with a gentle rocking of the plates. The medium was changed 6-10 hours later. The medium containing the lentiviral particles was harvested 36-48 hours later, removed of cellular debris by centrifugation (2000 rpm, for 5 minutes) and filtration through 0.2  $\mu$ m sterile filter units (Schleicher-Schuell). Filtered medium containing lentiviral particles can be aliquoted and stored at -70°C in unconcentrated form. Alternatively media containing lentiviral particles was purified and concentrated (about 100 times) by ultracentrifugation in SW40 rotor at 26,000 rpm for 2hours and resuspending invisible viral pellet in 50-100  $\mu$ l PBS.

### 3.8.2. Lentiviral titer determination

The functional titer of GFP-carrying lentivectors was estimated by infecting HEK293T cells with limiting virus dilutions and quantification of GFP-positive cells by FACS after 5 days. Briefly, the day before transduction 30,000 HEK293T cells per well of a 24 well plate were plated in 1 ml

medium. Next day cells in one well were counted using a hemocytometer (cell number usually ranged between 60,000 - 80,000) and transduced with six 4-fold serial dilutions in 250 $\mu$ l total volume. 50 $\mu$ l of unconcentrated or 1 $\mu$ l of concentrated virus prep served as starting dilution. Three days after transduction, 1ml of fresh medium was added, and 2 days later cells were detached from the bottom of the wells and analyzed for GFP fluorescence by FACS. When 5-10 % of the cells were GFP-positive, the fluorescence intensity values were in linear range. Values from linear range were used for titer estimation. Titer is defined by the number (percentage) of cells transduced by a given volume and counted on day 2, e.g. if 1 $\mu$ l gives 10% of GFP-positive cells and if we had 50,000 cells on day 2, the titer is (50,000 \* 10%) or 5,000TU/ $\mu$ l =  $5 \cdot 10^6$  TU/ml. (TU = transduction units, each transduction unit represents one functional lentiviral particle).

### 3.8.3. Lentiviral transductions

#### 3.8.3.1. Immortalized mouse myoblast culture- H-2K<sup>b</sup>-tsA58 cells

Myoblasts isolated from male homozygous H-2K<sup>b</sup>-tsA58 (immorto) mice were grown under permissive conditions at a temperature of 33°C in proliferation medium (see below) containing interferon- $\gamma$  (IFN-  $\gamma$ , tebu-bio, Offenbach) as previously described (Morgan et al., 1994). Proliferating cells were split upon reaching 60-70 % confluence in collagen- (10 $\mu$ g/ml PBS) or Matrigel<sup>TM</sup> coated (1:100 dilution in DMEM) petri dishes for up to 20 passages. At approximately 30-40 % confluence cells were transduced with lentiviral constructs and either expanded or induced to differentiate at 70-80 % confluence. Expanded cells were selected for GFP expression by FACS (see below). Stably selected cells were differentiated either in Matrigel<sup>TM</sup> coated petri dishes (for RNA extraction and western blots) or on Matrigel<sup>TM</sup> coated coverslips (for immunofluorescence studies).

Proliferation medium:           DMEM, 20 % fetal calf serum, 2 % L-glutamine,  
   2 % Na-Pyruvate, 1 % Penicillin/Streptomycin, 20 U/ml IFN-  $\gamma$

Differentiation medium:       DMEM, 2 % horse serum, 2 % L-glutamine, 2 % Na-Pyruvate  
   1 % Penicillin/Streptomycin

#### 3.8.3.2. C2C12 and human skeletal muscle (HSKM) cells

The myogenic cell line, C2C12 (ECACC#CB2438) and primary cultures from human skeletal muscle (HSKM) cells, were cultured as previously described (van der Ven et al., 1993).

Composition of the culture media is shown below. C2C12 and HSKM cells were seeded on 6 well or 12 well plates for lentiviral transductions. Transductions were performed at 30 % confluence at a multiplicity of infection (MOI) of 10 - 20 (i.e. 10-20 viral particles per cell). Transduced cells were selected for GFP expression by FACS, and selected cells were used for differentiation studies. Differentiation was induced by switching to differentiation media.

Proliferation medium: DMEM, 20 % fetal calf serum, 2 % L-glutamine,  
2 % Na-Pyruvate, 1 % Penicillin/Streptomycin, 0.4 % Ultrosor G,  
Differentiation medium: DMEM, 2 % horse serum, 2 % L-glutamine, 2 % Na-Pyruvate

#### 3.8.3.4. FACS-based sorting and establishment of stable cell lines

GFP-positive cells were sorted using FACSDiva (BD Biosciences), at the FACS core facility of the University of Bonn. Cells were excited with a blue laser (Enterprise II ion laser, Coherent, Santa Clara, CA, USA) with excitation wavelength of 488 nm. The power of excitation was about 80 mW. GFP-positive cells were collected with a 530/20 band pass filter where 20 stands for the width of the band pass in nm and 530 stands for the average wavelength of the band pass i.e. from 520-540 nm. The usual flow speed ranged between 100-5000 cells/sec. Data were collected with BD FACSDiva software version 5.03.

#### 3.8.3.5. Satellite cell isolation from wild type (strain SV129) and Xin knockout mice

The following protocol was employed for the purification of a population of muscle-derived cells from the diaphragm muscles of mice. The diaphragm of 6-8 weeks old SV129 wild type and Xin knockout mice was carefully excised and placed in ice-cold PBS. The diaphragm was carefully cleared of adventitious tissues and blood vessels and minced to small pieces. The minced tissue was digested for 1 hour with 750  $\mu$ l Collagenase B (1mg/ml) at 37°C and resuspended every 15 minutes. Resuspension of cells was carried out first, with blue plastic pipette tip and in later stages with yellow pipette tip; both the pipette tips were cut at the tip to avoid clogging through small diameter. Subsequently, 250  $\mu$ l of trypsin (0.05%) was added and the tissue was incubated for a further 20 minutes at 37°C and again resuspended with a blunt yellow pipette tip. The cell suspension was filtered through a 40  $\mu$ m, nylon cell strainer with 10 ml medium (IMDM, 20% FCS, 1% FCS, 1% Pen-Strep, 1% non-essential amino acids (NEAA), 0.1%  $\beta$ -mercaptoethanol

and basic fibroblast growth factor (bFGF) 5ng/ml). The cell suspension that contained a mixture of many cell types including satellite cells, fibroblasts and other debris was centrifuged and the cell pellet was resuspended in 10 ml of medium. To enrich the cell population for muscle specific cells including satellite cells, cells were pre-plated twice, for 30-45 minutes, non-attached cells were collected, counted and plated on gelatin coated glass coverslips or Matrigel<sup>TM</sup> coated petri dishes. 250,000-500,000 cells were plated in each well of a 24 well plate (for differentiation) or alternatively in a 6 cm petri dish (for proliferation). The first medium change was done after 4 days and subsequently every alternate day. For immunofluorescence studies, cells were plated directly on gelatin coated glass coverslips, transduced and were allowed to differentiate. For RNA extraction and quantification of gene knockdown cells were plated in petri dishes.

## 3.9. RNA isolation

### 3.9.1. RNeasy mini kit protocol

RNA was isolated from a monolayer of cultured cells according to the RNeasy mini kit protocol from Qiagen. Skeletal muscle cells growing on a petri dish (10 cm dish for proliferating and 6 cm dish for differentiating cells) were lysed by the addition of 1ml of RLT buffer supplemented with 10 $\mu$ l of  $\beta$ -mercaptoethanol, immediately after aspirating the culture media from the dish. Cells were scraped of the dish with a sterile rubber policeman and suspended thoroughly with a pipette until no cell clumps were visible. The lysate was applied to a QIAshredder spin column and centrifuged at maximum speed in a table top centrifuge (13,000rpm, 2 min). The flow-through was mixed with 600 $\mu$ l of 70% ethanol, applied to an RNeasy mini spin column and centrifuged at 10,000 rpm for 15 sec. The flow-through was discarded and the RNeasy mini column was transferred to a new 2 ml collection tube. The column was washed twice with 500  $\mu$ l of RPE and RNA was eluted with 30-50 $\mu$ l of RNase-free water into a new eppendorf tube.

### 3.9.2. Total RNA isolation with TRIzol<sup>®</sup> reagent

Total RNA was isolated with the TRIzol<sup>®</sup> reagent (Invitrogen, Carlsbad, CA, USA) as per the instructions of the manufacturer. Briefly, skeletal muscle cells growing on a 10 cm dish were lysed by the addition of 1ml of TRIzol<sup>®</sup> reagent immediately after removal of culture media. Cells were scraped from the dish with a sterile rubber policeman. The lysate was thoroughly suspended and incubated at room temperature for 5 min. The lysate was then centrifuged at

13000 rpm for 10 min at 4°C and the supernatant was transferred to a fresh tube. 200µl of Chloroform was added to the lysate from above step and mixed well and allowed to incubate at room temperature for 5-15 min. The lysate and Chloroform mixture was centrifuged at 13000 rpm for 10-15 min at 4°C resulting in the aqueous phase, organic phase and the interface. The aqueous phase (top colorless layer) was transferred to a fresh tube. RNA remained exclusively in the aqueous phase, whereas DNA and protein were in interphase and organic phase (lower phase). 500 µl of isopropanol was added to the aqueous phase, vortexed briefly, incubated for 5-10 min and centrifuged for 10 min at 4-25°C. The supernatant was discarded and the pellet was washed with 1ml of 70% ethanol, centrifuged at 8000 rpm for 5 min. The ethanol was removed; the RNA pellet was allowed to air dry for 5-10 min and resuspended in RNase-free water.

### 3.9.2.1. DNase I treatment of RNA to remove traces of genomic DNA

RNA isolated from proliferating and differentiating skeletal muscle cells (C2C12, H-2K<sup>b</sup>-tsA58 and C2C12 and H-2K<sup>b</sup>-tsA58 cells stably expressing lentiviral knockdown constructs) were treated with DNase I for 15-20 min in a volume of 100 µl (87.5 µl RNA solution+10µl buffer RDD+2.5µl DNase I stock solution) and purified again by column as per the instructions of the manufacturer.

### 3.9.2.2. Measuring RNA quality, integrity, purity and concentration

The quality of RNA was visualized by running on a 1% agarose gel. The ribosomal RNA bands 18S and 28S should appear as sharp bands and the intensity of 28S ribosomal RNA band should be twice that of 18S RNA band. If the ribosomal bands in a given lane are not sharp, but appear as a smear of smaller sized RNAs, it is likely that the RNA sample suffered major degradation during preparation. The concentration and the quality (purity) of RNA were also measured by UV visible spectrophotometer.

The concentration of RNA can be determined by measuring the absorbance at 260 nm (A<sub>260</sub>) in a spectrophotometer. Absorbance readings should be greater than 0.15 to ensure significance. An absorbance of 1 unit at 260 nm corresponds to 40 µg of RNA per ml (A<sub>260</sub> = 1 = 40 µg/ml). This relationship is valid for measurements in water. Therefore, RNA is diluted in water to quantify it spectrophotometrically.

RNA concentration in  $\mu\text{g}/\mu\text{l} = (\text{A}_{260} - \text{A}_{320}) * 40 * \text{dilution factor} / 1000$

Purity of RNA can be evaluated by determining the ratio of absorbance readings at 260 nm and 280 nm ( $\text{A}_{260}/\text{A}_{280}$ ). This ratio provides an estimate of the purity of RNA with respect to contaminants that absorb in the UV range, such as protein. The  $\text{A}_{260}/\text{A}_{280}$  ratio is influenced considerably by pH in which RNA is measured. As water is unbuffered, the pH and the resulting 260/280 ratio can vary greatly. Hence, for an accurate determination of purity, the 260/280 absorbance was measured by diluting RNA in 10 mM Tris-Cl, pH 7.5. The spectrophotometer was also calibrated with the TE buffer. Pure RNA has an  $\text{A}_{260}/\text{A}_{280}$  ratio of 1.9-2.1. However, values up to 2.3 are routinely obtained for pure RNA (in 10 mM Tris, pH 7.5) with some spectrophotometers. Lower pH results in lower  $\text{A}_{260}/\text{A}_{280}$  ratio which hampers the sensitivity to detect protein contamination. A control PCR with Xin specific primer pair was done on each sample of DNase treated RNA to ensure that no genomic DNA was present in the sample of RNA.

### 3.10. Reverse Transcription-PCR

RNA was reverse transcribed to cDNA using random nonamers as per the instructions of the reverse transcription kit from Solis BioDyne. Briefly, 1  $\mu\text{g}$  of RNA was mixed in a PCR tube with 2  $\mu\text{l}$  of random nonamers (100 nM). The volume was adjusted to 11  $\mu\text{l}$  with PCR water and incubated at 70°C for 5 min. The PCR tube was placed immediately on ice and 4  $\mu\text{l}$  of 5x reverse transcription buffer 1 (contains  $\text{MgCl}_2$  and DTT) and 1  $\mu\text{l}$  of dNTPs (20mM) was added. The volume was adjusted to 19  $\mu\text{l}$  with PCR water and the tube was incubated at 25°C for 5 min and afterwards placed on ice. 1  $\mu\text{l}$  of M-MLV RNase H<sup>-</sup> Reverse transcriptase (Solis BioDyne) was added, and the sample was incubated at 42°C for 1 hour. This was followed by an incubation step of 10 min at 70°C. The cDNA obtained after reverse transcription was stored at -20°C and subsequently used for semi-quantitative and quantitative Real-time PCR experiments.

#### 3.10.1. Semi quantitative RT-PCR

Semi quantitative RT-PCR was performed to quantify transcript abundance in cDNA samples generated from the reverse transcription of the RNAs isolated from the cells at different stages of differentiation. Initial experiments for knockdown confirmation were also done with semi quantitative PCR.

**Table 3.10. Semi quantitative RT-PCR reaction setup**

<b>Single reaction</b>	<b>Master mix for 4 reactions</b>
36 $\mu$ l PCR water .....	144 $\mu$ l
5 $\mu$ l Taq polymerase buffer (10X).....	20 $\mu$ l
3 $\mu$ l MgCl <sub>2</sub> (25mM).....	12 $\mu$ l
1 $\mu$ l dNTPS (20mM).....	4 $\mu$ l
1 $\mu$ l Primer 1.....	4 $\mu$ l
1 $\mu$ l Primer 2.....	4 $\mu$ l
1 $\mu$ l Taq polymerase.....	4 $\mu$ l
48 $\mu$ l	192 $\mu$ l

Each single reaction was aliquoted from the Master mix as described in Table 3.10. In the final step, 2  $\mu$ l of individual cDNAs (e.g. cDNAs from proliferating cells and cells differentiated for 1, 3 or 6 days) were added to makeup a single reaction of 50  $\mu$ l. The 50  $\mu$ l reaction was equally split into four separate tubes (e.g. 12  $\mu$ l each) and run at different cycle numbers as shown in Figure 3.1. The conditions for semi qRT-PCR are depicted in Table 3.11.

**Table 3.11. Semi qRT-PCR conditions for amplification of *Xin*, *Xirp2* and *Gapdh***

<b>Step</b>	<b>Time</b>	<b>Temperature</b>		
Denaturation	2 min	94°C		
Denaturation	30sec	94°C		
Annealing	30sec	60°C		
Extension	30sec	72°C	2	# Cycles
Final extension	10 min	72°C		
Pause	----	4°C		

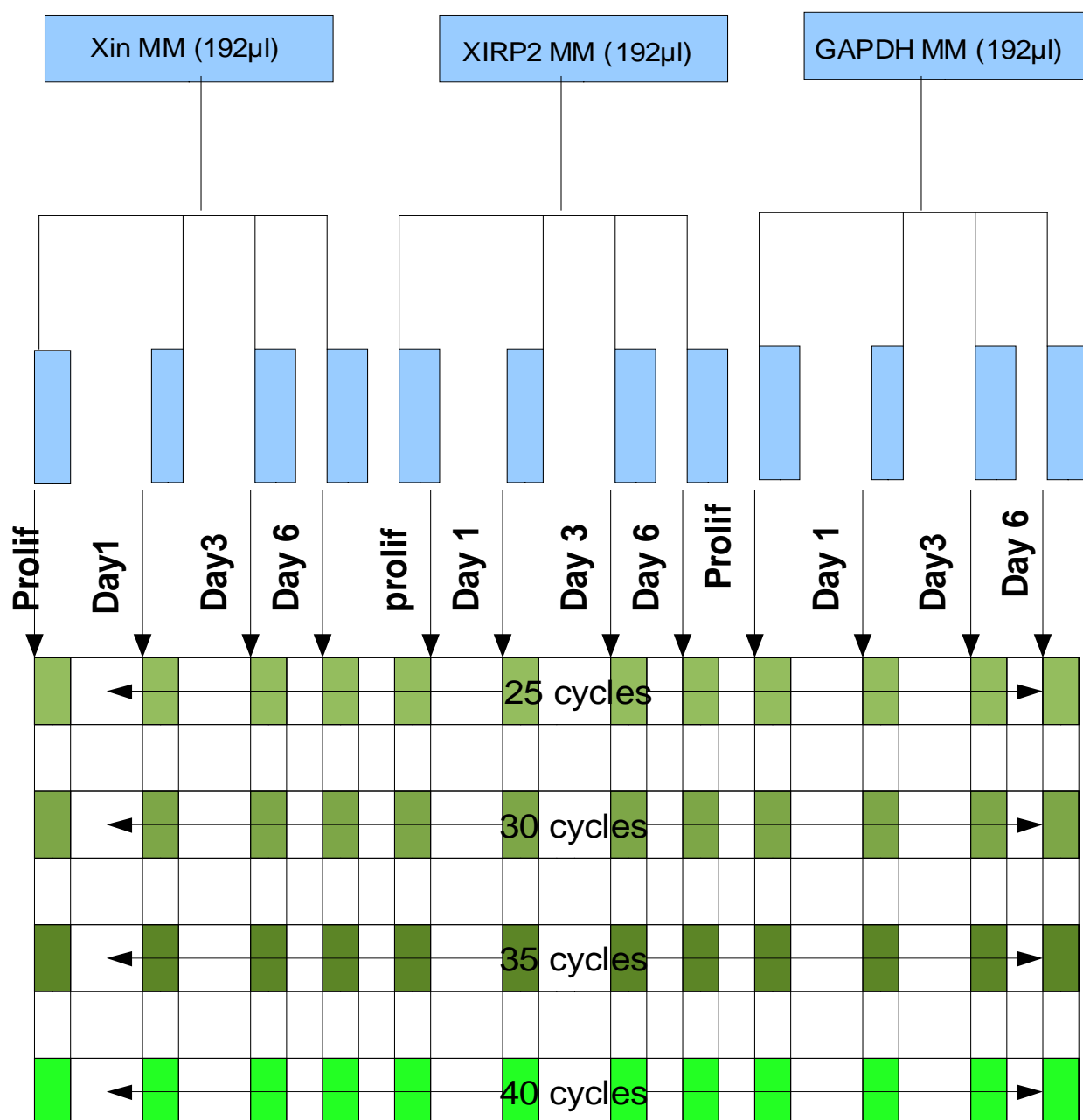


**Figure 3.1. Semi quantitative RT-PCR reaction setup.** Semi quantitative PCR experiments in a 50 µl reaction were setup as shown in the Figure. Each reaction was divided into four separate tubes (e.g.12 µl in each tube) and the reactions were run for different cycle numbers (25, 30, 35 and 40 cycles) with identical PCR conditions. The PCR products were run on a 2 % agarose gel. For the *Xin* and *Xirp2* expression profile experiment, primer pairs of *Xin*, *Xirp2* and *Gapdh* (as loading control) were used in 3 separate master mixes. The cDNAs from four different stages of differentiation (proliferating and differentiation days 1, 3 and 6) were added to the aliquoted reactions. Primers were chosen in such a way that the amplicons generated were in the size range of 100-200 bp in length. The experimental setup also included a no template (no cDNA) control.

### 3.10.2. Quantitative Real time PCR (q-RTPCR)

Quantitative Real time PCR was used to quantify the knockdown levels of genes in cells transduced with lentiviral knockdown constructs. The cDNAs from control cells and knockdown cells (see RNA isolation and reverse transcription steps above) were used with SYBR green based quantitative Real time PCR with QuantiFast SYBR green PCR kit from Qiagen on a Bio-Rad iCycler<sup>®</sup> instrument. The QuantiFast SYBR green PCR kit was based on a two-step cycling protocol, with a denaturation step of 95°C and a combined annealing/extension step at 60°C. This protocol was also meant for primers with melting point ( $T_m$ ) well below 60°C. The QuantiFast SYBR green PCR kit included 2xSYBR green Master mix which contained all the necessary components for the quantitative PCR including SYBR green dye, all the buffers and Hot Start Taq plus DNA polymerase. The Hot Start Taq polymerase required initial incubation step of 5 minutes at 95°C to activate it.

**Table 3.12. Reaction setup in a 96 well plate on iCycler<sup>®</sup> instrument**

<b>Single reaction</b>	<b>Master mix</b>
12.5 µl 2x QuantiFast SYBR green PCR master mix .....	137.5 µl (for 10+1 reactions)
0.5 µl Primer 1.....	5.5 µl
0.5 µl Primer 2.....	5.5 µl
10.5 µl RNase free water.....	115.5 µl
25 µl final volume	264 µl

Note: The Master mix was prepared in excess for one reaction. 24 µl of Master mix was aliquoted into each of the wells and 1 µl template cDNA was added in the final step. The number of cycles was set to 40. Since SYBR green dye intercalates in an unspecific manner to all double-stranded DNA, this method required validation. The validation method included melting curve analysis. A melting curve analysis was performed on PCR products to check each primer set. All three sets of primers Xin, Xirp2 and Gapdh produced single peaks in the melting curve analysis (see Figures of melting curves in Appendix). The end PCR products were also run on a 2% agarose gel to confirm the presence of a single band. From these validation methods it was concluded that the amplification was specific and no primer-dimer combinations or unspecific products were amplified in this protocol.

**Table 3.13. PCR conditions for Real time PCR with QuantiFast SYBR green PCR kit**

Step	Time	Temperature	Ramp rate	Additional comments
PCR initial activation step	5 min	95°C	Maximal/fast mode	Hot start Taq polymerase was activated in this step
<b>Two-step cycling</b>				
Denaturation	10s	95°C	Maximal/fast mode	
Combined annealing/extension	30s	60°C	Maximal/fast mode	Performed fluorescence data collection

### 3.11. Polymerase chain reaction

PCR was used to amplify specific DNA fragments according to established protocols (Saiki et al., 1985). For amplification of GC rich miR30 regions and PCR based double strand generation of hair pin sequences, DMSO at 5% concentration was included in the PCR reaction and the PCR was performed with Pfu polymerase, an enzyme with proof reading capacity. Plasmid clones purchased from Addgene and Open Biosystems were used as templates in PCR mixtures of 50  $\mu$ l reaction volume, containing 20 pM oligonucleotides, 2mM of dNTPs (Fermentas), 5 $\mu$ l Pfu buffer (10x) and 2.5 Units or 1  $\mu$ l of Pfu polymerase. Desired DNA fragments were amplified by programming the thermo cycler (TRIO-Thermo block, Biometra) according to the conditions given below.

**Table 3.14. Thermo cycler setting**


---

Denaturation 2.0 min at 94°C

35 Cycles of Denaturation, Annealing and Elongation

1) Denaturation 45 sec at 94°

2) Annealing 30 sec between 55-65°C

3) Elongation 2 min per each kb length at 72°C

Elongation 10 min at 72°C

Cooling or hold at 4°C.

---

## 3.12. Standard molecular cloning techniques

### 3.12.1. Blunting of DNA fragments

Where necessary, the sticky ends of DNA fragments, resulting from the digestion of the DNA with a restriction enzyme were blunted, using the Pfu polymerase. Briefly 1 µg of plasmid DNA was incubated with 2 mM dNTPS and 1 U of Pfu polymerase and 5 µl Pfu buffer in 50µl reaction volume at 72°C for 30 minutes. The reaction mix was then separated by agarose gel electrophoresis and purified from the gel using the QIAquick Gel Extraction Kit (Qiagen, Hilden) (see below).

### 3.12.2. Dephosphorylation of vector DNA

To avoid self-ligation of the vector, 5' ends of the linearized plasmids were dephosphorylated by incubation with calf intestinal alkaline phosphatase (CIAP, Roche Diagnostics, Mannheim). Briefly, 1-5 µg of the linearized vector DNA was incubated with 1 U calf intestinal alkaline phosphatase (CIAP) in CIAP buffer (provided by the manufacturer) in a total volume of 50 µl at 37°C for 30 min. By adjusting the concentration of EGTA to 5mM, the enzyme is inactivated upon incubation at 65°C for 10 min. Dephosphorylated DNA was separated by agarose gel electrophoresis and purified from the gel using the QIAquick Gel Extraction Kit (Qiagen, Hilden)

### 3.12.3. Ligation

The respective DNA insert fragment and the linearized (where necessary dephosphorylated) plasmid were mixed in equi-molar amounts together with ligation buffer and 0.5 U of T4 DNA ligase (MBI, Fermentas). The reaction mixture was kept at 22°C for 1 h or at 16°C for overnight.

The ligated product was transformed into *E. coli*, JM109 or DH5α cells.

### 3.12.4. Transformation of *E. coli* by heat shock

Competent bacteria (*E. coli* JM 109, DH5α or BL21CP) were thawed on ice. 5–10 µl of a ligation mix or approximately 0.1 µg plasmid DNA was incubated with 100 µl of bacteria for 30 min on ice. Subsequently, bacterial cells containing DNA were incubated at 42°C for 80 seconds and then placed on ice for 2 min. Subsequently, 1 ml of SOC broth was added to the bacteria and they were incubated in for 1 hr at 37°C under continuous shaking. Finally, cells were centrifuged

at 6000 rpm for 5 min, resuspended in 100  $\mu$ l of LB broth and plated on LB agar plates with suitable antibiotic selection marker. Plated bacterial cells were incubated overnight at 37°C.

### 3.12.5. Bacterial mini overnight cultures

Bacterial overnight cultures were grown by picking single colonies from the agar plates containing the transformed *E. coli*, the subsequent day and grown in 3 ml of LB broth with respective selected antibiotics.

### 3.12.6. Plasmid DNA preparation

#### 3.12.6.1. Mini preparation of plasmid DNA (mini preps)

Plasmid DNA was isolated either using Promega SV Wizard mini extraction kits or by TELT-mini preparations. 1.5 ml of bacterial overnight culture was centrifuged (6000 rpm, 5 min) and the supernatant was discarded. The pellet was dissolved in TELT lysis buffer (50 mM Tris pH 8.0, 62.5 mM EDTA pH 8.0, 2.5 M. LiCl, 4% Triton X-100) and centrifuged at 13,000 rpm for 5 min and the pellet was removed with a toothpick. From the supernatant, DNA was precipitated by addition of 0.8 times volume of isopropanol and centrifuged for 15 min at 13,000 rpm. The pelleted DNA was washed with 70 % ethanol, air dried and dissolved in 30  $\mu$ l of TE buffer, pH 8.8. The presence of plasmid was confirmed by restriction enzyme digests and subsequent agarose gel electrophoresis. Plasmid DNA for sequencing was prepared using the Promega SV Wizard mini extraction kits as per the instructions of the manufacturer. Sequencing was performed using the single read economy sequencing method by AGOWA GmbH, Berlin).

#### 3.12.6.2. Transfection quality plasmid DNA preparation: Midi preps and Maxi preps

Plasmids that were used for the transfection in eukaryotic cells were purified using the plasmid midi kit (Qiagen) or using maxi prep kits (Machery Nagel) from 100-250 ml of overnight cultures as described in the manufacturer's instructions. Isolated plasmid DNA was re-dissolved in 0.1x TE buffer (10 mM Tris-HCl, 1 mM EDTA, pH 8.0). The DNA concentration was calculated from the absorption value at 260 nm. The purity of the DNA was estimated from the ratio of absorptions of wavelengths at 260 nm and 280 nm. The plasmid integrity was also checked by running on 0.6% agarose gels by observing supercoiled plasmid DNA.

### 3.12.7. Restriction enzyme digests

Plasmid DNA was digested using the desired restriction enzymes. 1  $\mu\text{g}$  of the DNA of interest was incubated with restriction endonuclease (1 U/  $\mu\text{g}$  of DNA) in a total volume of 20  $\mu\text{l}$  in suitable buffers as suggested by the manufacturer for 1-3 hours at 37°C. For analysis, the digested samples were loaded onto 0.6% - 2 % agarose gels depending on the fragment sizes and compared with DNA standard ladder bands.

### 3.12.8. Agarose gel electrophoresis of DNA

Agarose gel electrophoresis was used to resolve the DNA fragments. 0.6% - 2 % agarose was dissolved in hot TAE buffer. After cooling to approximately 50°C, ethidium bromide was added to a final concentration of 0.5  $\mu\text{g}/\text{ml}$  and gels were cast. Electrophoresis in a horizontal electrophoresis tank containing 1x TAE buffer at 1-5 V/cm. DNA size markers (MBI Fermentas) were always loaded along with the DNA samples to estimate the size of the resolved DNA fragments. The gels were examined under UV light at 302nm and were photographed using 'Quantity one', gel-documentation software from Bio-Rad.

### 3.12.9. DNA fragment recovery from agarose gels

DNA fragments from restriction enzyme digests or PCR products were separated by agarose gel electrophoresis as described above. The desired DNA fragments were excised keeping the agarose gel under a low powered UV illuminator to avoid UV induced DNA mutations. The DNA fragment was then purified from the excised gel piece using the Qiagen gel extraction kit following the instructions supplied by the manufacturer.

## 3.13. Biochemical Methods

### 3.13.1. Protein expression

For the expression of recombinant proteins, pET expression vectors were used. The pET23aW1 vector was modified from original pET23a vector (Novagen) by introducing a three amino acid peptide, Glutamate-Glutamate-Phenylalanine (EEF) tag. The pET23a-T7 vector was modified from original pET23a vector (Novagen) by introducing a T7 immuno tag with amino acid sequence of MASMTGGQQMGR, an epitope derived from amino terminal portion of capsid protein of T7 phage. Expression of recombinant proteins from pET23a-EEF resulted in the

formation of a recombinant fusion protein with C-terminal 6x His tag and C-terminal EEF tag whereas, the expression from pET23a-T7 resulted in the formation of a recombinant fusion protein with C-terminal 6x His tag and N-terminal T7 tag. The *E. coli* strain BL21 CP was transformed with plasmids containing the relevant cDNA insert. Single colonies were picked from selection plates and grown overnight in LB selection medium. A mini expression culture of 4 ml total volume was performed to assess the expression and solubility of the fusion proteins.

### 3.13.2. Expression and purification of recombinant proteins

Recombinant proteins were expressed by inoculating 100-150 ml of LB medium containing chloramphenicol and carbenicillin as antibiotic selection markers. Expression was induced by 1mM IPTG for 3 hours after the culture has attained an  $O.D_{600}$  value of 0.6. Uninduced bacterial cultures (-IPTG) served as negative control. Bacterial cells were collected by centrifugation (5,000 rpm, Heraeus cool centrifuge) and kept at  $-20^{\circ}\text{C}$  until further use. Frozen pellets were thawed on ice, resuspended in lysis buffer and sonicated to reduce viscosity. Cell debris was removed by centrifugation (4,500 rpm, 30 min) and the supernatant was collected. 500-1000  $\mu\text{l}$  of pre-equilibrated Ni-NTA-Agarose beads (Qiagen) were added to the His-tagged fusion protein. The beads were incubated with the protein solution for approximately 1 h at  $4^{\circ}\text{C}$ . The fusion protein bound beads were washed thoroughly in wash buffer and fusion proteins were eluted in fractions by addition of respective elution buffer. The composition of the buffers is given below.

Lysis buffer: 50 mM  $\text{NaH}_2\text{PO}_4$ , 300 mM NaCl, 10 mM Imidazole, 1 mg/ml Lysozyme, pH 8.0

Wash buffer: 50 mM  $\text{NaH}_2\text{PO}_4$ , 300 mM NaCl, 20 mM Imidazole, pH 8.0

Elution buffer: 50 mM  $\text{NaH}_2\text{PO}_4$ , 300 mM NaCl, 250 mM Imidazole, pH 8.0.

### 3.13.3. Protein concentration determination

Protein concentration was determined by Bradford method. Protein Assay Dye reagent (Bio-Rad) was added to the protein solutions at required dilutions, incubated for 5 min and the O.D. was read at 595 nm wavelength. A series of  $\gamma$ - globulin dilutions served as standards. Both standard and samples were prepared in triplicate.

### 3.13.4.

**SDS-Polyacrylamide gel electrophoresis (SDS-PAGE):** SDS-polyacrylamide gel electrophoresis was performed using the discontinuous buffer system described by Laemmli (1970). For running gels, 6-14 % and for stacking gels 3 % acrylamide concentrations were used

(composition of the mixtures is given below). Where necessary, step gradient gels of 6 % to 14 % were used to resolve both high molecular and low molecular weight proteins in a single gel. The Bio-Rad Mini Protean II system was used with a spacer thickness of 0.75 mm.

**Table 3.15. SDS-PAGE Resolving gel composition**

Components	8 %	10 %	12 %	14 %	16 %
Acrylamide Solution (37.5:1):	1.07 ml	1.33 ml	1.60 ml	1.87 ml	2.13 ml
Resolving gel buffer:	1.00 ml				
Double distilled H <sub>2</sub> O:	1.93 ml	1.67 ml	1.40 ml	1.13 ml	0.87 ml

**Table 3.16. SDS-PAGE Stacking gel composition**

Components	3.0 %	4.5 %
Acrylamide Solution (19:1):	0.15 ml	0.23 ml
Stacking buffer:	0.38 ml	0.38 ml
Double distilled H <sub>2</sub> O:	0.98 ml	0.90 ml

**Table 3.17. Buffer composition**

Acrylamide solution:	30 % Acrylamide/Bis-Acrylamide (37.5:1)
Resolving gel buffer:	375 mM Tris-HCl, 0.2 % SDS, pH 8.8
Stacking gel buffer:	125 mM Tris-HCl, 0.2 % SDS, pH 6.8
Running buffer:	25 mM Tris, 250 mM glycine, 0.1 % SDS, pH 8.8
Coomassie staining:	0.1 % Coomassie Brilliant Blue G250, 50 % (v/v) methanol, 20 % (v/v) acetic acid
De-staining solution:	10 % (v/v) methanol, 7 % (v/v) acetic acid
Sample buffer:	125 mM Tris-HCl, 0.2 % SDS, pH 6.8
5 x SDS sample buffer:	5 mM EDTA, 30 % glycerol, 60 mM Tris-HCl, 15 % SDS, 0.1 % Bromophenol blue, pH 6.8, 7.5 % $\beta$ -mercaptoethanol

Purified protein solutions were mixed with 5 x sample buffer at a ratio of 1:5 (SDS sample buffer: Protein solution) and boiled at 95°C for 2-5 minutes to denature. Samples were loaded into the wells of the stacking gels along with molecular mass marker to allow for the determination of the apparent molecular mass of proteins. After loading the samples, gels were run at a constant

voltage of 100-150 V until the bromophenol blue dye front reached the bottom of the gel. Resolved proteins were either stained with Coomassie brilliant blue or transferred onto a nitrocellulose membrane for subsequent detection protocols.

### 3.13.5. Protein Transfer

#### 3.13.5.1. Semidry blot

Proteins resolved by SDS-PAGE were electrophoretically transferred from the gel to a nitrocellulose membrane by a semidry blotting method for proteins of sizes up to 150 kDa. The transfer was performed using a semi-dry blotting apparatus (Bio-Rad). A constant current of 1 mA/cm<sup>2</sup> of nitrocellulose membrane was applied for 90 min. The quality of the protein transfer was determined by staining the membrane with Ponceau red solution (Sigma) for 2 min at room temperature. After staining, membranes were washed with deionized water and photographed after molecular mass markers and/or protein bands of interest were marked.

Ponceau staining solution: 0.1 % (w/v) Ponceau-red in 3 % (w/v) acetic acid.

Semi dry blot buffer: 39 mM Glycine, 48 mM Tris, 0.037 % SDS, 20 % methanol, pH 8.3

#### 3.13.5.2. Tank blot

Proteins resolved by SDS-PAGE were electrophoretically transferred from the gel to a nitrocellulose membrane by tank blotting for proteins above 100 kDa and whenever quantitative transfer was required (in the case of comparing protein levels from control and knockdown cells). The transfer was performed using a tank blotting apparatus (Bio-Rad). A constant current of 250 mA was applied overnight at 4°C. Protein transfer was assessed by staining the membrane with Ponceau red as described above.

Tank blot buffer: 25mM Tris/ HCl, 192 mM Glycine, 18 % (v/v) methanol, 0.01 % SDS, p<sup>H</sup> 8.3

### 3.13.6. Immunodetection of membrane bound proteins

#### 3.13.6.1. ECL method

Transfer membranes prepared as described above were blocked with blocking buffer containing 4 % low-fat milk powder, either overnight at 4°C or at room temperature for 1-2 h. After blocking, the blot was incubated at room temperature with gentle agitation with either one of the desired primary antibodies with appropriate dilutions for 1-2 h at room temperature or overnight at 4°C.

The blot was washed 3 times with TBST (with 0.05 % tween-20) at room temperature for 5 min each. Subsequently, the blot was incubated with Horse Radish Peroxidase (HRP) conjugated secondary antibody directed against the primary antibody for 1 hr. After washing with TBST, substrate reaction was carried out using an enzymatic Enhanced Chemiluminescence (ECL) detection system (Pierce Biotechnology Inc.).

**Table 3.18. Composition of ECL solutions**

---

TBST: 50 mM Tris/HCl, 150 mM NaCl, 0.05 % tween-20, pH 7.9

ECL kit: Super signal West Pico Chemiluminescent substrate (Pierce Perbio Science GmbH, Germany, Bonn)

ECL-Film: Hyper film ECL (Amersham)

---

### 3.13.6.2. Odyssey infrared scanning method

Immunodetection using this method followed similar methods as described above with two exceptions. For washing the membranes, TBST with Triton X-100 is used to reduce the background which might appear with Tween. Additionally, the blots meant for detection by Odyssey<sup>®</sup> were incubated with an IR DYE 800-conjugated goat anti-mouse IgG antibody (Rockland Immunochemicals, Gilbertsville, USA). The obtained signals were quantified using an Odyssey<sup>®</sup> infrared scanner (LI-COR Biosciences, Bad Homburg, Germany).

### 3.13.6.3. Western blot overlay

Western blot overlay experiments were performed with recombinantly expressed and purified proteins at a concentration of 1 µg/µl, electrophoretically transferred to a nitrocellulose membrane (BA-85, Schleicher and Schuell). The blot membrane was stained with Ponceau<sup>®</sup> red to identify the electrophoresed proteins; afterwards the membrane was photographed and blocked with blocking buffer overnight at 4°C. The membrane was washed briefly with PBST and overlaid with purified recombinant protein diluted in blocking buffer (4 % (W/V) low fat milk powder in PBST) to concentrations between 1 to 20 µg for 1-2 h at room temperature. The overlaid protein that was bound to the blotted protein was immunodetected as described above.

#### 3.13.6.4. Dot blot overlay

Dot blot assays were performed by spotting and drying of the protein of interest along with necessary positive and negative control proteins. Blocking of the membrane, overlaying with protein of interest and Immunodetection were performed as described above.

### 3.14. Fixation and Permeabilization of cells

Cells grown on glass cover slips were washed twice in warm PBS and treated with either paraformaldehyde or with methanol and acetone as follows

#### 3.14.1. Paraformaldehyde fixation

Cells were incubated in 4 % Paraformaldehyde in PBS at room temperature for 15 min. The cells were permeabilized by incubating in 0.5 % Triton-X 100 for 15 min. The coverslips were subsequently washed twice in PBS and stored in sterile PBS until further use.

#### 3.14.2. Methanol- acetone fixation

Cells cultured on the coverslips were incubated in a 1:1 methanol-acetone mixture at -20°C for 15 min. Subsequently, the coverslips were air dried and stored desiccated at -80°C until further use. Alternatively they are stored in sterile PBS until further use.

### 3.15. Immunohistochemical staining of tissue sections

Frozen cryosections (on glass cover slides) with a thickness of 6-10  $\mu\text{m}$  were fixed in cold methanol-acetone and blocked with blocking solution (10 % normal goat serum in PBS containing 0.1 % Tween 20 ) for 30 min at room temperature. Primary antibodies were diluted appropriately in PBST (PBS containing 0.1 % Tween 20) and incubated on sections for one hour at room temperature or overnight at 4°C. The sections were washed twice with PBST and incubated with secondary antibody at room temperature for 45 minutes. Finally, the sections were washed twice with PBST and mounted with Mowiol® and covered with big rectangular glass coverslips. Stained sections were analyzed by imaging in a confocal microscope (see below).

## 3.16. Microscopy

### 3.16.1. Confocal and epifluorescence microscopy

To observe the localization of proteins in stained cells and tissues, images were acquired with Confocal laser scanning microscope (LSM 510, Carl Zeiss, Jena, Germany) or epifluorescence microscope (Nikon TE2000, Nikon, Japan). Nikon microscope was fitted with a 60x/1.25 NA oil immersion objective. A cooled CCD camera (Visitron, Puchheim) was used to record images on the epifluorescence microscopes. Images on Nikon TE2000 microscope were acquired with NISElements V2.0 (Nikon, USA) software and were processed either with Image J or Adobe Photoshop CS3 (Adobe Systems Inc., USA). Confocal fluorescence images of stained cells on coverslips and immunolabelled specimens (6 to 10  $\mu\text{m}$  thick tissue sections ) were recorded using a Zeiss LSM 510 confocal microscope equipped with a 488 nm argon laser, a 543 nm helium-neon laser and a 633 nm helium-neon laser at 63x/1.3 NA oil immersion objective. For the excitation of GFP fluorescence, the 488nm argon laser was used, whereas, the 543 nm laser was used to excite Cy3, TRITC or Texas red. The Nikon TE 2000 was fitted with 6 fluorescent filter blocks in rotating turret with shutter. The filter combinations were selected to avoid any bleed-through. The images from green and red channels were independently attributed with color codes and then superimposed using the accompanying software. Further image processing was done with Image J and Adobe Illustrator CS3 (Adobe Systems Inc., USA).

## 4. Results

---

### 4.1. Expression patterns of *Xin* and *Xirp2* in skeletal muscle cells

#### 4.1.1. Comparative expression levels of *Xirp1* and *Xirp2* by semi-quantitative RT-PCR

To test the temporal expression of *Xirp1* and *Xirp2* in differentiating skeletal muscle cells, the immortal mouse skeletal muscle cell line H-2K<sup>b</sup>-tsA58 (Morgan et al., 1994), that typically differentiates up to the stage of cross striated and contracting myotubes *in vitro* was chosen. Since our efforts to produce an antibody that recognizes mouse *Xirp2* protein were unsuccessful, the simultaneous expression of these genes at the protein level by western blotting could not be tested. Therefore, a semi-quantitative RT-PCR method was used to analyze their expression patterns at the mRNA level. RNA was isolated from proliferating and differentiating cells. The isolated RNA was reverse-transcribed to cDNA and subsequently used as a template for quantifying transcript abundance of *Xin* and *Xirp2* using gene specific primers (Appendix Table 1). The housekeeping gene *Gapdh* served as reference. Expression of *Xirp1* was already observed in proliferating cells at the RNA level (Figure 4.1). The expression of *Xirp1* increased with time and reached its maximum expression level after 3 days of differentiation, after which there was no further increase in its expression. By contrast, only minimal expression levels of *Xirp2* were detected in proliferating cells as well as in early differentiating cells up to day 3. Robust expression of *Xirp2* was only found from day 3 onwards and the expression remained stable up to day 6. These results indicate that, at least at the RNA level, *Xirp1* is expressed even before the initiation of differentiation in skeletal muscle cells, whereas *Xirp2* is only expressed at a considerably more advanced differentiation stage.

Semi quantitative-RT-PCR expression profile of *Xirp1* and *Xirp2* in H-2K<sup>b</sup>-tsA58 muscle cells

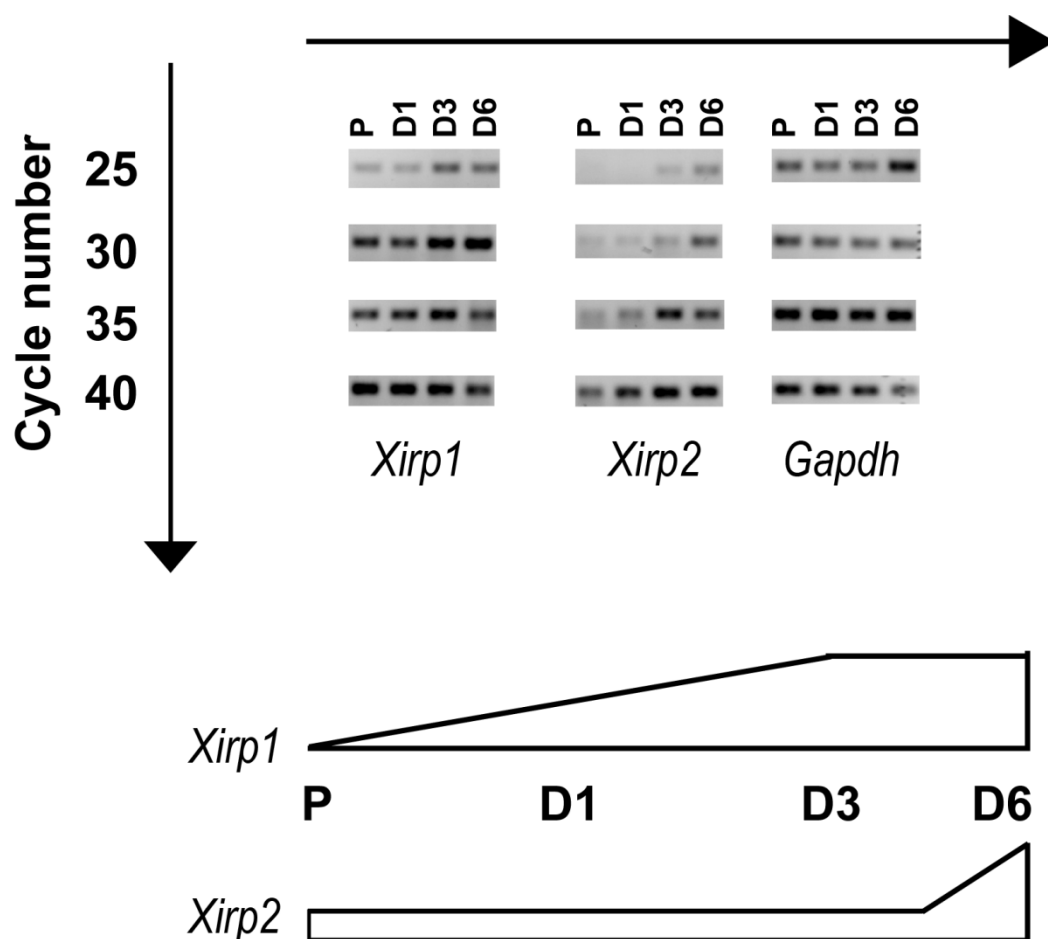


**Figure 4.1. Expression patterns of *Xirp1* and *Xirp2* at mRNA level in differentiating H-2K<sup>b</sup>-tsA58 mouse immortal cells.** RNA was isolated from H-2K<sup>b</sup>-tsA58 cells undergoing differentiation at different time points (Proliferation (P) and differentiation days 1, 3 or 6 (D1, D3 or D6)). Isolated RNA was reverse transcribed to cDNA and used as template for analyzing expression of *Xirp1* and *Xirp2* genes with gene specific primers in a semi quantitative PCR. *Gapdh* served as a reference. *Xirp1* expression increased from D1 up to D3 and thereafter the expression level reached a plateau. For *Xirp2*, in the early stages of P, D1, D3, expression was minimal and towards the end of differentiation (D6) expression reached robust levels.

#### 4.1.2. Localization of Xin protein in proliferating and differentiating cells

Although *Xirp1* gene transcripts were detected in proliferating cells at the RNA level (Figure 4.1), the protein (Xin) is absent in proliferating cells (Figure 4.2 B). Xin protein is also not detected in striations in maturely differentiated myotubes (Figure 4.2 J).

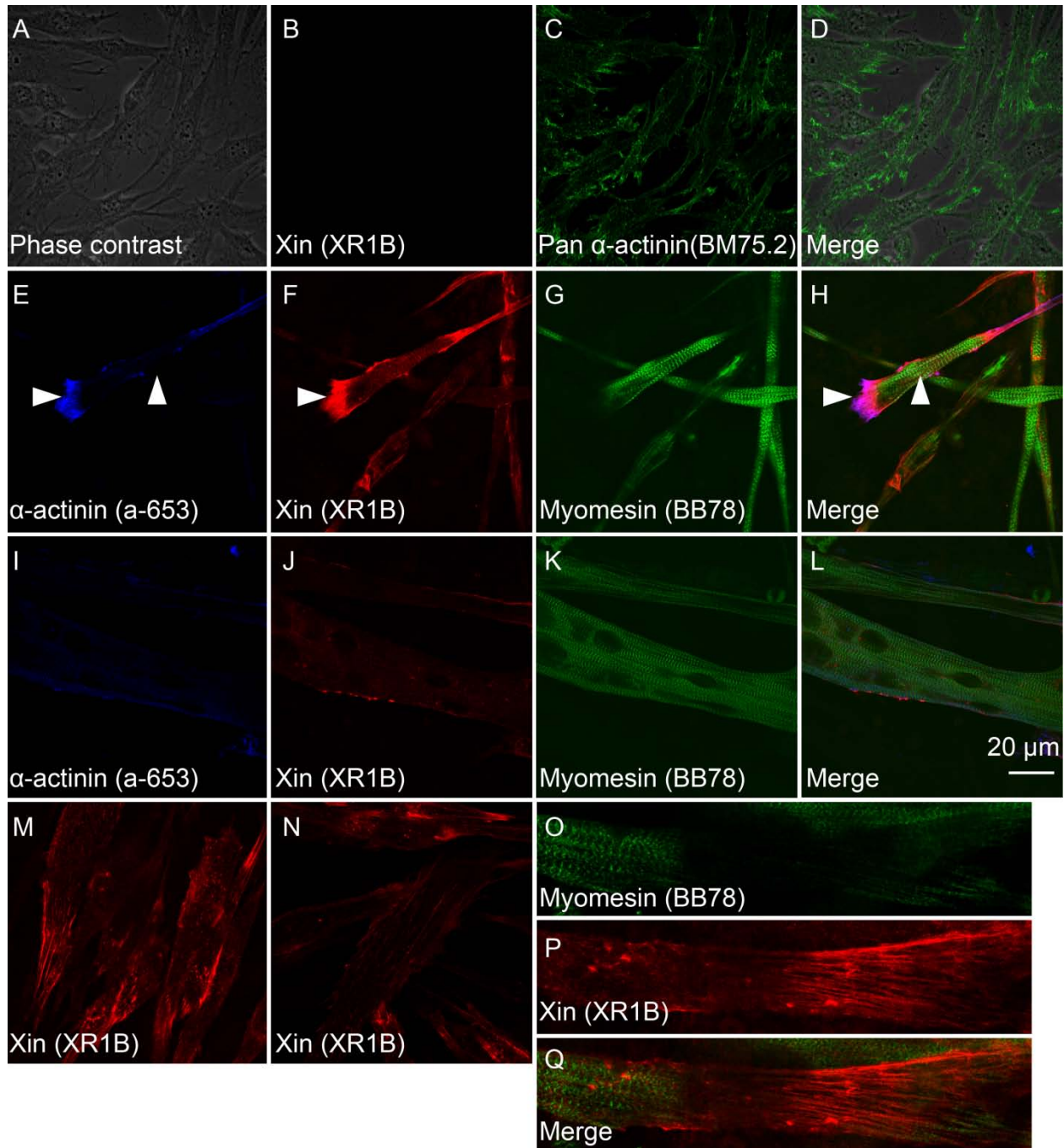


**Figure 4.2. Localization of Xin in proliferating and differentiating H-2K<sup>b</sup>-tsA58 cells.** Proliferating cells (A-D) were stained for Xin with XR1B, an antibody recognizing XinA and XinB isoforms (B) and BM75.2, an antibody recognizing all  $\alpha$ -actinin isoforms (C). Note that Xin protein was not detected in these cells (B). Non striated myofibrils (NSMF) of differentiating myotubes (E-H) show colocalization of Xin (side arrow head, F) with  $\alpha$ -actinin (detected by a-653, side arrow head, E). Panels I-L show fully differentiated cells, in which Xin staining (J) does not colocalize either with Z-disk protein  $\alpha$ -actinin (I) or with M-band protein myomesin (detected with BB 78, K). M and N show typical Xin stainings at the myotube ends and along the stress fibers respectively. Panels O-Q display SMF and NSMF regions in a single developing myotube and the corresponding stainings of Xin and myomesin.

Intriguingly, within a single myotube which shows both striated and non-striated regions, Xin colocalizes with  $\alpha$ -actinin in the non-striated myofibrils (NSMF) but not in the striated myofibrils (SMF, Fig. 4.2 E-H)). After induction of differentiation, Xin staining prominently appears in the regions where the myofibrils begin to form, typically myotube ends and the sites of new myofibril formation (Fig. 4.2 M-Q). In summary, Xin is localized to myotendinous junctions or the ends of myotubes and the sites where new myofibrils begin to form, but it is absent in mature, striated myofibrils.

### 4.1.3. Expression of Xirp2 in various muscle cells, primary cells and tissue samples

The efforts to study simultaneous expression profiles of Xin and Xirp2 proteins were complicated by the lack of proper differentiation in human skeletal muscle (HSKM) cells. At the same time, the lack of antibodies recognizing mouse Xirp2 protein hindered similar experiments with the well-differentiating mouse cell lines. This further compromised the studies on localization patterns of Xirp2 during differentiation in mouse cells. It must be noted that probably due to the relatively poor differentiation of the HSKM cells, Xirp2 staining appeared weak in differentiating HSKM cells (Figure 4.3). It was detectable only in the 1-2% of myotubes differentiated for six days, which contained mature myofibrils with distinct Z-disks. In these cells Xirp2 was localized in a doublet band flanking the Z-disk (Figure 4.4). By contrast, in cryosections from adult human skeletal muscle tissue, all available Xirp2 antibodies revealed a colocalization with  $\alpha$ -actinin in the Z-disk (Figure 4.5). This implies that the layout of the Xirp2 molecule changes from regions flanking the Z-disk to the Z-disk itself during the differentiation process. Expression of Xin was detectable in HSKM cells which were switched to differentiation, even when the cells were not completely differentiated also in cells showing no Xirp2 expression. This finding again confirms the conclusion that Xin is expressed earlier than Xirp2 in skeletal muscle cells. Extrapolating these results, we predict a role for Xirp2 in the later stages of myofibril formation, whereas Xin probably plays a role in early myofibrillogenesis.

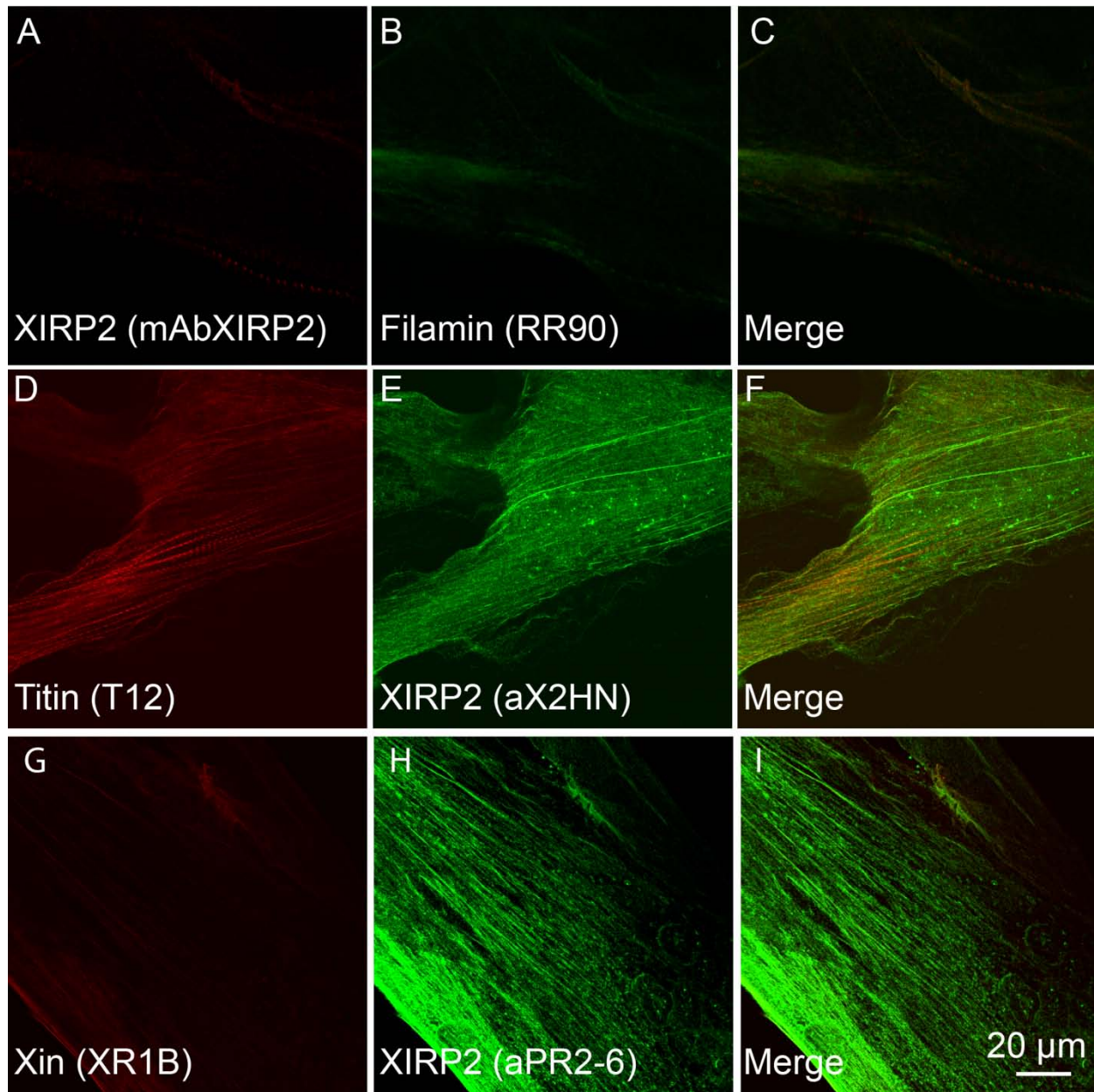


**Figure 4.3. Localization of human Xirp2 protein in cultured human skeletal muscle (HSKM) cells undergoing differentiation.** The differentiating HSKM cells were stained for Xirp2 either with a monoclonal antibody (mAb XIRP2) (A) or two distinct polyclonal antibodies (aX2HN, E) and (aPR2-6, H). The cells were counterstained with filamin (RR90, B), titin (T12, D) or Xin (XR1B). Note that Xirp2 was localized along premyofibrils in E and H. Panel A shows a more ordered localization of Xirp2 flanking the Z-disk at the periphery of the cell.

The localization of Xirp2 was also studied in adult human skeletal muscle tissue sections with different antibodies targeting various regions of the human Xirp2 protein. All three available antibodies namely mAbXIRP2, the polyclonal antibodies anti PR2-6 and antiX2HN decorated the Z-disk region and mainly colocalized with  $\alpha$ -actinin (Figure 4.5). The differences in localization

pattern of Xirp2 observed with mAb and polyclonal antibodies are due to possible impurities in polyclonal antibodies.

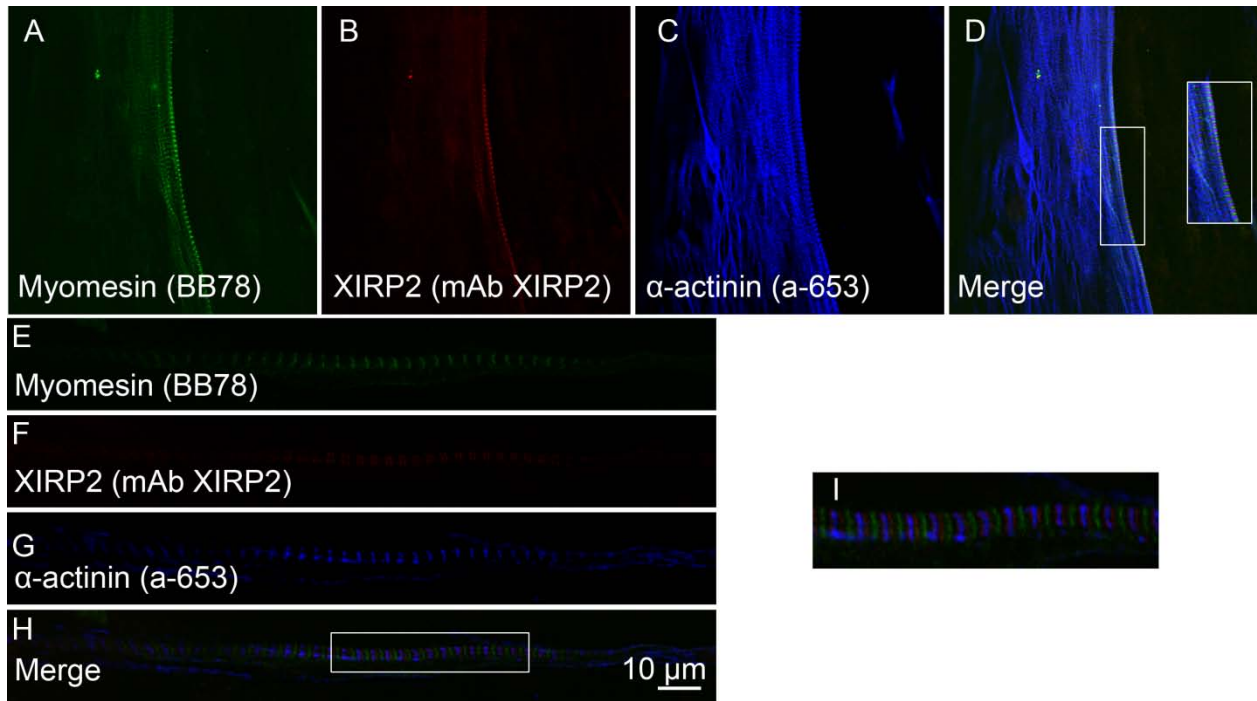


**Figure 4.4. Xirp2 doublet band flanking the Z-disk in differentiating HSKM cells.** Differentiating HSKM cells were stained with a monoclonal Xirp2 antibody (mAbXIRP2, B, F) and counterstained for Z-disk protein  $\alpha$ -actinin (a-653, C, G) and M-band protein myomesin (BB78, A, E). Note that Xirp2 staining was visible in a doublet band flanking the Z-disk identified by the staining of  $\alpha$ -actinin (D, H, I).

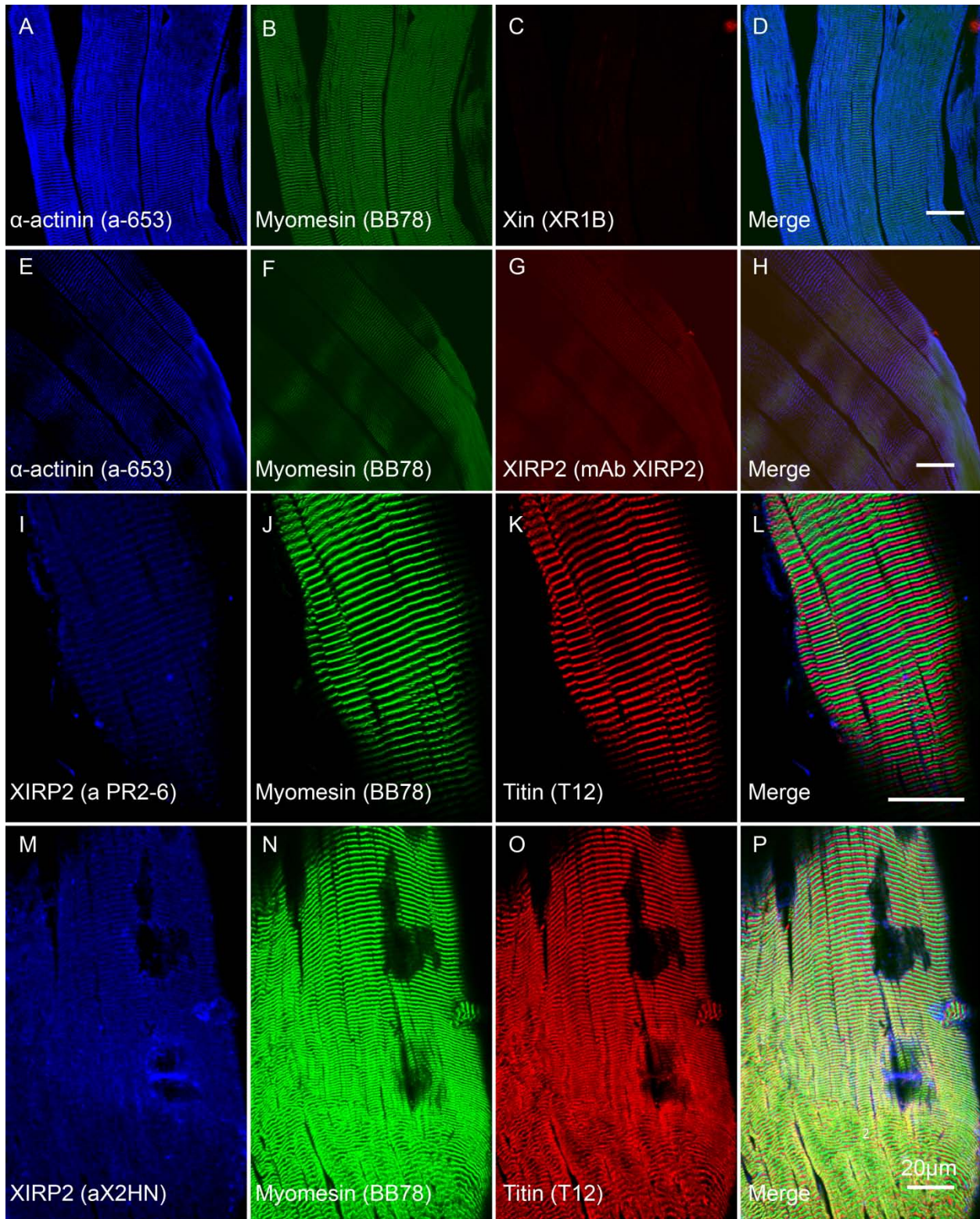


**Figure 4.5. Localization of Xin and Xirp2 in adult human skeletal muscle tissues.** Longitudinal sections of human skeletal muscle tissues (Vastus lateralis, a kind gift from Dr. Dirk Anhuf, Universitätsklinikum, Bonn ) were stained for Xin (C) and different antibodies targeted against human Xirp2 protein as indicated (G, I, M). Tissue sections were counterstained for  $\alpha$ -actinin (A and E), or titin (K and P) to visualize the Z-disk. Scale bar: 20 $\mu$ m

## 4.2. Knockdown of Xirp2 expression in muscle cells

To elucidate the possible role of Xirp2 in myofibrillogenesis and myodifferentiation, a functional knockdown of Xirp2 via RNAi was attempted. Earlier attempts in the laboratory to knockout Xirp2 gene in mice were unsuccessful owing to its complex gene structure. Xirp2 gene consists of 9 exons. The exon 7 is the largest one and contains most of the coding sequence. Multiple alternative forms of the protein can result due to splicing events and differential transcriptional start sites predicted for this gene. Therefore conventional knockout methods were unsuccessful in this laboratory. (A very recent report described successful knockout of Xirp2 (Wang et al., 2010)). Therefore RNAi was chosen as an alternative method for Xirp2 depletion. To effectively use RNAi method and to develop the knockdown system in hard to transfect muscle cell lines and primary muscle cells a lentiviral based gene knockdown method was selected. However, our experience with the existing lentiviral based systems and their inflexibility has motivated us to develop a novel general purpose modular lentiviral system. The system was intended for simple use, yet the modular approach was designed for multiple tasks without compromising the performance of the system.

### 4.2.1. Construction of multipurpose modular lentiviral vectors

Recently, a novel inducible lentiviral system based on a single vector was described that relied on the promiscuous activity of tTRKRAB, a fusion protein between the Krüppel-associated box (KRAB) domain and the tetracycline repressor (tetR) of *Escherichia coli* (Szulc et al., 2006). The tTRKRAB-mediated epigenetic repression of cellular Pol II and Pol III promoters juxtaposed to tet operator (TetO) sequences was shown to be reversibly controlled by doxycycline (Szulc et al., 2006). The conditional vectors of this system allowed the expression of shRNAs from Pol III promoters and enabled reversible gene knockdown in vitro and in vivo without substantial leakiness (Szulc et al., 2006). However the vectors described in this reference used only shRNAs driven by the H1 (Pol III) promoter. Public libraries of gene knockdown clones (Silva et al., 2005) as well as many vectors meant for gene knockdown also use shRNAs driven by other Pol III promoters (U6) and shRNAmirs driven by H1 and U6 promoters as well as a host of Pol II promoters. Since the tTRKRAB fusion protein can control both Pol II and Pol III promoters, the vectors described in the reference were modified as described below to allow for expression of both shRNAs and shRNAmirs from Pol III and Pol II promoters respectively.

#### 4.2.1.1. Construction of the plasmid- pLVmir

The construction of pLVmir (Figure 4.6) is based on the lentiviral vectors pLVCT-tTRKRAB (Appendix Figure 1) and pGIPZ (Appendix Figure 2 & 2.1) (Stegmeier et al., 2005; Szulc et al., 2006). The vector map including unique restriction sites and modules is displayed in Figure 4.7. First, the vector pLVCT-tTRKRAB was cut with restriction enzyme SpeI to give two fragments 4372bp and 8505bp respectively (Figure 4.6). The 8505 bp fragment was self-ligated to yield a new vector pLVCT $\Delta$ (SpeI-SpeI). An XhoI site present just upstream of TetO sequence was deleted by digesting with XhoI, blunting the resulting sticky ends and finally religating to generate a new plasmid pLVCT $\Delta$ (SpeI-SpeI) $\Delta$ XhoI. In the next step, the shRNAmir-WPRE portion from the vector pGIPZ was amplified with two primers incorporating SpeI and MscI restriction sites in the forward and reverse primer respectively (a list of primers used for constructing various modular vectors is given in Appendix Table 2). The resulting amplicon was double digested with SpeI and MscI and cloned into the same restriction sites present in the plasmid pLVCT $\Delta$ (SpeI-SpeI) $\Delta$ XhoI, to generate a new plasmid, which was named pLVmir. This resulting plasmid harbors unique XhoI, EcoRI and MluI sites to facilitate direct cloning of miRNA30 based short hairpin sequences from public libraries from Open Biosystems (Chang et al., 2006). To further simplify the cloning protocol a stuffer sequence of 4.3 kb was introduced into the XhoI and EcoRI sites. We named the final version of the vector as pLVmir-stuffer. A schematic representation of the cloning is shown in Figure 4.6. The resulting vector including its unique restriction sites and modules is given in Figure 4.7.

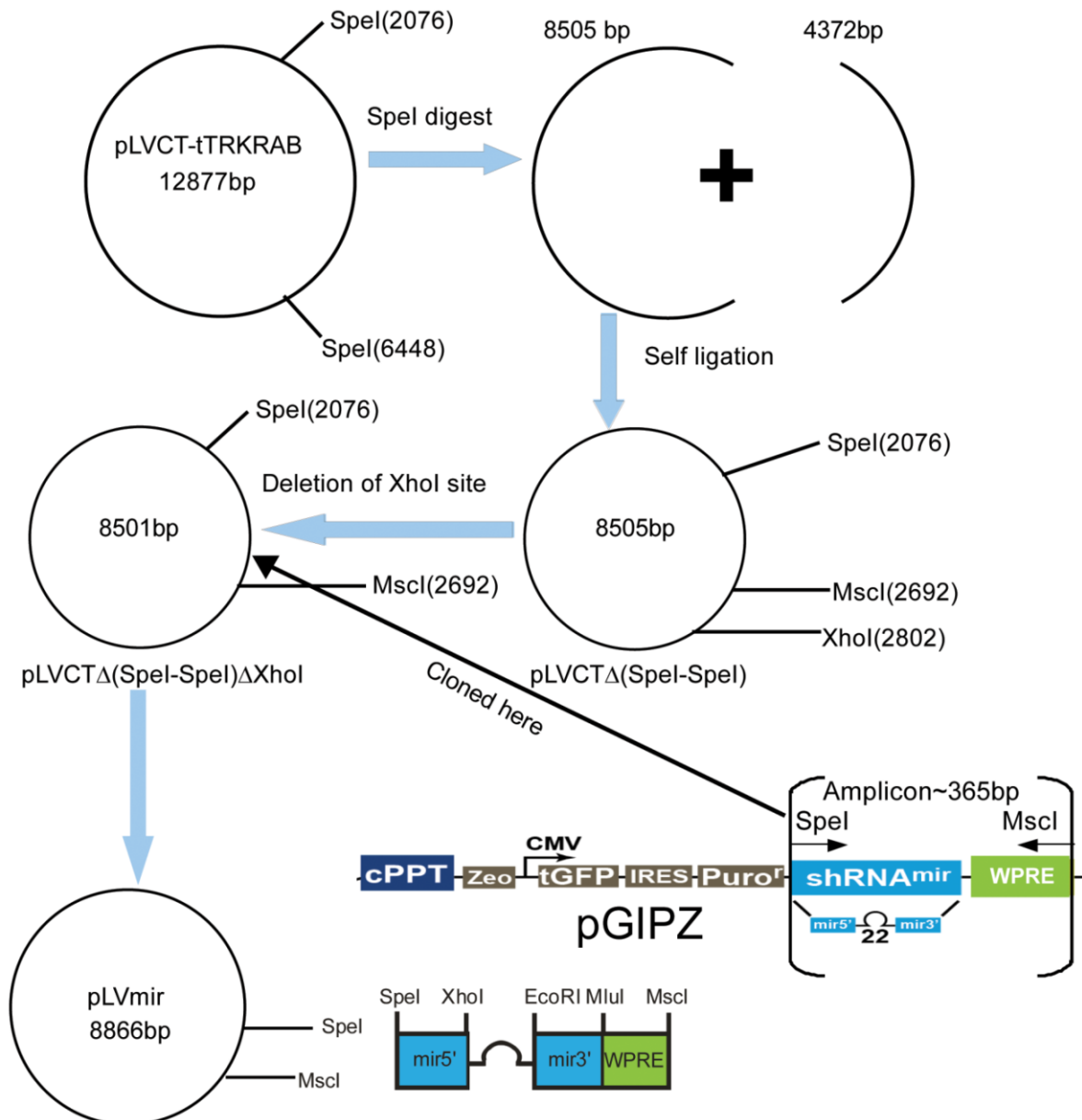


**Figure 4.6. Schematic representation of the cloning steps performed to construct the vector pLVmir from pLVCT-tTRKRAB and pGIPZ.** For details of the cloning steps, see text.

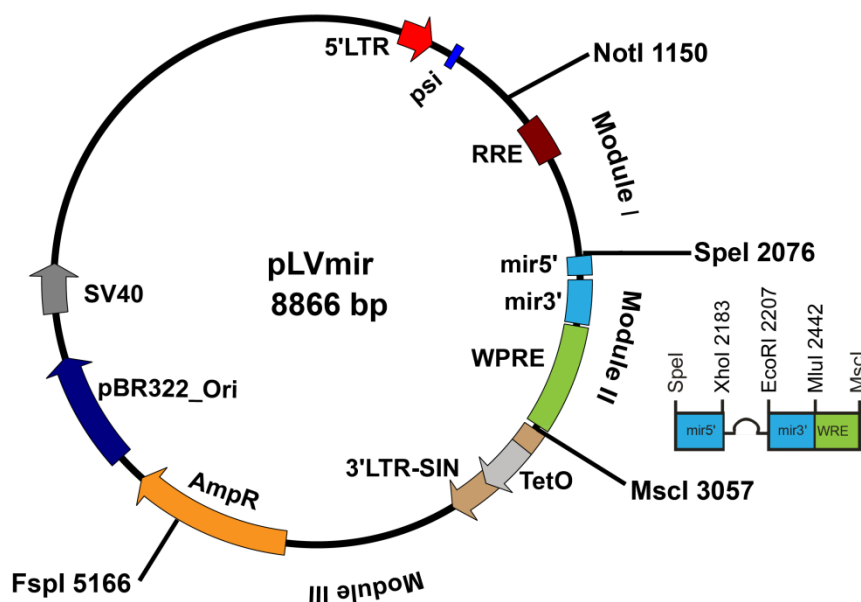


**Figure 4.7. Vector map of pLVmir with its unique restriction sites emphasizing its modular design.** Modules are defined as the regions between the indicated restriction sites: module I is located between NotI and SpeI, module II between SpeI and MscI, module III between MscI and FspI, respectively. The choice of usable modules is given in Figure 4.9. 5' LTR - 5' long terminal repeat; 3' LTR-SIN - 3' long terminal repeat-self inactivating unit; TetO - tetracycline operator; psi - packaging signal; RRE - reverse response element; mir5' and mir3' - 5' and 3' context sequences of miR30; WPRE - woodchuck hepatitis virus post-transcriptional regulatory element; AmpR- ampicillin resistance; pBR322\_ori- pBR322 origin of replication; SV40 - simian virus 40 polyadenylation signal.

#### 4.2.1.2. Designing and cloning of shRNAmirs into modular lentivectors

The two step protocol for cloning shRNAmirs into pLVmir and the subsequent construction of modular vectors for designated purposes is illustrated in detail in Figures 4.8 and 4.9. This protocol was applied for cloning shRNAmirs targeting mouse Xirp2 mRNA (NM\_001024618). In the first step, sequences predicted to target Xirp2 mRNA ( see Appendix Table 4 for the actual sequences) were selected based on the siDESIGN algorithm (Dharmacon, Lafayette, USA) and converted to shRNAmir sequences with XhoI and EcoRI ends as shown in Figure 4.8., using a previously published protocol (Paddison et al., 2004a).

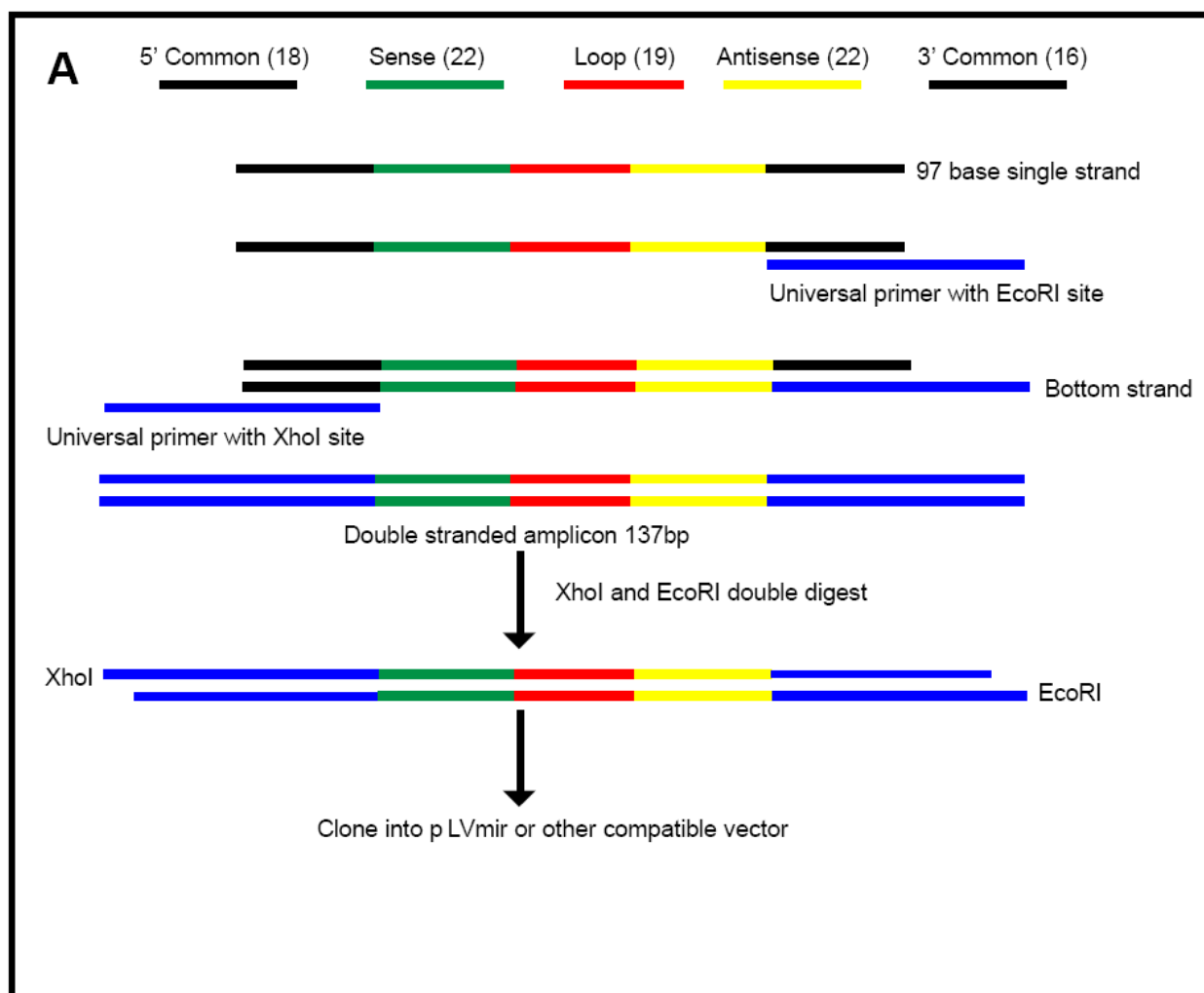


**Figure 4.8. Schematic diagram showing the designing and cloning of shRNAmirs.** Panel A shows the method for the conversion of siRNAs into shRNAmirs. To start with, a 22 nucleotide sense sequence that can potentially target the mRNA of a gene under consideration is identified with siDESIGN algorithm (<http://www.dharmacon.com/DesignCenter/DesignCenterPage.aspx>). Subsequently, a 97 base single strand is designed based on RNAi oligo retriever (<http://www.cshl.org/public/SCIENCE/hannon.html>) as shown in the Figure. Universal primers with XhoI and EcoRI in forward and reverse direction respectively amplify the single strand DNA to a double strand. The resulting amplicon is double digested with these enzymes and cloned into pLVmir or other compatible vectors. B) Shows the alignment of universal primers with the 97-base single strand nucleotide.

The shRNAmir sequences generated from this protocol were double digested with XhoI and EcoRI and cloned into the correspondingly prepared pLVmir-stuffer. Successful cloning removes

the stuffer sequence (4.3kb) and introduces a short fragment of 110 bp consisting of the hairpin sequence. Alternatively, shRNAmir clones from pSM2 (retroviral) or pGIPZ (lentiviral) public libraries can be excised and cloned into pLVmir using the same restriction sites.

#### 4.2.1.3. Construction of modular vectors based on pLVmir

In the second step, the NotI and SpeI double digested fragment of pLVTHM (the 3184bp shorter fragment also designated as module IA, Appendix Figure 3 and Figure 4.9) was cloned into correspondingly prepared pLVmir harboring the hairpin sequence (from step one) to generate a lentiviral vector pLVET-mir, constitutively expressing GFP and cloned shRNAmir sequence under the control of EF1 $\alpha$  (Elongation factor 1 $\alpha$ ) promoter.

Repeating the same step with NotI and SpeI double digested fragment of pLVET-tTRKRAB ( the 4811 bp, shorter fragment, designated as module IB, Appendix Figure 4 and Figure 4.9) generated a lentiviral vector ( pLVET-tTRKRAB mir) conditionally expressing GFP and the shRNAmir sequence under the control of EF1-alfa promoter. The tTRKRAB module provides conditionality to the system (Szulc et al., 2006). The EF1-alfa promoter can be exchanged with the CAG (cytomegalovirus (CMV) early enhancer element and chicken beta-actin combination) promoter in both constitutive and conditional versions by cutting and replacing NotI and PacI fragment in these vectors with that of pLVCT-tTRKRAB (Appendix Figures 1 and 4). Alternatively, the 4372 bp, SpeI digested fragment (Figure 4.6 and cloning scheme ) of pLVCT-tTRKRAB can be replaced into pLVmir containing the cloned shRNAmir sequence from step one by using single restriction site SpeI and selecting clones containing the 4732 bp insert in the right orientation to give pLVCT-mir or pLVCT-tTRKRABmir versions. The Tet-off version, pLVCT-rtTRKRAB-2SM2 (Appendix Figure 5) was generated following a similar protocol.

The scope of the modular design was further extended by transferring additional Pol III based shRNA or shRNAmir expression cassettes into the plasmid, pLVTHM using EcoRI and ClaI sites. All existing shRNA or shRNAmir expression cassettes once transferred into the above restriction sites in pLVTHM backbone are amenable to this modular design. As example, three new plasmids pLVTU6+1, pLVTHM-mir, pLVTU6-mir harboring U6-shRNA, H1-shRNAmir and U6-shRNAmir expression cassettes respectively, were created (Figure 4.9, modules IIIB, IIIC and IIID). Plasmid pLVTHM is designated as module IIIA.

#### 4.2.1.3.1. Construction of pLVTHM-mir

A new plasmid pLVTHM-mir for expression of shRNAmir's from H1 promoter was constructed based on pLVTHM backbone as described in the steps below.

In a first step the SalI site positioned directly upstream of the EF1 alpha promoter in pLVTHM was destroyed by digesting with SalI, blunting the resulting sticky ends and religating to give a new plasmid pLVTHM $\Delta$ SalI. Subsequently, a small stuffer sequence [sequence corresponding to the cDNA encoding the C-terminal region or tail portion of desmin, (accession number [NM\\_001927.3](#))] was amplified with a forward primer containing an MluI site and a reverse primer containing both a SalI and a ClaI site. The above amplicon was cloned into MluI and ClaI sites in pLVTHM $\Delta$ SalI, resulting in a further new plasmid called mpLVTHM $\Delta$ SalI, with a new SalI site introduced between MluI and ClaI. Finally, the miR30 sequence from the vector pSM2(Chang et al., 2006) was amplified with a forward primer containing MluI site and a reverse primer containing a SalI site and cloned into MluI and SalI sites in mpLVTHM $\Delta$ SalI to give a new vector, pLVTHM-mir. This vector expresses the shRNAmir from the H1 promoter.

#### 4.2.1.3.2. Construction of pLVTU6+1

The U6-shRNA cassette from the plasmid pTZU6+1 is a kind gift from Prof. John. J. Rossi, (Beckmann Research Institute, City of Hope, CA, USA), (Lee et al., 2002) was transferred to pLVTHM $\Delta$ SalI XbaI (plasmid generated by successive deletion of SalI and XbaI restriction sites at positions 2028 and 5885 respectively) using the EcoRI and ClaI sites to give the new plasmid pLVTU6+1 which can be used for expression of shRNA from U6 promoter.

#### 4.2.1.3.3. Construction of pLVTU6-mir

The U6-shRNAmir cassette from pSM2 was transferred to pLVTHM $\Delta$ SalI using BamHI (blunted) and MluI sites on the former and EcoRI (blunted) and MluI sites on the later, to create a new plasmid pLVTU6-mir which can be used for expression of shRNAmir from U6 promoter.

#### 4.2.1.4. Construction of constitutive and conditional transgene modules

A lentivirus that enables expression of actin-GFP was constructed by the transfer of the actin-GFP sequence from a pMypG vector to pLVCT-tTRKRAB using MluI and XbaI (blunted) on pMypG and MluI and SmaI sites on pLVCT-tTRKRAB to give the conditional version of

transgene module i.e. pLVCT-Actin-GFP-tTRKRAB. Digesting the conditional version with EcoRI and self-ligating the larger fragment yields the constitutive version of the transgene module. The constitutive version of the vector can be used to clone any gene by replacing actin sequence using the PmeI, BamHI or MluI and the SalI sites. Schematic representation of all the cloned vectors and the corresponding modules are shown in Figure 4.9.

#### 4.2.1.5. Compatible vectors for cloning into Pol III modular vectors

The modular vectors constructed in this work are not limited to the expression cassettes described above in this work. This system can be used to exchange the expression cassettes from various other vectors enabling these expression cassettes to be used in this modular setting. A list of the compatible vectors and their cassettes is given in Table 4.1 below.

**Table 4.1. Compatible vectors for cloning into Pol III modular vectors**

Source vector	Expression cassette from source vector	Target vector	Expression cassette replaced from target vector
pSUPER	EcoRI-ClaI (H1-shRNA)	pLVTHM or pLVTHM-mir *	EcoRI-ClaI (H1-shRNA)
pRSC	EcoRI-XhoI (H1-shRNA)	pLVTHM-mir **	EcoRI-Sal (H1-shRNAmir)
pSM2	SalI-MluI (shRNAmir)	pLVTU6-mir	Sal-Mlu (shRNAmir)
pSM2 and pGIPZ	XhoI-EcoRI (hairpin)	pLVmir	Xho-EcoRI (hairpin)

pSUPER is the first plasmid-based vector for shRNA expression (developed at Netherlands Cancer Institute (NKI)) and one of the most popular vectors in the scientific community (Brummelkamp et al., 2002). pRSC (Retro Super Cam) is a retroviral library vector developed at NKI. The NKI library targets about 8000 human genes and 15000 mouse genes with 3 or 2 shRNA constructs per gene, respectively. Hannon-Elledge libraries are second generation libraries utilizing shRNAmir design instead of shRNA design. These libraries include both pSM2 (Retroviral library) and pGIPZ (Lentiviral library) and are marketed by Open Biosystems and cover 30,000 human and 30,000 mouse genes with 3 constructs per gene. In pSM2 vectors shRNAmir is driven by a U6 (Pol III) promoter whereas in pGIPZ vectors shRNAmirs are driven by the CMV (Pol II) promoter. Although the Hannon-Elledge library also exists as conditional vectors (Tet-repressor system), the system only allows for control of a Pol II promoter and the system tends to be leaky.

\*The H1-shRNA cassette from pSUPER can also be cloned into pLVTHM-mir using the same EcoRI-Cla sites. In this case the H1- shRNA cassette from pSUPER replaces the H1-shRNAmir cassette in pLVTHM-mir.

\*\*XhoI and SalI sites are compatible and the H1- shRNA cassette from pRSC replaces the H1-shRNAmir cassette in pLVTHM-mir.

#### 4.2.1.6. The modular nature of the vectors

The core of this vector system is based on the lentivirus transfer vector, pLVmir (Figure 4.7), which was constructed from pLVCT-tTRKRAB and pGIPZ. Defined portions of this vector may be replaced by distinct modules from various other vectors using simple cloning steps (Figure 4.9). Module I, offers the possibility to select from a variety of constitutive and conditional gene expression control regions, while in module IIB, present in pLVmir, any available shRNAmir sequence can be cloned, the expression of which is driven by the promoter chosen in module I. Alternatively, the shRNAmir cassette can be excluded by choosing module IIA from pLVTHM. Module III (IIIA, IIIC, IIID or IIIE) offers additional Pol III promoter-driven shRNA or shRNAmir expression cassettes. The Pol III expression cassette can be excluded by choosing module IIIB from pLVmir. In principle, all permutations and combinations of modules I, II and III are possible. The complete list of combinations of modules, the resulting vectors and their potential applications are given in Table 4.3. Since there is no promoter in the pLVmir, it cannot be used as a stand-alone vector. However, it offers high flexibility in that any desired promoter (e.g. tissue-specific, ubiquitous Pol II such as CAG, CMV, or Pol III (H1 or U6) can be inserted upstream of the SpeI restriction site. Table 4.2. presents a comparison of the vectors generated in this work with various currently available vectors for RNAi emphasizing on the method of selection of stable RNAi clones, the silencing triggers and their expression from various promoters.

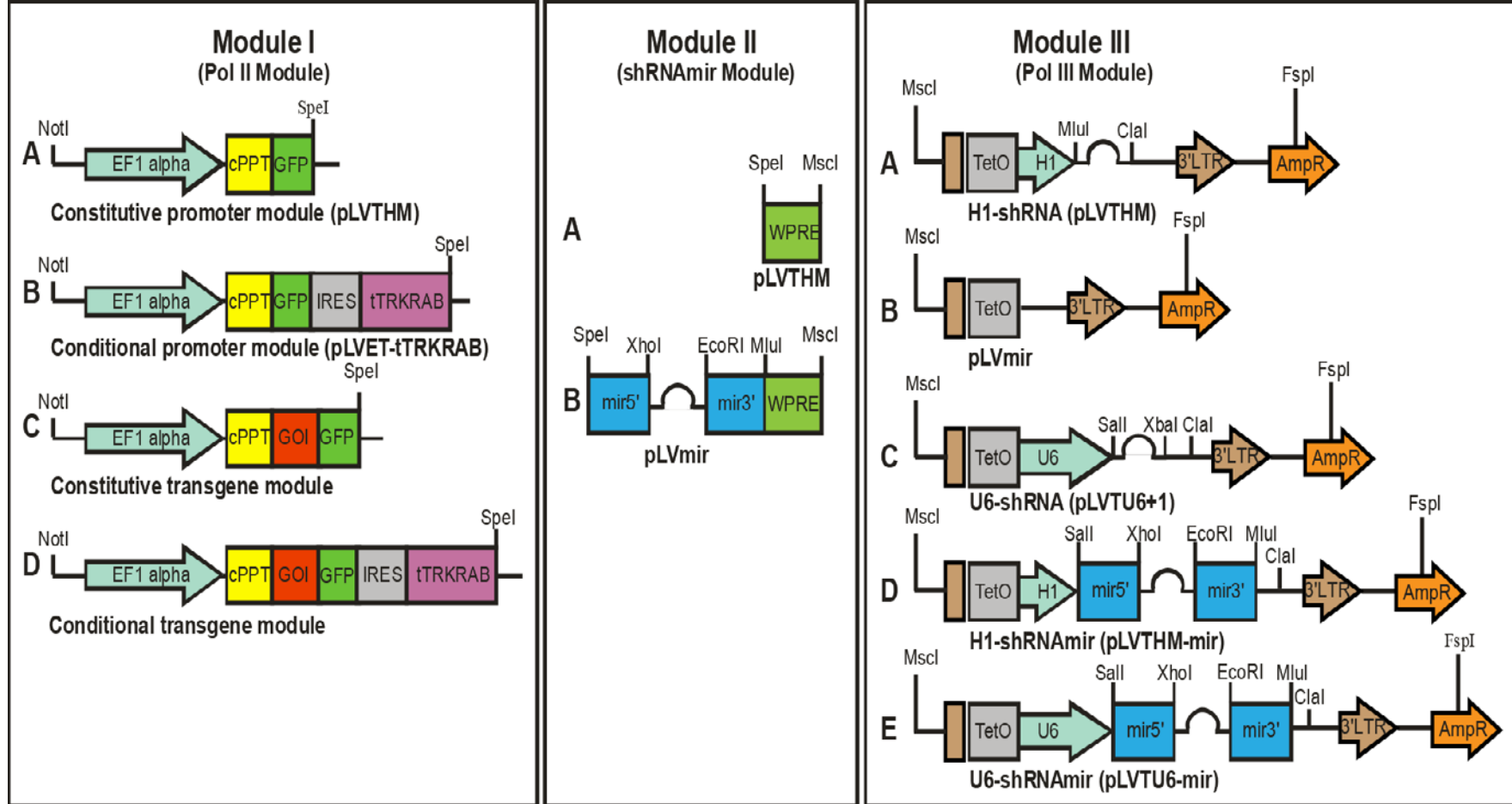


**Figure 4.9. Schematic diagram showing all modules that may be combined to achieve transgene expression and/or knockdown.** The complete list of combinations of modules, the resulting vectors and their potential uses are given in Table 4.3. All vectors except pLVTHM were constructed in this work. EF 1 alpha - Elongation factor 1 alpha promoter; cPPT - central polypurine tract; GFP - Green fluorescence protein; GOI-GFP - a GFP fusion protein of gene of interest; IRES - internal ribosomal entry site; tTRKRAB - a fusion protein of tetracycline repressor (tetR) and Krüppel-associated box (KRAB) domain; GFP, GOI-GFP, tTRKRAB and the shRNAmir in module IIB are expressed from the EF-1 alpha promoter. shRNAmirs in pLVTHM-mir and pLVTU6-mir are expressed from the H1 and the U6 promoters, respectively. shRNAs in pLVTHM and pLVTU6+1 are expressed from the H1 and the U6 promoters, respectively.

**Table 4.2. Comparison of the vectors generated in this work with currently available vectors for RNAi**

<b>Vector</b>	<b>FACS-based selection</b>	<b>Antibiotic selection</b>	<b>shRNAmir expression</b>	<b>shRNA expression</b>
pSM2	No	Yes	Constitutive from U6(Pol III) promoter	No
pGIPZ	Yes	Yes	Constitutive from CMV(Pol II) promoter	No
pLVTHM	Yes	No	No	Constitutive (H1-shRNA)
PLVET-tTRKRAB or pLVCT-tTRKRAB	Yes	No	No	Conditional if H1-shRNA from pLVTHM is cloned
pLVmir * *Vector constructed in this study	Yes	No	Constitutive/ conditional from Pol II (CAG or ET) if module IA + module IIB+ module IIIB is chosen, from Pol III (H1 or U6) if module IA + module IIA + module IIID or IIIE is chosen	Module IIIA or IIIC should be cloned. Constitutive/ Conditional depending on module I chosen
pSico	Yes	No	No	A functional U6-shRNA expression cassette is restored after Cre based excision of CMV-GFP and sorting GFP-negative cells.
pSico-R	Yes	No	No	A functional U6-shRNA expression cassette is removed after Cre based excision of U6-shRNA cassette and sorting for GFP -positive cells.

**Table 4.3. List of combinations of modules, the resulting vectors and their potential use.**

<b>A) Vectors for gene knockdown from Pol III promoters</b>				
<b>Module I</b>	<b>Module II</b>	<b>Module III</b>	<b>Name of the vector</b>	<b>Proposed uses</b>
IA	IIA	IIIA	pLVTHM (Addgene)	Constitutive single gene knockdown (H1-shRNA)
IA	IIA	IIIC	pLVTU6+1	Constitutive single gene knockdown (U6-shRNA)
IA	IIA	IIID	pLVTHM-mir	Constitutive single gene knockdown (H1-shRNAmir)
IA	IIA	IIIE	pLVTU6-mir	Constitutive single gene knockdown (U6-shRNAmir)
Replacing IA with IB in the above vectors yields corresponding conditional single gene knockdown vectors.				
<b>B) Vectors for gene knockdown from Pol II promoters</b>				
IA	IIB	IIIB	pLVET-mir	Constitutive single gene knockdown
IB	IIB	IIIB	pLVET-Kmir	Conditional single gene knockdown
K= IRES-tTRKRAB				
<b>C) Vectors for transgene expression</b>				
IC	IIA	IIIB	pLVET-GOI-GFP	Constitutive transgene expression
ID	IIA	IIIB	pLVET-GOI-GFP-K	Conditional transgene expression
<b>D) Vectors for combined transgene expression and gene knockdown with shRNAmirs/shRNAs or rescue plasmids</b>				
IC	IIB	IIIB	pLVET-GOI-GFP-mir	Constitutive rescue plasmid, shRNAmir expressed from EF1 $\alpha$ promoter
IC	IIA	IIID	pLVET-GOI-GFP-Hmir	Constitutive rescue plasmid, shRNAmir expressed from H1 promoter
IC	IIA	IIIE	pLVET-GOI-GFP-U6mir	Constitutive rescue plasmid, shRNAmir expressed from U6 promoter

IC	IIA	IIIA	pLVET-GOI-GFP-Hs	Constitutive rescue plasmid, shRNA expressed from H1 promoter
IC	IIA	IIIC	pLVET-GOI-GFP-U6s	Constitutive rescue plasmid, shRNA expressed from U6 promoter

Module IC can be replaced with ID to get corresponding conditional versions. GOI-GFP is expressed from EF1 alpha promoter in both constitutive and conditional versions.

### E) Vectors for synergistic effect and simultaneous knockdown

IA	IIB	IIIA or	pLVET-mirHs	Constitutive synergistic effect or simultaneous knockdown
		IIIC or	pLVET-mirU6s	
		IIID or	pLVET-mirHmir	
		IIIE	pLVET-mirU6mir	
IB	IIB	IIIA or	pLVET-KmirHs	Conditional synergistic effect or simultaneous knockdown
		IIIC or	pLVET-KmirU6s	
		IIID or	pLVET-KmirHmir	
		IIIE	pLVET-KmirU6mir	

## 4.2.2. Validation of the modular vectors

### 4.2.2.1. Confirmation of hairpins after cloning into modular vectors

The modular vectors constructed in this work and the method of cloning hairpins (shRNAs and shRNAmirs) into such vectors was validated by performing control restriction digests and comparing the shorter fragments as shown in Figure 4.10. The comparison gives a guide for selection of right clones of modular lentiviral vectors harboring the required number of hairpins for synergistic and multiple gene knockdown strategies. Primers suggested for sequencing the shRNAmir/shRNA hairpins in the modular vectors are given in Appendix Table 2.

### 4.2.2.2. FACS based validation of cloned vectors demonstrates functionality of the modular design

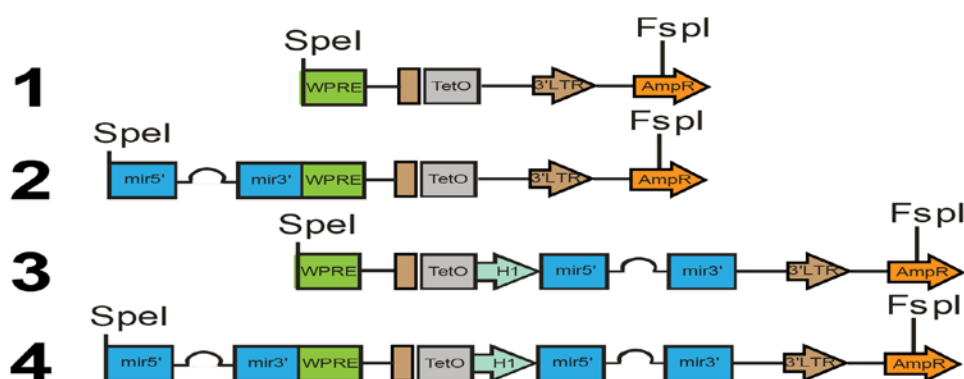
The functionality of selected module combinations in this design was tested experimentally. To do this, HEK293T cells were transduced with a lentivirus consisting of modules IB and IIB (Figure 4.11A). The module IB contains the EF1 $\alpha$  promoter that can be controlled by the tTRKRAB component of the module. Module IIB contains the shRNAmir sequence cloned into this module. Since the region containing the module IIB differs from the original lentiviral vector (see pLVCT-tTRKRAB and module IB in Appendix Figure 1 and Figure 4.9, respectively), the lentiviral vectors created by combining these modules were characterized for their functionality

and reversibility of the system. HEK293T cells carrying the virus were first maintained in medium containing high concentrations of doxycycline (1 $\mu$ g/ml). The cells were subsequently split into two dishes and further maintained in the presence or absence of doxycycline respectively.

**A**

Sr. No	Number of hairpins in the vector	Vector name	Modules
1	No hairpins	pLVCT-tTRKRAB	IIA+ IIIB
2	One hairpin from Pol II	pLVET-mir	IIB+ IIIB
3	One hairpin from Pol III	pLVTHM-mir	IIA+ IIID
4	One hairpin each from Pol II & Pol III	pLVET-mirHmir	IIA+ IIID

**B**



**C**

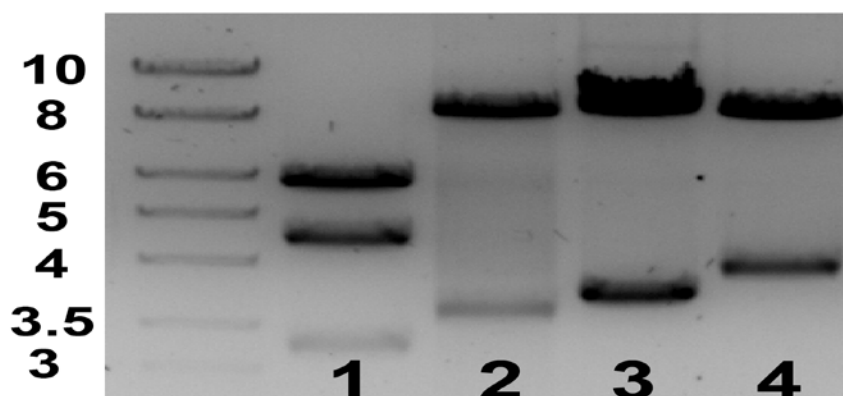


**Figure 4.10. Cloning of hairpins (shRNAmirs) into the modular vectors and confirmation of the presence of hairpins.** Successful cloning of one or two hairpins into modular vectors can be confirmed by SpeI and FspI double digests of vectors containing these hairpins by comparing the size of the smallest fragment. pLVCT-t TRKRAB containing no hairpin (1), pLVET-mir containing single hairpin from Pol II promoter (2), pLVTHM-mir containing single hairpin from a Pol III promoter (3) and pLVET-mirHmir

containing two hairpins one each from Pol II and Pol III (4) are described in (A) and depicted in (B). The smallest restriction fragments (C) match the expected size as schematically represented in (B).

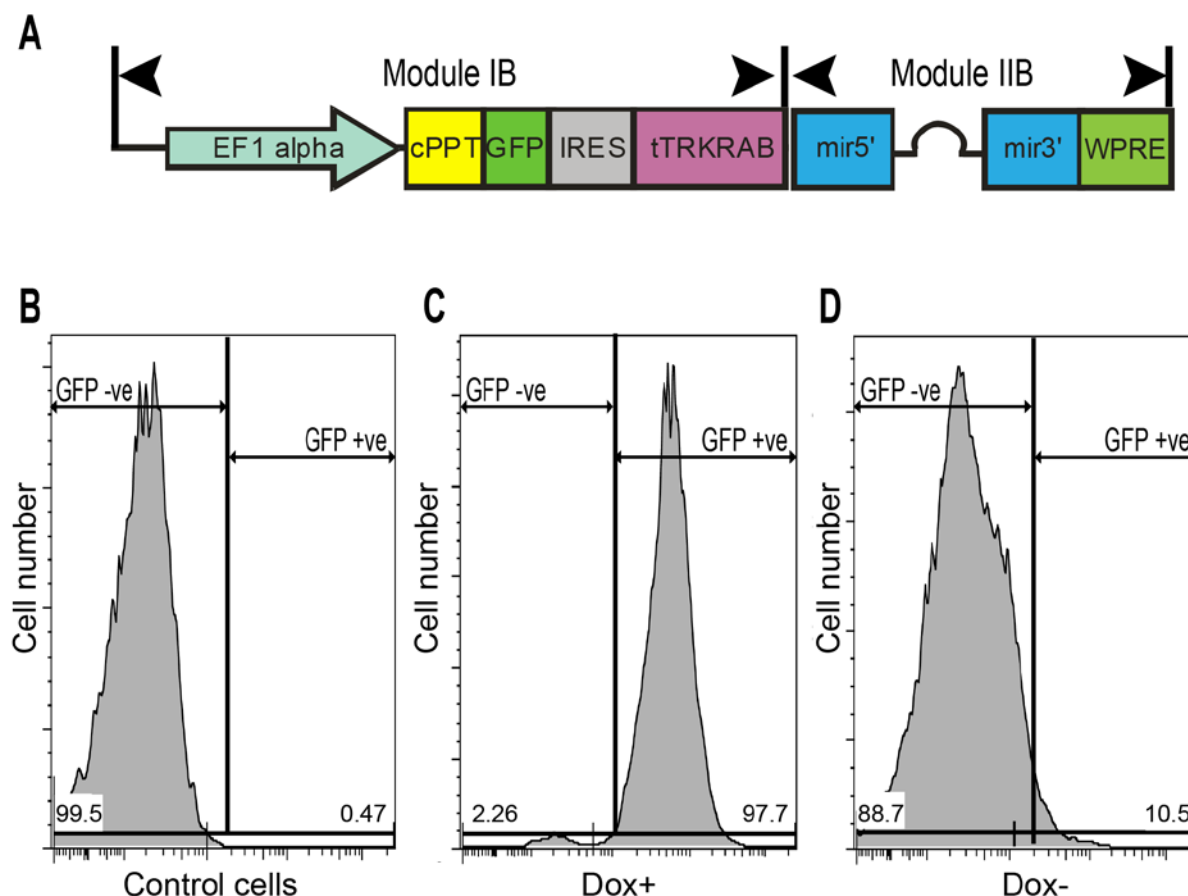


**Figure 4.11. FACS-based validation of the combination of modules IB and IIB in conditional lentiviral vector.** (A) Gives a schematic representation of the modules chosen to construct a conditional lentiviral vector expressing a *Xirp2*-specific shRNAmir. (B-D) FACS analysis of control (untransduced) and transduced HEK293T cells for GFP expression, 48 hours after induction or withdrawal of doxycycline (1 $\mu$ g/ml). Panel B shows control (untransduced) cells. Panel C shows a GFP-positive population of transduced cells subjected to doxycycline treatment. Panel D shows the same cells upon withdrawal of doxycycline. Note that nearly all GFP-positive cells turned GFP-negative in the absence of doxycycline and the GFP expression of cells in panel D is essentially identical to control cells in panel B. Higher doxycycline concentration (1 $\mu$ g/ml) and a relatively quick (within 48 hours) analysis of GFP expression could possibly explain a fast induction (Dox + cells) but a slow tapering of GFP expression (upon Dox withdrawal).

Two days later the cells were analyzed by FACS for GFP expression. FACS results indicated that the cells maintained in the absence of doxycycline (Dox-) were essentially identical to control cells (Figure 4.11D). In contrast, cells maintained in the presence of doxycycline (Dox+) were almost exclusively GFP-positive (Figure 4.11C). These results demonstrated the full reversibility of the system since cells that were GFP-positive in the presence of doxycycline,

were fully converted to GFP-negative cells in the absence of doxycycline within 48 hours. Most importantly, the introduction of module IIB did not compromise the original functionality of the system as evidenced by the expression of GFP, which confirms the functionality of the promoters in module I, and the working of the “on-off” switch, which confirms the inducibility of the system.

Any functional shRNA or shRNAmir sequence expressed from a Pol III promoter (a list of compatible vectors was provided in Table 4.1) can be transferred to the modular vectors created in this study. Since each module functions individually, the combination of the modules would be expected to be functional. Some examples of combinations of modules are shown below.

#### 4.2.2.3. Validation of constitutive transgene modules by the analysis of protein expression and localization

To test if the modular lentiviral vectors could be used for constitutive transgene expression, the muscle specific transcription factor MyoD and Ig-like domains 18-21 of the cross striated muscle specific protein filamin C (FLNC d18-21) were expressed in HEK293 cells using lentiviral transduction as shown below.

##### 4.2.2.3.1. Expression of MyoD in HEK293 cells

To test the constitutive transgene module, a lentivirus expressing a C-terminal fusion of MyoD with GFP was produced and transduced into HEK293 cells. The results (Figure 4.12) show that the transcription factor MyoD localized to the nucleus as expected confirming that the lentiviruses constructed by this method can be used for gene expression.

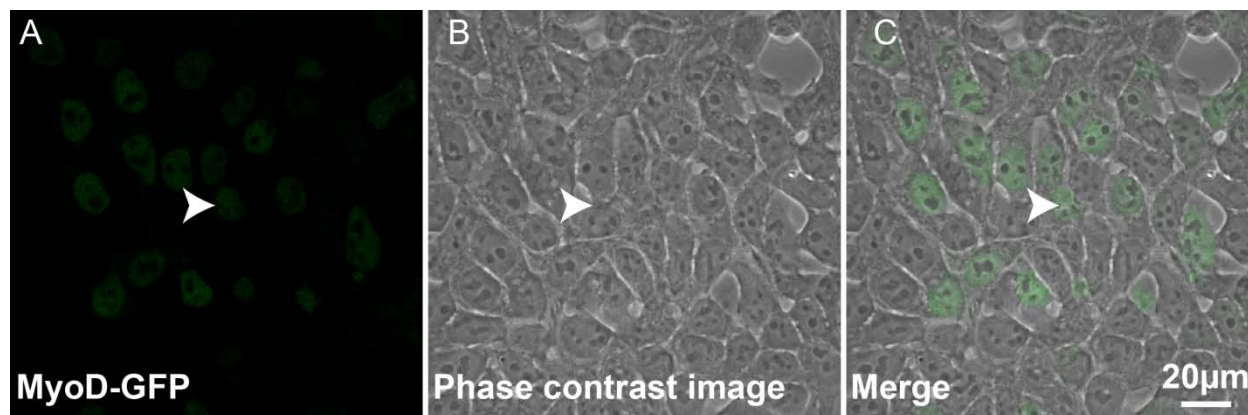


**Figure 4.12. Expression of MyoD-GFP in HEK293 cells.** HEK293 cells were transduced with a virus resulting in constitutive expression of a C-terminal GFP fusion protein of MyoD. Note that the transcription factor MyoD is expressed and localized to the nucleus of these cells (arrow head). Transduced cells were not selected for GFP expression by FACS. Therefore, not all cells are transduced and express GFP.

#### 4.2.2.3.2. Expression of filamin C d 18-21 in HEK 293 cells

The filamin C domain 18-21 (FLNCd18-21) region, which is known to contain several protein-protein interaction motifs, was expressed as a C-terminal GFP fusion protein in a constitutive manner from the EF1 $\alpha$  promoter using a lentiviral transduction in HEK293 cells. For this purpose, the cDNA of ACTA was replaced with the cDNA of filamin C domain 18-21, in the constitutive transgene module (Figure 4.9). Lentiviruses generated using this construct were transduced into HEK293 cells and stable cell lines were generated by FACS selection. A control lentivirus expressing GFP alone was also used for comparison of protein extracts by Western blotting. Expression of the construct resulted in the protein of expected size (~ 78kD). The resulting cells could be used for biochemical studies of protein-protein interactions.

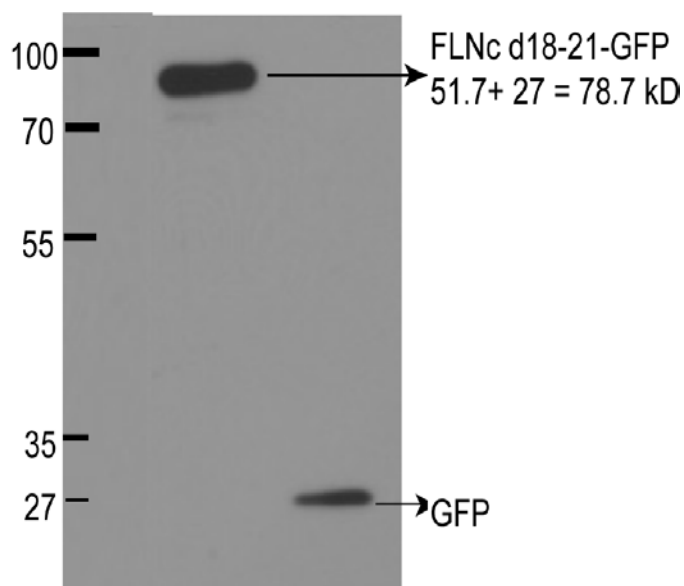


**Figure 4.13. Analysis of expression of FLNCd18-21-GFP fusion protein and GFP control protein in HEK293 cells by Western blotting.** Lentiviruses constitutively expressing either a FLNC d18-21-GFP fusion protein or a control GFP protein were transduced into HEK293 cells. The resulting cells were further allowed to proliferate. Western blots were performed to confirm the expression of proteins of expected size. Cells harboring the GFP virus showed the GFP protein band at 27 kD, whereas cells harboring a GFP fusion of FLNC d18-21 showed the expected protein band at 78 kD.

### 4.2.3.1 Selection of siRNAs

To elucidate the possible role of Xirp2 in myofibrillogenesis and myodifferentiation, a functional knockdown of Xirp2 via RNAi was attempted. The mouse *Xirp2* gene (NM\_001024618.2) contains a total of 9 exons. The exon 7 is the largest exon and harbors most of the entire coding information. Differential splicing results in alternative usage of exons 8 or 9 resulting in expression of Xirp2 protein isoforms 1 and 2, respectively (Fig.4.14). A total of three siRNAs that target Xirp2 were selected based on the siDESIGN algorithm (Table 4.2). The positions of siRNAs are schematically represented in Figure 4.14. The chosen siRNAs target different splice variants. In this case sequence #1 and #2 target isoform 1, and isoforms 1 and 2, respectively. Selected siRNAs were converted to shRNAmirs and cloned into modular lentiviral vectors as shown in Figure 4.8.

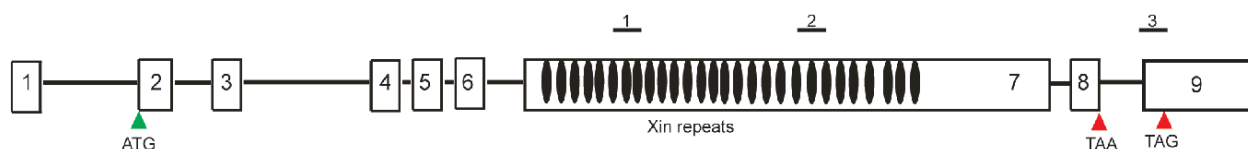


**Figure 4.14. Selection of siRNAs targeting *Xirp2* gene.** A total of three siRNAs predicted to target mouse *Xirp2* (NM\_001024618.2) were selected based on siDESIGN algorithm). siRNAs # 1 and #2 target in exon 7, whereas siRNA# 3 targets in exon 9. siRNA #1 targets both mouse *Xirp2* (NM\_001024618.2) and human *XIRP2* (NM\_152381.4).

### 4.2.3.2. Lentiviral transduction and establishment of stable cell lines from mouse and human skeletal muscle cell lines

Whereas HEK293 cells could be transduced with a high efficiency with non-concentrated lentiviral supernatants (titers  $\approx 10^6$  particles/ml, 50 to 100  $\mu$ l was sufficient to obtain 100% transduction in a 12 well plate), only poor transductions were achieved in case of both, primary skeletal muscle cells and muscle cell lines. Lentivirus was therefore concentrated to titers of  $\approx 1 \times 10^9$  particles/ml using an ultracentrifuge (Materials & Methods). Additionally, a higher Multiplicity of Infection (MOI) of 20-30 was used, resulting in approximately 50-70 % GFP-positive cells as recorded by FACS analysis. GFP-positive muscle cell lines were collected and grown further, thereby establishing stable cell lines. Transduced skeletal muscle cells containing conditional versions of shRNAmir sequences displayed their conditionality and reversibility. When these GFP-positive sorted muscle cell lines were cultured in media containing doxycycline, GFP expression remained stable even after 15 passages confirming stable long-term

GFP-expression in these cultures. On the other hand, culturing this GFP-positive sorted cells in the absence of doxycycline, turned them to GFP-negative cells confirming that the EF1 $\alpha$  promoter can be effectively switched off in skeletal muscle cells (Figure 4.15).

#### 4.2.3.2.1. Significance of fixation methods in Xin and Xirp2 antibody staining in Xirp2 knockdown cells

HSKM, H-2K<sup>b</sup>-tsA58 and C2C12 cells expressing lentiviral knockdown constructs were differentiated and processed for immunofluorescence by either paraformaldehyde (PFA) fixation or methanol-acetone fixation. PFA fixation preserves the cytosolic GFP in transduced cells enabling the visualization of transduced cells along with additional antibody stainings. However, XR1B and mAb XIRP2 or polyclonal XIRP2 antibodies were not reactive upon PFA fixation. Moreover, simultaneous labeling with three antibodies could not be achieved with this method. Methanol-acetone fixation removed cytosolic GFP from transduced cells, enabling triple labeling with three antibodies in these cells. Since primary murine muscle cells were not stably selected after transduction with lentiviral constructs, these cells were fixed using PFA fixation to be able to optically confirm the transduction efficiency. Subsequently, methanol-acetone fixed cells were used to study the myofibrillar arrangement with antibodies directed against three different proteins that were applied simultaneously.

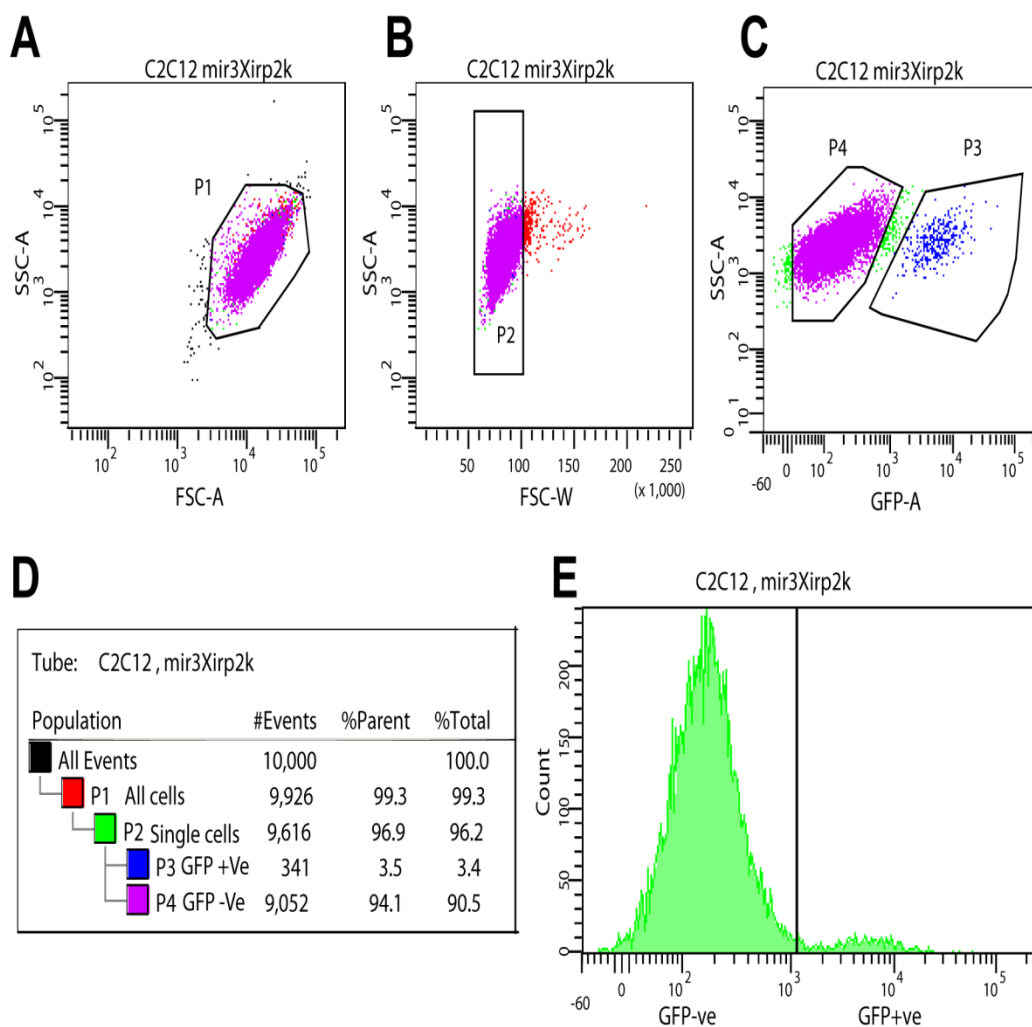


**Figure 4.15. FACS-based testing of promoter switch off in the absence of tetracycline in C2C12 cells transduced with a conditional version of shRNAmir targeting Xirp2.** C2C12 cells were transduced with lentivirus conditionally expressing shRNAmir driven by the EF1 $\alpha$  promoter. Transduced cells were cultured in proliferation media containing doxycycline and GFP-positive cells were sorted. Subsequently, these cells were maintained in the absence of doxycycline for 3 days and GFP expression was analyzed by FACS to quantify the percentage of GFP-positive cells. Panel A shows all the cells that were analyzed, Panel B shows single cells (free of clusters and doublets of cells) and Panel C shows the GFP-positive (P3) and GFP-negative (P4) gates used for sorting the cells on a BD FACSDIVA flow sorter. Panel D gives a table summarizing the percentage of each population of cells. Panel E shows a relative percentage of GFP-negative (P4 gate) and GFP-positive (P3 gate) cells. This result demonstrates that the EF1 $\alpha$  promoter can be switched off effectively in muscle cells.

#### 4.2.3.3. Confirmation of Xirp2 knockdown

To quantify the level of Xirp2 knockdown in C2C12 and H-2K<sup>b</sup>-tsA58 cells, RNA was isolated from transduced and stably selected cells. Isolated RNA was reverse transcribed and quantitative real time PCR (qRT-PCR) was performed (see Materials & Methods). For confirmation of

knockdown in HSKM cells a Western blot was performed. The schematic representations of the modules used to construct these lentiviruses is shown in Figure 4.16A. Sequences mir1Xirp2 and mir2Xirp2 are expressed constitutively from EF1 $\alpha$  promoter, whereas sequence mir3Xirp2K is expressed conditionally from the same promoter. Cells transduced with the latter virus were maintained in the presence of medium containing doxycycline at 1 $\mu$ g/ml concentration to induce the expression of GFP and the shRNAmir sequence.

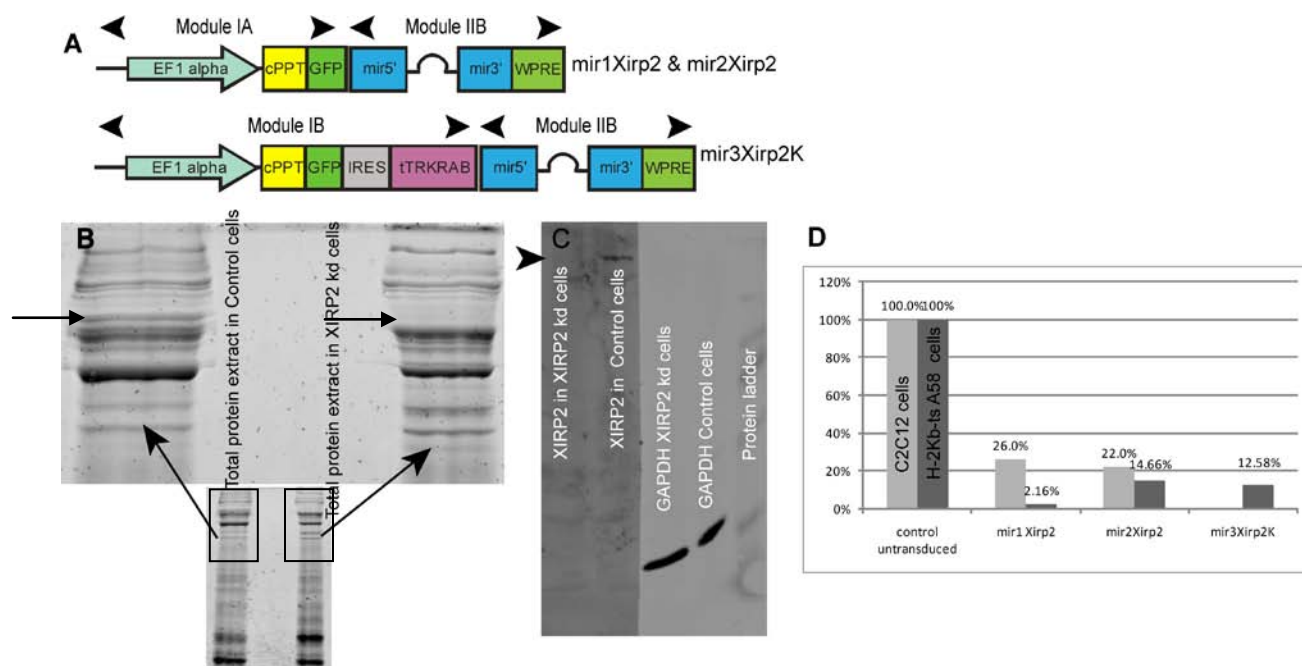


**Figure 4.16. Knockdown levels obtained with different shRNAmir sequences targeting the endogenous *Xirp2* mRNA in HSKM, H-2K<sup>b</sup>-tsA58 and C2C12 cells.** (A) Schematic representation of the modules used to construct the viruses. (B) Coomassie staining of total protein extracts from untransduced HSKM cells and HSKM-Xirp2 knockdown cells confirming the nearly identical total protein expression profiles. Note that one specific band that might represent Xirp2 is missing in knockdown cells (arrow). (C) Western blot comparing Xirp2 expression in untransduced HSKM cells and HSKM-Xirp2 knockdown cells. Note the disappearance of Xirp2 protein band in HSKM-Xirp2 knockdown cells (arrowhead). (D) Remaining percentage of endogenous *Xirp2* mRNA (by a q-RTPCR experiment) in C2C12 and H-2K<sup>b</sup>-tsA58 from stably transduced and FACS-sorted cells undergoing differentiation for six days. GAPDH served as control for equal protein loading.

Analysis of total protein extracts from HSKM cells transduced with mir1Xirp2 sequence showed a nearly identical total protein expression profile, except for one band that might represent human Xirp2 (Figure 4.17B). Western blots performed to compare Xirp2 expression in untransduced HSKM cells and HSKM-Xirp2 knockdown cells at the protein level showed efficient knockdown. q-RTPCR experiments indicated that all three sequences mediated

significant knockdown of the target mRNA to between approximately 2 and 25% of the original level. The results from Western blot and qRT-PCR validated the *Xirp2* knockdown achieved by the shRNAmir sequences and the lentiviral vectors constructed in this study.

### 4. 3. Consequences of *Xirp2* knockdown in muscle cell lines

#### 4.3.1. *Xin* expression level is unchanged upon knockdown of *Xirp2* in H-2K<sup>b</sup>-tsA58 cells

To determine if *Xirp2* knockdown had any effect on the expression of the closely related *Xin* protein, semi-quantitative RT-PCR and Western blot analysis were performed. H-2K<sup>b</sup>-tsA58 cells stably transduced with lentiviral shRNAmir sequences targeting *Xirp2* were differentiated for six days and RNA and total protein extracts were made from these cells. A semi-quantitative RT-PCR comparison of *Xirp1* and *Xirp2* expression in control H-2K<sup>b</sup>-tsA58 and H-2K<sup>b</sup>-tsA58-*Xirp2* knockdown cells (Figure 4.17A) indicates that there is no change in the expression levels of *Xin* in the knockdown cells compared to control cells. Western blots performed using extracts from differentiating H-2K<sup>b</sup>-tsA58-*Xirp2* knockdown cells (Figure 4.17B) indicated that irrespective of the shRNAmir sequence used to knockdown *Xirp2* in these cells, the expression of *XinA* and *XinB* protein isoforms displayed no significant differences compared to control cells. These results indicated no significant changes in *Xin* expression levels both at the mRNA level or protein level consequent to *Xirp2* knockdown.

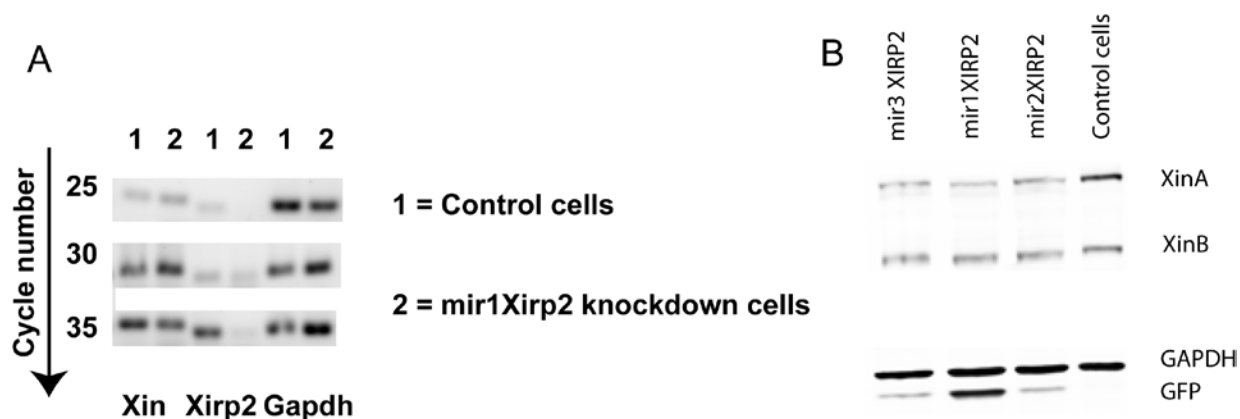


**Figure 4.17. *Xin* expression is unchanged in *Xirp2* knockdown cells both at RNA and protein level.** Panel A depicts a semi-quantitative RT-PCR comparison of *Xin* and *Xirp2* expression levels at the mRNA level in control H-2K<sup>b</sup>-tsA58 and H-2K<sup>b</sup>-tsA58-*Xirp2* (mir1XIRP2) knockdown cells. Gapdh served as

a control. Panel B, shows a Western blot with total protein extracts from various Xirp2 knockdown cells differentiated for six days. At the RNA level the expression of the Xirp2-related gene *Xirp1* was essentially identical in control and Xirp2 knockdown cells. Western blot demonstrates that also at the protein level the expression of Xin did not change significantly. GAPDH served as a loading control. Different GFP signal intensities probably result from varying copy numbers of integrated viruses. Higher GFP-levels (mir1Xirp2) are associated with higher knockdown efficiency (Figure 4.16D).

---

## 4.3.2. Effects of Xirp2 knockdown on muscle cell differentiation

### 4.3.2.1 Knockdown of Xirp2 in human skeletal muscle (HSKM) cells

In HSKM cells, transduction with mir1XIRP2 resulted in a highly specific and efficient knockdown with no significant changes in the expression of related proteins (Figure 4.16A). Cells transduced with mir1XIRP2 normally fused to form elongated multinucleated myotubes (Figure 4.18 A). However, the developing myofibrils appeared severely disrupted and showed no cross-striations (Figure 4.18 C). Xin was localized along actin stress fibers and in myotube ends (Panels I and J) and displayed no significant changes when compared to control cells (Panels E and F). However, control cells transduced with lentivirus containing sequences which were not predicted to target human *XIRP2* and mock-transduced HSKM cells also showed poor differentiation, i.e. fusion but only limited striations. From these results it was concluded that HSKM cell differentiation was not optimal independent of the transduced virus and hence these cells were not used for further experiments. Instead a panel of mouse cells including C2C12, H-2K<sup>b</sup>-tsA58 and primary cells was used.

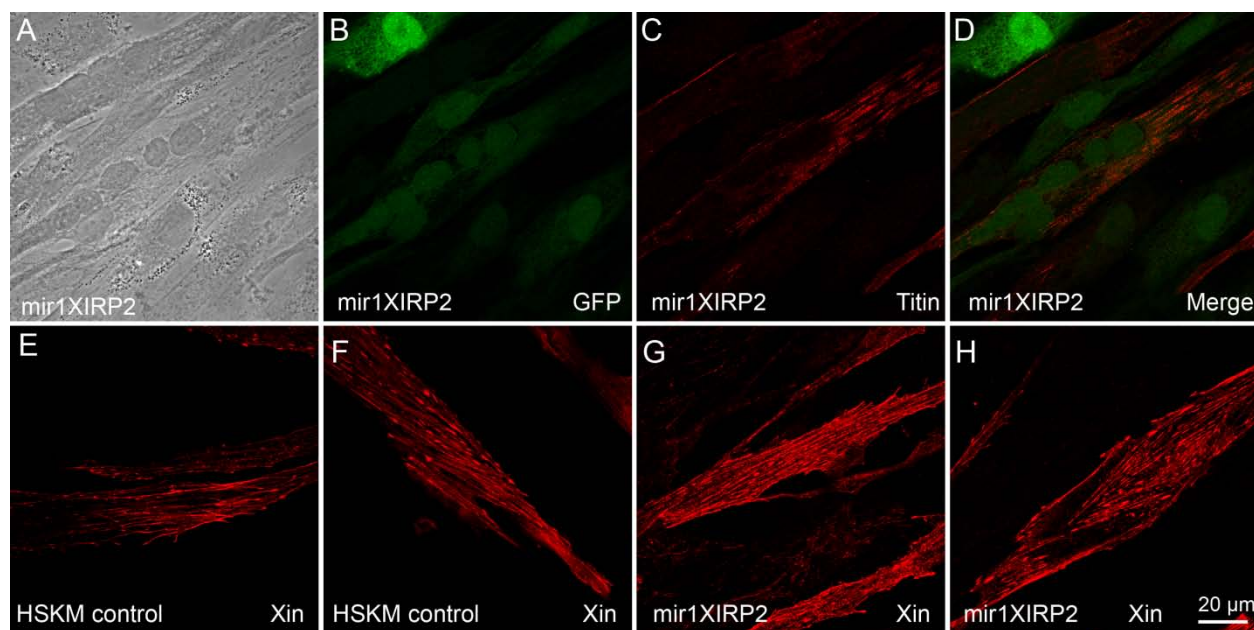


**Figure 4.18. Phenotype in HSKM-Xirp2 knockdown cells.** HSKM-Xirp2 knockdown cells (mir1Xirp2) were differentiated for six days, fixed with PFA (A-D) or methanol/acetone (E-H) and stained for myofibrillar proteins. Panel A, depicts a phase contrast image clearly indicating fusion of cells (multinucleated cell). Panel B, depicts cytosolic GFP confirming successful transduction. Panel C, depicts titin (T12) staining. Note the near complete absence of mature myofibrils in C. Panels E-H depict typical Xin staining patterns along the actin stress fibers and at myotube ends in HSKM control cells (E, F) and HSKM-Xirp2 knockdown cells (G, H). Immunofluorescence images were captured with a LSM 510 confocal laser scanning microscope.

#### 4.3.2.2 Knockdown of Xirp2 in H-2Kb-ts A58 cells

In H-2Kb-ts A58 immortalized mouse muscle cells, Xirp2 knockdown was achieved by three independent shRNAmir sequences mir1Xirp2, mir2Xirp2 and mir3Xirp2K resulting in specific and efficient knockdown (Figure 4.16). Xirp2 knockdown did not alter the expression levels of Xin both at mRNA level and protein level (Figure 4.17). To evaluate if Xirp2 knockdown altered the localization of Xin and other myofibrillar proteins, immunolocalization studies were performed. H-2Kb-ts A58-Xirp2 knockdown cells normally fused to form elongated multinucleated myotubes (Figure 4.19) and displayed typical Xin staining as seen in control cells (Figure 4.19N). Myofibril development was also not significantly altered in knockdown cells. However, a weaker Z-disk staining with T12, an antibody against Z-disk titin, was observed in knockdown cells. In contrast staining for the M-band component myomesin (BB78) appeared normal.

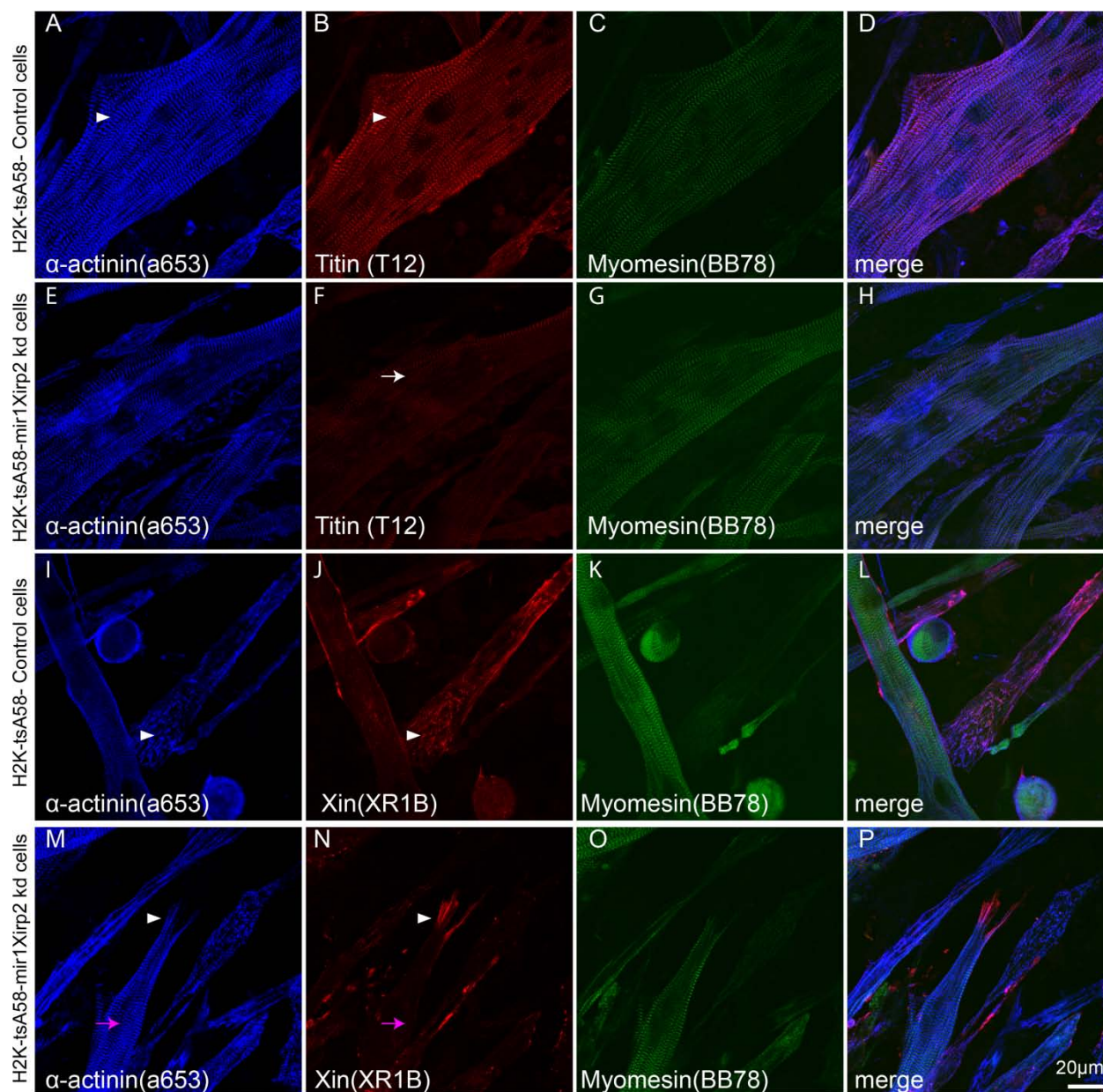


**Figure 4.19. Localization of myofibrillar proteins in untransduced and H-2K<sup>b</sup>-tsA58-Xirp2 knockdown cells.** H-2K<sup>b</sup>-tsA58-Xirp2 knockdown cells differentiated for six days and fixed with methanol/acetone were stained for  $\alpha$ -actinin, titin, Xin and/or myomesin and images were captured with LSM 510 confocal laser scanning microscope. Staining of transduced cells by T12 (F, white arrow) reveals a less intense staining of Z-disks in Xirp2 knockdown cells compared to untransduced control cells (B, arrowhead). Note that Xin (arrowheads in J and N) colocalizes with  $\alpha$  actinin (arrow heads I and M) in non-striated myofibrils (NSMF, but does not colocalize with  $\alpha$ -actinin in striated myofibrils (SMF, pink arrows in M and N) in both control and Xirp2 knockdown cells. The expression of Xin and the M-band protein myomesin are not altered in Xirp2 knockdown cells.

### 4.3.2.3. Knockdown of *Xirp2* in C2C12 mouse myoblasts

Proliferating C2C12 cells were transduced with lentiviral constructs targeting *Xirp2* (Figure 4.16A) and stable cell lines were established in a similar manner to H-2K<sup>b</sup>-tsA58 cells.

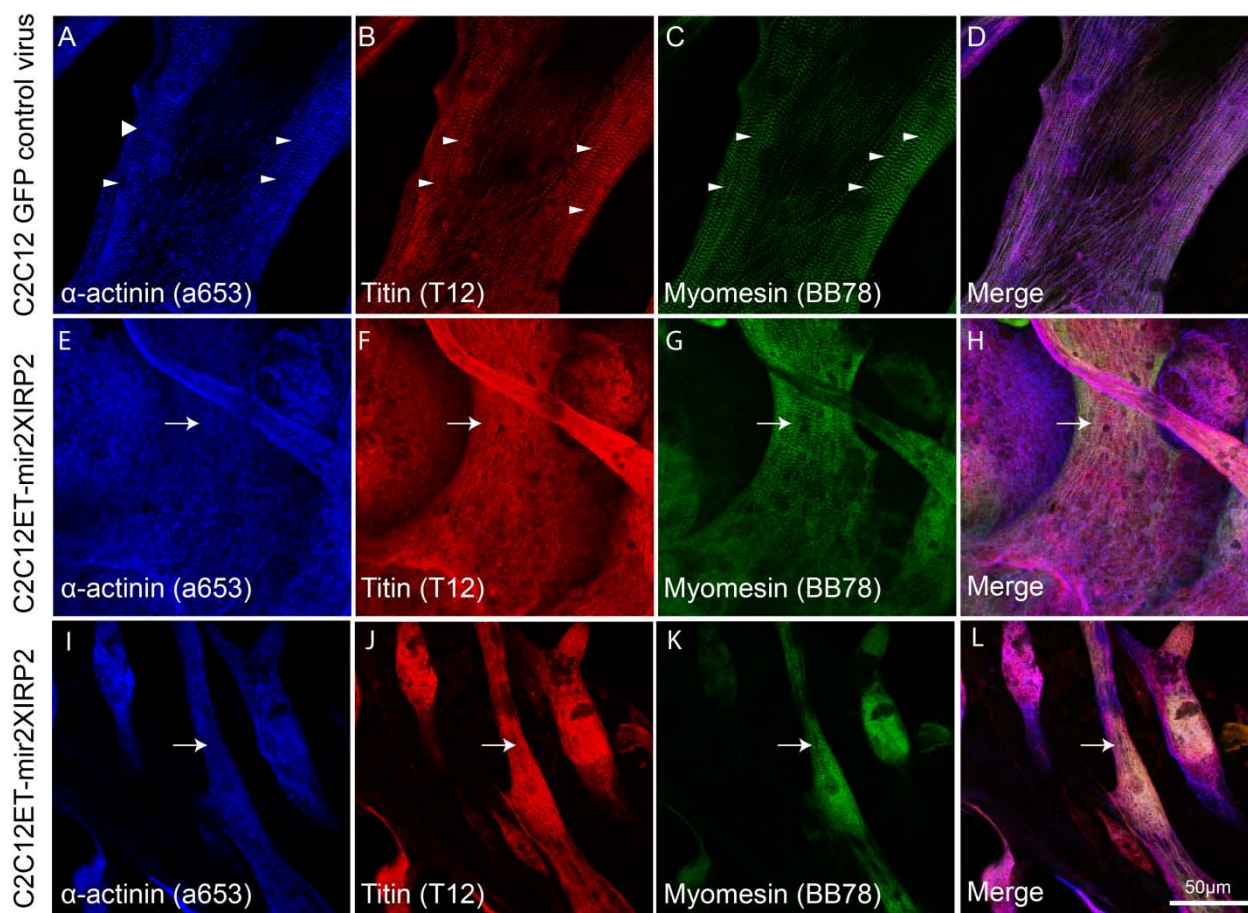


**Figure 4.20. Localization of myofibrillar proteins in mock transduced C2C12 and C2C12- *Xirp2* knockdown cells.** C2C12-*Xirp2* knockdown cells were processed by methanol/acetone fixation after six days differentiation and stained for  $\alpha$ -actinin, titin and myomesin. Immunofluorescence images were captured with LSM 510 confocal laser scanning microscope. Note that upon staining with T12, Z-disks appear disrupted in *Xirp2* knockdown cells (F, J) but not in mock-transduced control cells (B). The expression of  $\alpha$ -actinin and the M-band protein myomesin are relatively normal.

Subsequent immunofluorescence stainings of differentiated C2C12-*Xirp2* knockdown cells with T12, an antibody targeting an epitope in the Z-disk of titin, revealed a disorganization of Z-disks (Figure 4.20, F, J) that was not observed in mock-transduced control cells (B). These cells contained perfectly striated myofibrils. In contrast, the expression of *Xirp2* shRNA did not obviously alter the spatial and temporal expression of the M-band protein myomesin. From these results it can be concluded that fusion of myoblasts to form myotubes is not affected in the

absence of Xirp2. In contrast, Z-disks are disorganized to some degree, whereas significant changes in M-band assembly are not observed.

#### 4.3.2.4. Establishment and transduction of primary muscle cells derived from wild type and Xin knockout mice

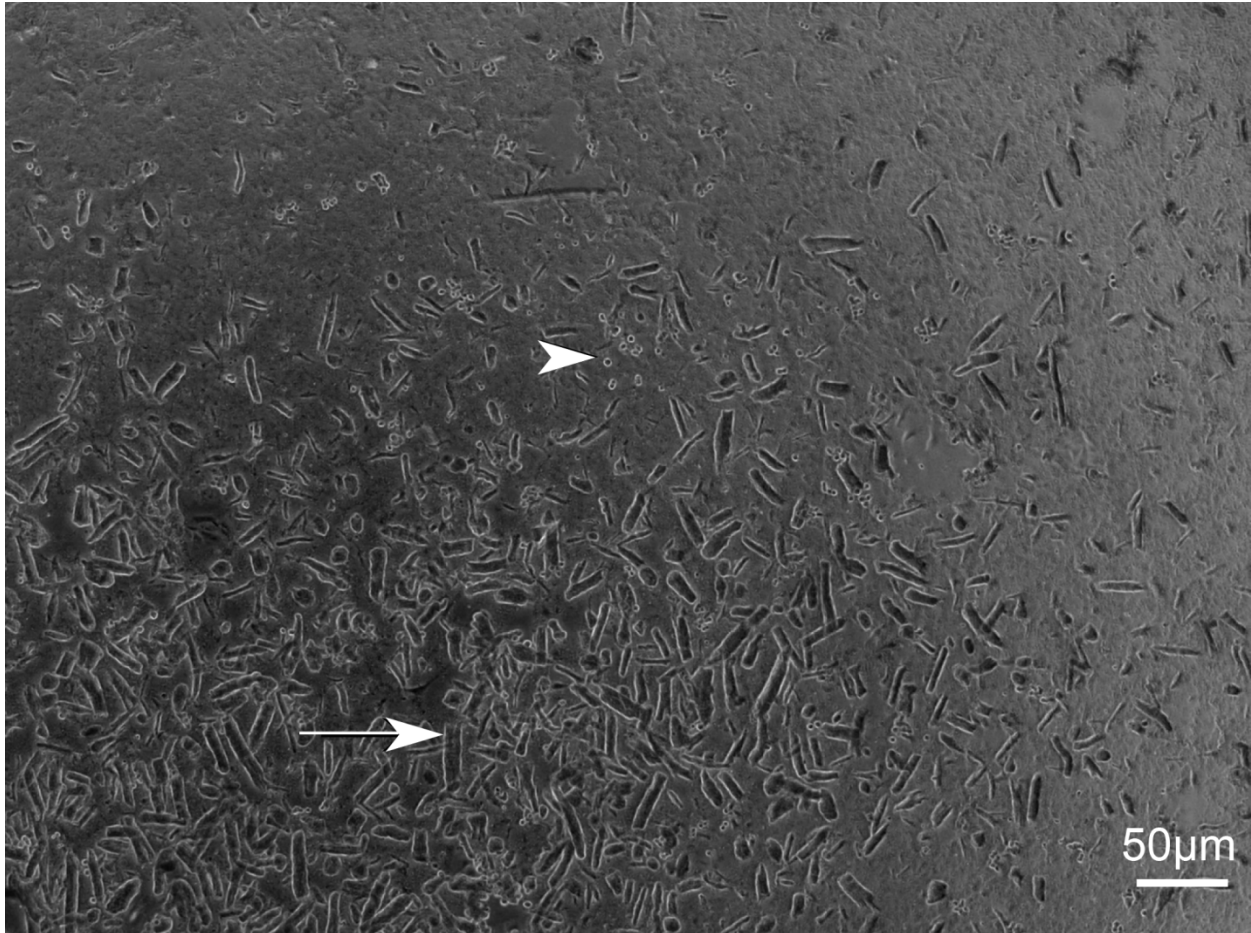


**Figure 4.21. Myoblast cultures established from single myofibers of diaphragm muscles of wild type and  $Xin^{-/-}$  mice.** Primary muscle cell cultures one day post isolation. Note the presence of small round satellite cells (indicated by arrow head) and single myofibers (indicated by arrow). After four days in culture the medium was changed to remove cellular debris. The attached satellite cells started proliferating rapidly giving rise to muscle progenitor cells and some cells were already entering differentiation from day 6 onwards. With time, the percentage of differentiating cells increased.

Primary muscle cells were isolated from wild type (SV129 strain) and  $Xin^{-/-}$  mice as described in Materials & Methods. Figure 4.21 represents the initial stages of a primary muscle cell culture one day post isolation. Isolated cells were transduced immediately after the first medium change (4 days post isolation) at an MOI of 30. The medium was changed again after 16 hours and thereafter every alternate day. The cells were allowed to differentiate without changing the

medium to a low-nutrition medium (Becher et al., 2009). Initially an attempt was made to select transduced cells via FACS sorting, however, in addition to proliferating cells, all cultures contained differentiating cells and this population increased rapidly over time, therefore these cells could not be processed by FACS. From these observations it can be concluded that most of the satellite cells and muscle specific cells were inherently committed to differentiate. After reaching nearly confluence, the percentage of proliferating cells decreased dramatically while the percentage of differentiating cells increased.

#### 4.3.2.4.1. Transduction efficiencies in wild type and $Xin^{-/-}$ primary muscle cells

Transduction of primary muscle cells isolated from wild type and  $Xin^{-/-}$  mouse skeletal muscle specimens was efficient ( $\approx 70\%$ ) with *Xirp2* knockdown constructs when transduced 4 days post isolation. GFP fluorescence intensity varied between different myotubes probably depending on the number of copies of viral particles present in these cells. Significantly myotubes containing higher copies of lentiviral knockdown constructs (indicated by stronger GFP fluorescence, arrows) displayed comparatively immature myofibrils compared to myotubes containing fewer lentiviral knockdown constructs (indicated by weaker GFP fluorescence, arrowheads).

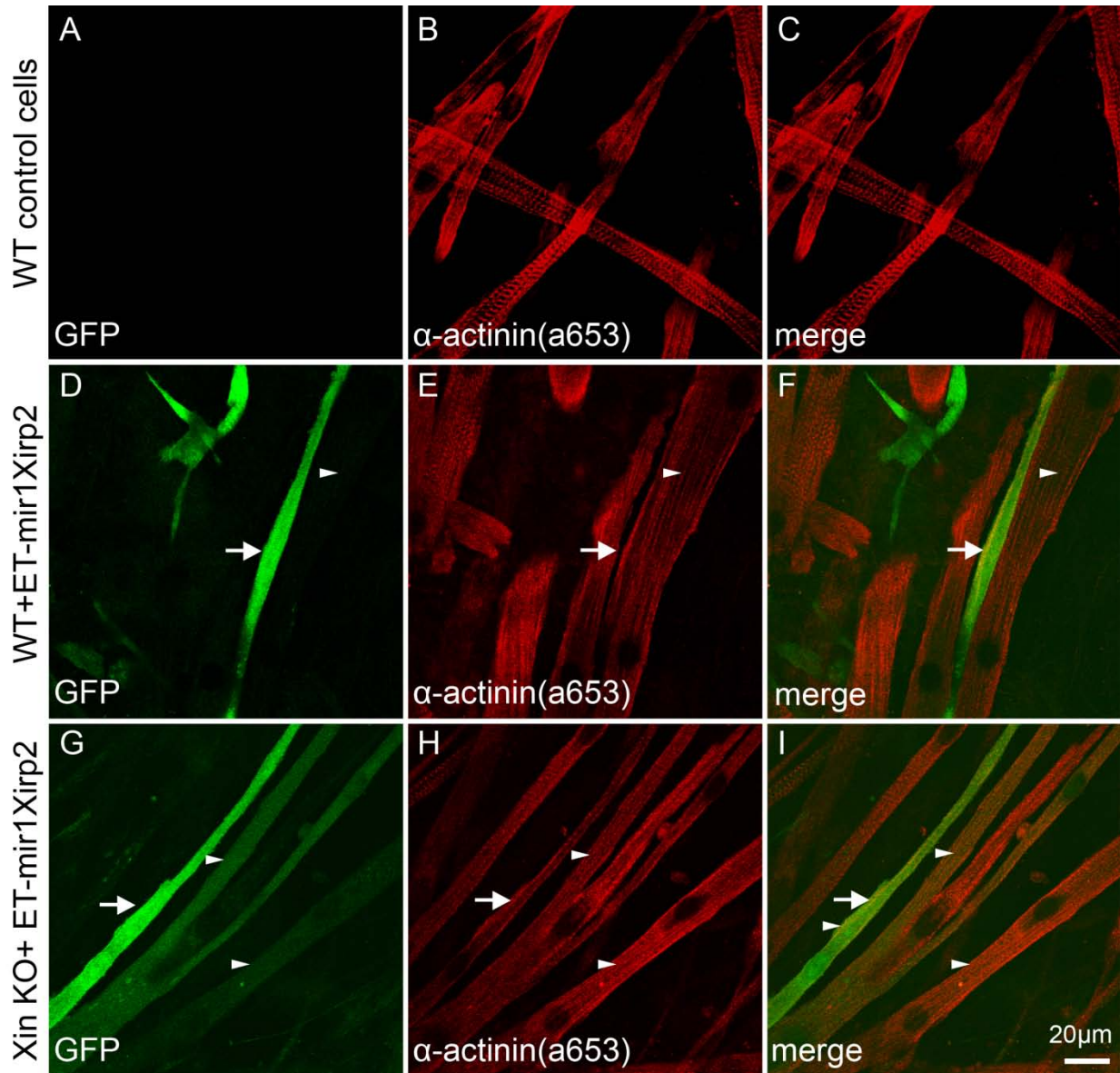


**Figure 4.22. Transduction efficiencies and myofibrillar structures in differentiating wild type and *Xin*<sup>-/-</sup> myotubes.** Primary muscle cells from wild type (SV129 strain) and *Xin*<sup>-/-</sup> mice were isolated and transduced with lentiviral shRNAmir constructs targeting *Xirp2* and co-expressing GFP reporter. Transduced cells were differentiated and processed for immunofluorescence by fixing with PFA to ensure that transduced cells retain GFP fluorescence enabling easy identification of transduced cells. Wild type cells served as control. Note that optimal differentiation as indicated by striated pattern revealed by  $\alpha$ -actinin staining is observed only in untransduced wild type myotubes (B). Wild type and *Xin*<sup>-/-</sup> myotubes transduced with lentiviruses expressing *Xirp2* knockdown constructs displayed immaturely organized myofibrils with very few striations (E, H).

#### 4.3.2.5. Knockdown of *Xirp2* in wild type mouse primary myoblasts

Having established transduction of primary myoblasts, the phenotype of *Xirp2* knockdown in wild type myotubes was determined by immunolocalization of sarcomeric  $\alpha$ -actinin and *Xin*.

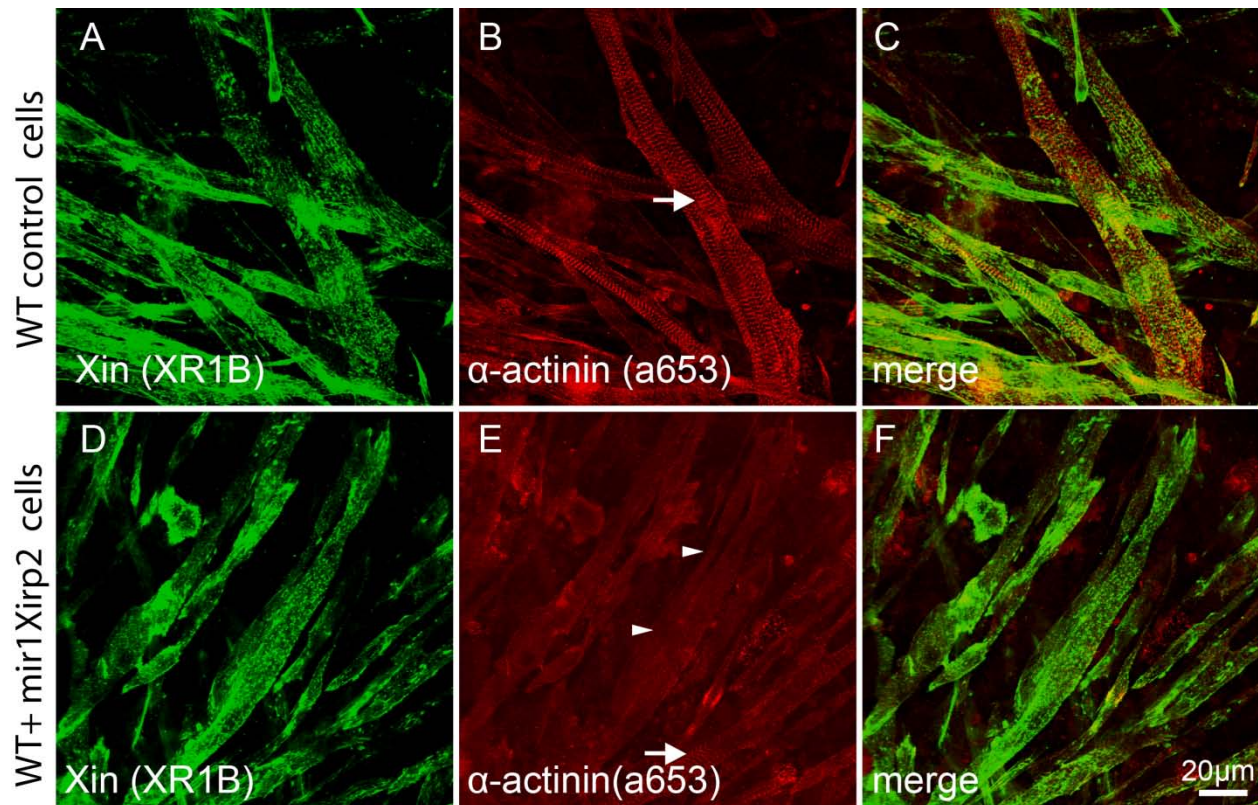


**Figure 4.23. Effect of Xirp2 knockdown in wild type myotubes.** Primary muscle cells were isolated from diaphragm muscles of wild type SV129 mice. Xirp2 was knocked down in these cells by mir1XIRP2 lentiviral construct. Wild type and wildtype-Xirp2 knockdown cells were differentiated and stained for myofibrillar markers Xin (XR1B) and  $\alpha$ -actinin (a653). Whereas a normal striated pattern is visible in wild type control myotubes (B), a massive disruption of myofibrillar structures is seen in wild type-Xirp2 knockdown myotubes (E). The localization of Xin along the actin stress fibers remained unaltered (D) compared to untransduced myotubes (A).

Xirp2 knockdown led to major disruption of myofibrils in wild type myotubes. Very few mature striations were observed in these cells compared to untransduced wild type cells (arrows in B and E). Areas indicated with arrowheads displayed a complete loss of striations (E). In contrast Xin staining along the actin stress fibers (D) is not significantly altered compared to control cells (A).

### 4.3.2.6. Knockdown of Xirp2 in $Xin^{-/-}$ mouse primary muscle cells

#### 4.3.2.6.1 Consequences of Xirp2 knockdown in $Xin^{-/-}$ primary muscle cells

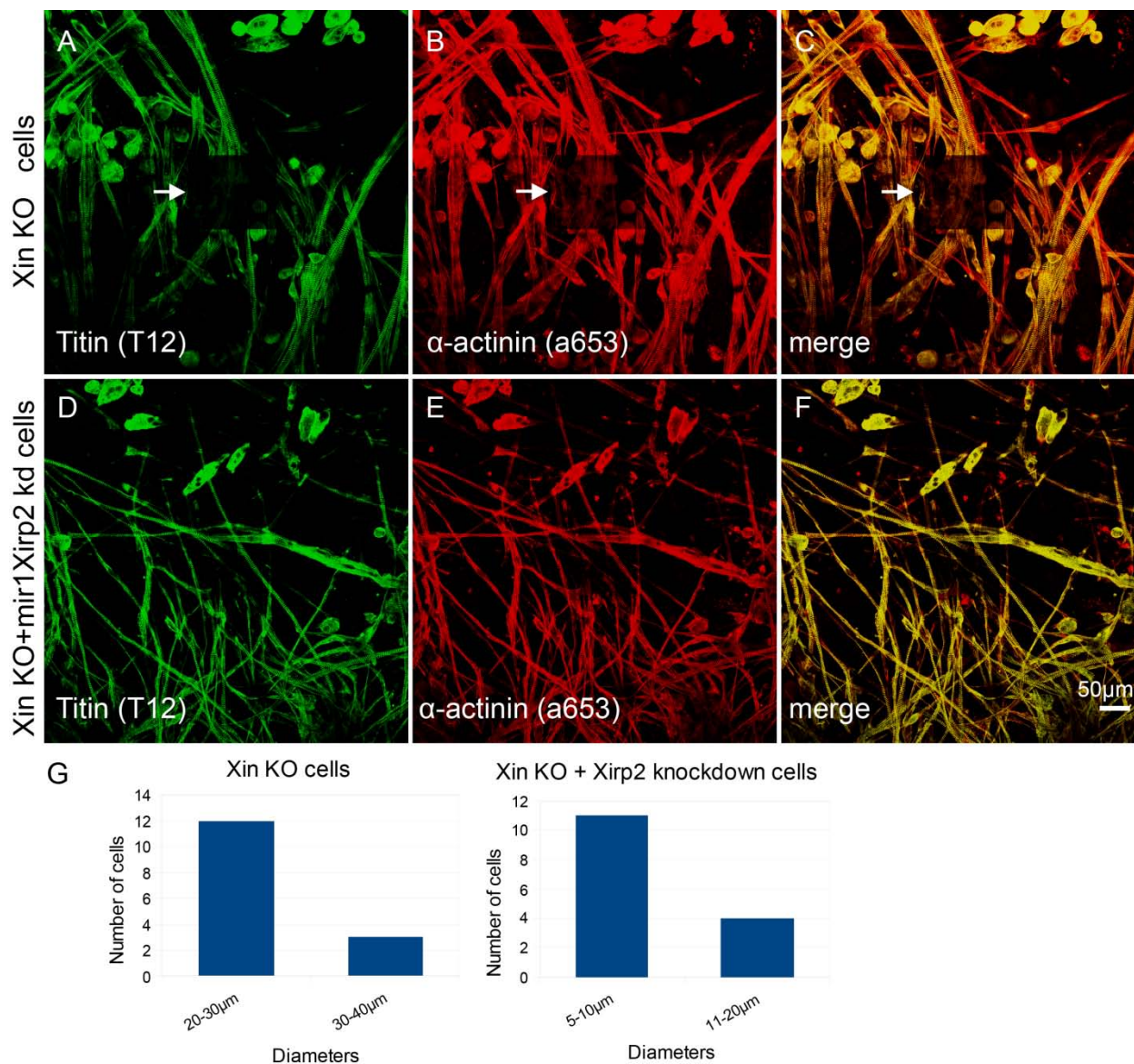


**Figure 4.24. Overview images of myotube cultures derived from  $Xin^{-/-}$  mice:  $Xin^{-/-}$  control and  $Xin^{-/-}$ -Xirp2 knockdown cells.** Primary muscle cells isolated from diaphragm muscles of  $Xin^{-/-}$  mice were transduced with the mir1Xirp2 knockdown virus. Differentiated cells were methanol/acetone fixed and stained for myofibrillar markers titin and  $\alpha$ -actinin. Panel G compares diameters of myotubes from  $Xin^{-/-}$  and  $Xin^{-/-}$ -Xirp2 knockdown cells. Overview images and panel G suggest that  $Xin^{-/-}$ -Xirp2 knockdown cells show thinner myotubes (D, E and F) compared to control  $Xin^{-/-}$  satellite cells (A, B and C).

Primary muscle cells isolated from  $Xin^{-/-}$  mice differentiated to mature myotubes with the expression of typical myofibrillar markers  $\alpha$ -actinin and titin in striated pattern (Figure 4.25A and B). Xirp2 knockdown in primary muscle cells from  $Xin^{-/-}$  mice did not inhibit their fusion to myotube structures; however, myotubes in the later cultures appeared thinner compared to  $Xin^{-/-}$  cells (D and E). A random

measure of diameters of myotubes in  $Xin^{-/-}$  and  $Xin^{-/-}$ -Xirp2 cultures is presented in panel G. While the diameter of the majority of myotubes in  $Xin^{-/-}$  cultures was 20-30 $\mu$ m, myotubes in  $Xin^{-/-}$ -Xirp2 cultures measured only 5-10  $\mu$ m.

#### 4.3.2.6.2 Comparison of myotubes developed from wild type and double gene depleted satellite cells

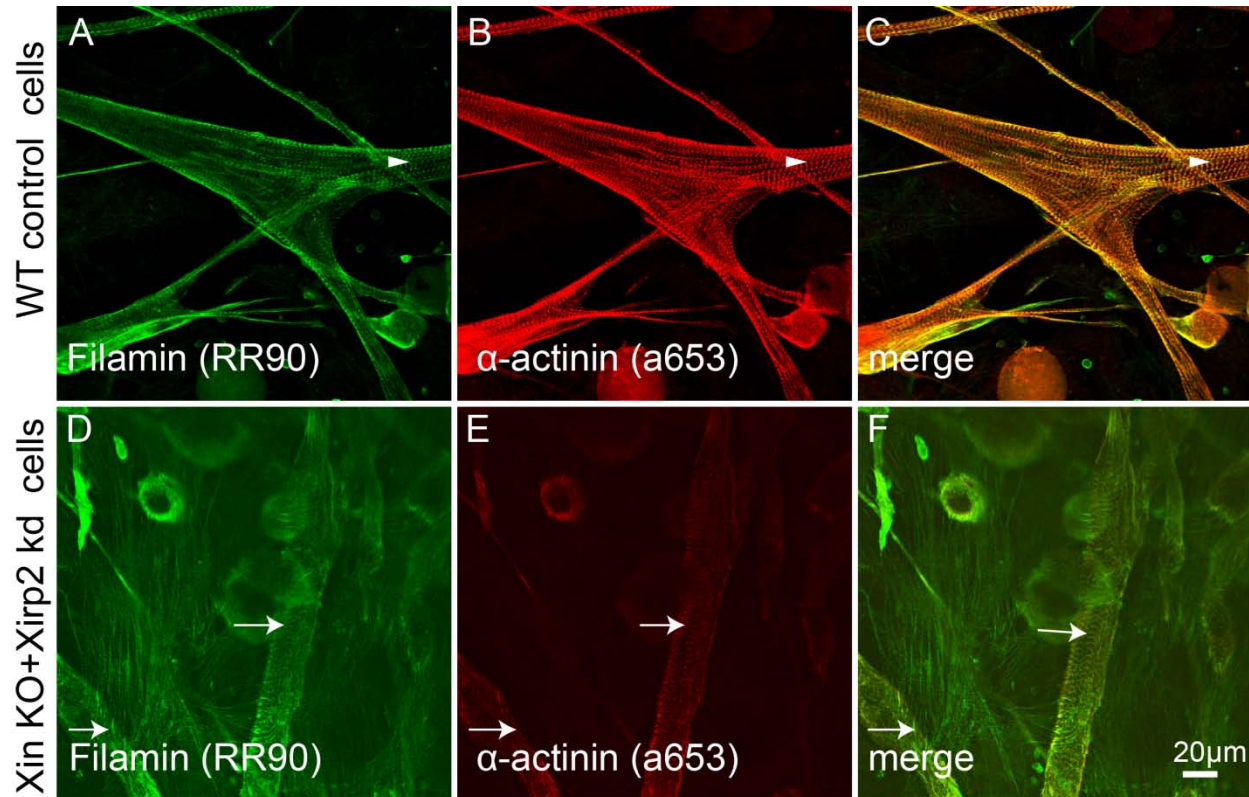


**Figure 4.25. Confocal microscopy images of myofibrillar markers in wild type and double gene depleted myotubes.** Differentiated wild type and  $Xin^{-/-}$ -Xirp2 knockdown cells were fixed with methanol/acetone and stained for myofibrillar markers filamin C and  $\alpha$ -actinin. Immunofluorescence images were captured with LSM 510 confocal laser scanning microscope. The localization of filamin C (RR90, green) and  $\alpha$ -actinin (a-653, red) were indicated as shown. As revealed by the filamin C staining in D and  $\alpha$ -actinin staining in E, myotubes depleted of both  $Xin$  and Xirp2 displayed immature myofibrils (arrows in D,E and F) with few observable striations compared to wild type control myotubes (arrowheads in A and B).

To investigate the effect of the depletion of  $Xin^{-/-}$  and Xirp2 on myodifferentiation,  $Xin^{-/-}$  primary cells were transduced with Xirp2 knockdown lentiviruses and differentiated cells were stained for Z-disk markers filamin C and  $\alpha$ -actinin. While a perfect colocalization of filamin C (arrowheads, A) and  $\alpha$ -actinin (arrowheads, B) in Z-disks was apparent in wild type control cells, the degree of differentiation in double gene depleted cells was comparatively minimal. Since the RR90 antibody also detects filamin A, the filamin isoform expressed predominantly in undifferentiated cells, this antibody also stains cells that do not contain sarcomeric  $\alpha$ -actinin.

## 5. Discussion

---

The striated muscle specific proteins Xin and Xirp2 have been predicted to play vital roles in cardiac and skeletal muscle development. However, in recent years conflicting data have emerged from literature on the roles of these proteins. Whereas the treatment of developing chick embryos with antisense oligonucleotides targeting the Xin mRNA resulted in abnormal cardiac morphogenesis in chicken (Wang et al., 1999), in two different mouse models, the ablation of *Xirp1* (the gene encoding Xin) only resulted in mild hypertrophic response and knockout mice were found to be viable and fertile (Gustafson-Wagner et al., 2007; Otten et al., 2010). *XinA<sup>-/-</sup>* mice lacking XinA and XinB isoforms (Gustafson-Wagner et al., 2007) displayed comparatively severe phenotype and an upregulation of Xirp2 in contrast to *XinABC<sup>-/-</sup>* mice developed by our group (Otten et al., 2010), which displayed no alteration in Xirp2 levels. Interestingly, XinC isoform was detected in hypertrophic hearts (Otten et al., 2010). At the time of beginning this dissertation work, there was no report describing the functional role of Xirp2 in either cardiac or skeletal muscle. Two recent reports have described the functional role of Xirp2 in mice: *Xirp2* hypomorphic model described by Mc Calmon et al (McCalmon et al., 2010) and mXin $\beta$  knockout model described by Qinchuan Wang et al (Qinchuan Wang et al., 2010). Both the reports gave an account of cardiac phenotype with varying degree of severity. However, neither of them described the skeletal muscle phenotype. In light of these observations, much about the functions of Xirp proteins in skeletal muscle remained unclear and therefore a lentiviral based Xirp2 knockdown was chosen as a method to understand the role of Xirp2 in skeletal muscle differentiation model and possible compensatory mechanisms resulting from Xirp2 knockdown in this setting. Primary muscle cells isolated from *XinABC<sup>-/-</sup>* mice were used to understand the functional role of Xin and/or Xirp2 either individually or by combined depletion.

### 5.1. Expression patterns of Xin and Xirp2 in skeletal muscle cells

Comparative expression levels of *Xirp1* and *Xirp2* at the RNA level by semi-Quantitative RT-PCR in proliferating and differentiating skeletal muscle cells indicated that *Xirp1* is expressed prior to *Xirp2* in differentiating cells (this work). These results also indicated that, at least at the RNA level, *Xirp1* is expressed in proliferating cells even before the initiation of differentiation in

skeletal muscle cells, whereas *Xirp2* is only expressed at a considerably more advanced differentiation stage (see section 4.1). Previous literature has described a robust increase in *Xirp1* mRNA expression upon muscle injury and it was localized to muscle satellite cells as well as within primary muscle myoblast cultures (Hawke et al., 2007). However, at the protein level, *Xirp1* expression was not detected in proliferating cells (present study). Expression of Xin in myoblasts induced to differentiate is consistent with earlier literature (van der Ven et al., 2006). Some experiments involving *Xin* knockdown in C2C12 cells (Hawke et al., 2007) were reported to show an increase in proliferation rate compared to control cells albeit without any differences in their differentiation capacity. Moreover there was no explanation for the increase in cell proliferation rate after the knockdown of *Xin* mRNA expression.

### 5.1.1. Localization of Xin and Xirp2 in skeletal muscle cells

Localization of Xin protein to non-striated regions of premyofibrils and nascent myofibrils in differentiating cells and in the myotendinous junctions of maturely differentiated muscle fibers are consistent with previous work reported in the literature (Pacholsky et al., 2004; van der Ven et al., 2006). Myomaxin, the mouse orthologue of human XIRP2 was reported to localize to striated myofibrils in skeletal muscle sections (Huang et al., 2006). However, there were no reports of localization of Xirp2 protein during skeletal muscle differentiation. Since the antibody used in the present work detects only human Xirp2 but not mouse Xirp2, its localization was studied only in HSKM cells. Expression of Xirp2 was only rarely observed in HSKM myotubes, indicating a relatively poor differentiation capacity of these cells, and at the same time a delayed initiation of Xirp2 expression (Figure 4.3). Xirp2 staining was detectable only in 1-2% of myotubes which were more terminally differentiated and contained myofibrils with distinct Z-disks. In these cells human Xirp2 was localized in a doublet band flanking the Z-disk (Figure 4.4). By contrast, in cryosections from adult human skeletal muscle tissue, all available Xirp2 antibodies revealed a colocalization with  $\alpha$ -actinin in the Z-disk (Figure 4.5). This implies that the layout of the Xirp2 molecule changes from regions flanking the Z-disk to the Z-disk itself during the differentiation process. Expression of Xin was already detectable in HSKM cells shortly after initiation of differentiation, again confirming the conclusion that *Xin* is expressed earlier than *Xirp2*. Extrapolating from these results, *Xirp2* is suggested to play a role in later stages of myofibril formation, whereas *Xin* may play a role in early myofibrillogenesis.

## 5.2. The role of Xirp proteins in muscle cells

The first ever functional characterization of a Xirp protein was performed by knocking-down cXin in the chicken via antisense oligonucleotides (Wang et al., 1999). cXin deficient embryos displayed severe heart looping defects, cardiac edema and heart beating defects. It was suggested that the asymmetric expression of cXin in the heart of untreated chicken embryos correlates with normal asymmetric looping of the heart (Wang et al., 1999). In mouse, Xirp1 and Xirp2 were found to be expressed in striated muscles, the heart and the skeletal muscle. Surprisingly, the xirp1 knockout mouse is viable (Gustafson-Wagner et al., 2007), although adult knockout mice developed cardiac hypertrophy (larger hearts, thicker ventricles), fibrosis and conduction defects leading to arrhythmia. Ultrastructural analysis of cardiomyocytes revealed decreased myofiber width, disarrayed myofibrils (no clear A/I bands boundary), broader Z-discs, shorter sarcomeres and abnormal ICD. Moreover, the expression of various proteins was found to be misregulated (e.g. Connexin43, N-Cadherin and  $\beta$ -Catenin). In contrast, *Xin* knockout mice developed in our laboratory (Otten et al., 2010) displayed even milder cardiac phenotype. It was demonstrated by Otten et al, that *Xin* knockout strategy adapted by Jim Lin group (Gustafson-Wagner et al., 2007) resulted in only partial knockout of *Xin* ( knocking out *XinA* and *XinB* isoforms but leaving *XinC* isoform intact). Interestingly, *XinC* isoforms was found to be expressed in hypertrophic hearts, which could explain the hypertrophic effects of *Xin* knockout mice developed by Jim Lin group. In contrast to, *XinAB*<sup>-/-</sup> mice (Gustafson-Wagner et al., 2007) *XinABC*<sup>-/-</sup> mice (Otten et al., 2010) displayed no upregulation of Xirp2. *XinABC*<sup>-/-</sup> mice displayed increased perivascular fibrosis in young hearts. Isolated cardiomyocytes from *XinABC*<sup>-/-</sup> mice displayed increase in cell length and increased number of non-terminally localized intercalated disk (ICD)-like structures. Furthermore, resting sarcomere length was increased, sarcomeres shortening, peak shortening at 0.5-1 Hz, and the duration of shortening were decreased. Sarcomere shortening and relengthening velocities were accelerated at frequencies above 4 Hz in *XinABC*<sup>-/-</sup> mice. Interestingly, Xirp2 were found to be upregulated in mouse models of hypertension: one hypertension model where mice were treated with Angiotensin II and another model for pressure overload (Duka et al., 2006; Jung-Ching Lin et al., 2005). In addition, Xirp1 was found to be upregulated in mouse satellite cells and in a muscle regeneration model based on eccentric exercise in mouse (Barash et al., 2004; Hawke et al., 2007). Moreover, mdx mice and ky/ky mice

models also displayed upregulation and ectopic localization of *Xin* in regenerating muscles (Beatham et al., 2006; Hawke et al., 2007).

There are two recent reports describing the functional role of *Xirp2* in mice hearts (McCalmon et al., 2010; Wang et al., 2010). In the first report, Mc Calmon et al. have demonstrated that upregulation of *Xirp2* in Angiotensin II infused animals was direct effect of the hormone and was a not attributable to secondary effect resulting from pressure overload (McCalmon et al., 2010). To substantiate their point the authors have also identified and mapped an Angiotensin II responsive region in the proximal 1.5 kb *Xirp2* promoter. An attempt has been made recently to elucidate the functional role of *Xirp2* in the heart by creating *Xirp2* hypomorphic allele mouse model (McCalmon et al., 2010). The *Xirp2* hypomorphic mice were viable but reduction of *Xirp2* expression in mouse hearts resulted in cardiac hypertrophy in adult unstressed mice. Interestingly, these mice displayed tapered response to Angiotensin II induced myocardial damage and diminished fibrosis and apoptosis compared to wild type mice exposed to chronic Angiotensin II infusion. Additionally, *Xirp2* hypomorphic mice did not show any altered cardiac function as measured by echocardiography (McCalmon et al., 2010). *Xirp2* hypomorphic mice displayed a modest increase in HW: BW ratio between 9 and 15 weeks postnatally. Morphometric analysis of ventricular myocytes in adult hypomorphic hearts revealed a significant increase in the cross-sectional area. However other hallmarks of cardiomyopathy such as fibrosis and apoptosis were not significantly altered. No obvious perturbations in myofibrillar structure in *Xirp2* hypomorphic mice cardiomyocytes were reported. The report did not describe the phenotype in skeletal muscle cells.

The cardiac phenotype of unstressed *Xirp2* hypomorphic allele is reminiscent of *Xin* knockout mice which also developed adult onset hypertrophy suggesting partial overlap of functions. However unlike *Xin* knockout mice model which demonstrated an upregulation of *Xirp2* (Gustafson-Wagner et al., 2007), the *Xirp2* hypomorphic mice model (McCalmon et al., 2010) displayed no alteration of *Xin* expression. Similar results were also obtained in the present study, i.e. *Xirp2* knockdown in several of muscle cell lines and primary cells did not alter *Xin* expression or its localization. *Xin* is also a MEF2 target however; its expression was not significantly induced in the heart by Ang II (McCalmon et al., 2010). *Xirp2* is required for proper physiological growth as a reduction in its expression resulted in enlarged cardiomyocyte

size. Cardiac hypertrophy in hypomorphic mice was accompanied by an upregulation of hypertrophic marker gene,  $\beta$ -MHC, and a downregulation of the calcineurin modulatory gene, RCAN1/MCIP1 (McCalmon et al., 2010). The downregulation of calcineurin modulator and increased calcineurin activity was speculated to be the plausible mechanism for hypertrophy in unstressed *Xirp2* hypomorphic allele mice. Further the upregulation of Pdlim3/ALP and MARCKS (myristoylated alanine-rich C kinase substrate), which encode cytoarchitectural proteins involved in actin dynamics localized to costameres and focal adhesions, was speculated to be a compensatory response to the reduction of *Xirp2* in these structures. The diminished cardiac hypertrophy in *Xirp2* hypomorphic mice compared to wild type mice after Ang II infusion was attributed to insufficient levels of *Xirp2* which in turn is direct effector of Ang II. An examination of phosphorylation levels of intracellular signaling molecules known to function downstream of Ang II revealed a downregulation of glycogen synthase kinase (GSK)-3  $\beta$  serine-9 phosphorylation in Ang II infused *Xirp2* hearts. Inhibition of GSK-3 $\beta$  kinase activity, a well established hypertrophic antagonist, through increased phosphorylation on serine-9, is associated with enhanced hypertrophy. A major target of active GSK-3  $\beta$  is  $\beta$ -catenin, which is phosphorylated by GSK-3  $\beta$  and is subsequently targeted for ubiquitination and degradation. Western blot analysis revealed that  $\beta$ -catenin levels are significantly diminished in Ang II-treated hypomorphic mice. Thus, the reduction in GSK-3  $\beta$  serine-9 phosphorylation in Ang II-treated hypomorphic mice is consistent with diminished cardiac hypertrophy (McCalmon et al., 2010).

In the second report by Qinchuan Wang et al, ablation of *mXin $\beta$*  (*Xirp2*) led to abnormal heart shape, ventricular septal defects, severe growth retardation and postnatal lethality (*mXin $\beta$*  null mice died before weaning) with no upregulation of the *mXin $\alpha$*  (*Xin*) (Wang et al., 2010). The *mXin $\beta$*  (*Xirp2*) null hearts displayed altered apoptosis and proliferation of cardiomyocytes and misorganized myocardium and impaired diastolic function and a delay in switching off the slow skeletal troponin I. Loss of *mXin $\beta$*  resulted in immature intercalated discs and the mislocalization of *mXin $\alpha$*  and N-cadherin. These observations are completely different from those reported by Mc Calmon et al, in their *Xirp2* hypomorphic mice, which displayed unaltered cardiac function and unperturbed myofibrillar structures. The complete loss of *mXin $\beta$*  (*Xirp2*) message in the *mXin $\beta$*  knockout model of Jim Lin group compared to reduced level of *Xirp2* in hypomorphic mice model of Frank Naya group could offer a potential explanation for the differences in these two models. Additionally, *mXin $\beta$*  null hearts displayed upregulation of

active stat3 (signal transducer and activator of transcription 3) and downregulation of activities of Rac1, insulin growth factor receptor, protein kinase B, and extracellular signal related kinases 1 and 2 (Wang et al., 2010).

In the present study, to evaluate the functional role of Xirp2 in myofibrillogenesis and myotube formation a lentiviral mediated shRNAmir knockdown was achieved in several muscle cell lines and primary muscle cells isolated from wild type and *Xin*<sup>-/-</sup> mice. Knocking down Xirp2 did not affect myotube formation in all cell lines and primary muscle cells. Xirp2 knock down in both wild type and primary muscle cells from *XinABC*<sup>-/-</sup> mice, disrupted Z-disk targeting of  $\alpha$ -actinin and filamin C. In contrast, the expression of the M-band protein myomesin was relatively unaffected. From these results it can be concluded that myotube formation per se is not altered in the absence of Xirp2; in contrast, Z-disks are disorganized to some degree, whereas no significant changes are observed in the M-band.

### 5.3. Xin expression levels are unchanged in Xirp2 knockdown cells – H-2Kb-tsA58 cells

Semi-Quantitative RT-PCR and western blot analysis of control and Xirp2 knockdown cells indicated no significant changes in Xin expression at the mRNA and protein level in the Xirp2 knockdown cells compared to the control cells (Figure 4.17). Furthermore, localization studies of Xin in Xirp2 knockdown cells revealed no alteration in the localization of Xin compared to control cells (Figure 4.19).

### 5.4. Possible role of Xin in satellite cells and their commitment to differentiation

According to a recent report, Xin is already expressed in activated satellite cells and in newly regenerated skeletal muscle fibers (Hawke et al., 2007). Xin mRNA was found to be upregulated more than 16 fold within 12 hours following skeletal muscle injury and was shown to localize to the muscle satellite cell population. It was also shown that Xin was expressed during muscle regeneration as well as in primary muscle satellite cell cultures but not in other stem cell populations. According to this study, Xin staining was also observed in satellite cells along with typical satellite cell marker syndecan-4 further indicating the expression of Xin in satellite cells.

In-situ hybridization studies on regenerating muscle fibers 5 to 7 days post injury confirmed Xin expression within these newly regenerating myofibers. Promoter-reporter assays demonstrated that known myogenic transcription factors such as the Myocyte enhancer factor-2 (MEF2), the Myogenic differentiation factor (MyoD) and the Myogenic factor-5 (Myf-5) transactivated Xin promoter constructs supporting the muscle specific expression of Xin (Hawke et al., 2007). Although the expression and localization were established, the actual functional role played by Xin was not fully understood. From the biochemical data of Xin interactions with actin and  $\beta$ -catenin (Choi et al., 2007; Pacholsky et al., 2004) and filamin C (van der Ven et al., 2006), it was predicted that Xin is involved in reorganization of the cytoskeleton and contributes to myofibril formation. However neither the functional knockout of Xin (previous results from this laboratory) nor Xin knockdown (Hawke et al., 2007) resulted in any overt differences in myofibrillogenesis. In a mouse model with a partial Xin knockout (targeting XinA and XinB isoforms but not XinC isoform) generated by Jim Lin group at the University of Iowa (Gustafson-Wagner et al., 2007), it was reported that Xirp2 expression was upregulated as a consequence of Xin knockout of this setting. A complete functional Xin knockout (targeting all three Xin isoforms, XinA, XinB and XinC) in this laboratory (Otten et al., 2010) had shown no upregulation of Xirp2 in these knockouts (present study). Both studies described only heart function avoiding any comment on the skeletal muscle function (Gustafson-Wagner et al., 2007; Otten et al.). Unpublished data from our laboratory showed the absence of major differences in skeletal muscle morphology and function. No differences in cardiac myofibril formation were observed in both studies irrespective of whether Xirp2 complemented the function of Xin or not. Since Xin is expressed earlier than Xirp2 in skeletal muscle differentiation and Xirp2 knockdown is not accompanied by any changes in either the expression or localization of Xin (from the results of this study), there was no strong evidence for the trans complementation of Xirp2 by Xin.

From the observations of Hawke et al (Hawke et al., 2007), it was tempting to predict a role for Xin proteins in cell fate determination and commitment. Xin was detected in satellite cells and early differentiation stages where satellite cells initially migrate, proliferate and ultimately differentiate to regenerate the injured tissue. A recent report also suggests the role of activated  $\beta$ -catenin in satellite cell proliferation, wherein localization of activated  $\beta$ -catenin in the nucleus of

satellite cells resulted in proliferation whereas its localization in the cytoplasm (out of the nucleus) resulted in satellite cell differentiation (Otto et al., 2008). A host of Wnt ligands which increased the level of activity of activated  $\beta$ -catenin, helped in satellite cell proliferation and other Wnt ligands, which decreased activity of activated  $\beta$ -catenin resulted in decreased proliferation and increased differentiation of the satellite cells demonstrating a role for  $\beta$ -catenin signaling in satellite cells. Since Xin proteins across the species were predicted to have a conserved  $\beta$ -catenin binding region (Grosskurth et al., 2008), Xin might influence  $\beta$ -catenin levels and the consequent decisions on satellite cell fate. It is also noteworthy that downregulation of Xin in cultured C2C12 cells increases the proliferation and migration of these cells (Hawke et al., 2007). Since Xin is known to be upregulated in the early differentiation stages, one could imagine that Xin plays a balancing role between proliferation and differentiation whereby higher or lower levels of Xin lead to differentiation or increased proliferation rates, respectively. Since the proliferation differences were studied only in cultured C2C12 cells, it will be interesting to investigate the role of Xin in satellite cells. More specifically: do satellite cells isolated from Xin knockout mice show increased proliferation compared to satellite cells isolated from wild type mice? Additional questions should address if any differences in the localization and distribution of activated  $\beta$ -catenin in the nucleus and the cytoplasm of the satellite cells from wild type and the Xin<sup>-/-</sup> mice exist. The satellite cell activation is characterized by the expression of the transcription factor, MyoD, which is the strongest transactivator of Xin. Xin is expressed in activated satellite cells and localizes to regions of early differentiation (eg. the injury site which is being repaired) leading to the prediction that Xin expression might determine satellite cell fate and their commitment to differentiation. It was also observed that Xin is expressed at the mRNA level in proliferating cells (present study), whereas at the protein level it is expressed only in differentiating cells indicating a role for Xin in subtle balancing of proliferation and differentiation commitments of muscle cells. However, the complete lack of Xin (satellite cells isolated from Xin<sup>-/-</sup> mice) did not prevent satellite cell commitment to differentiation (results from this study).

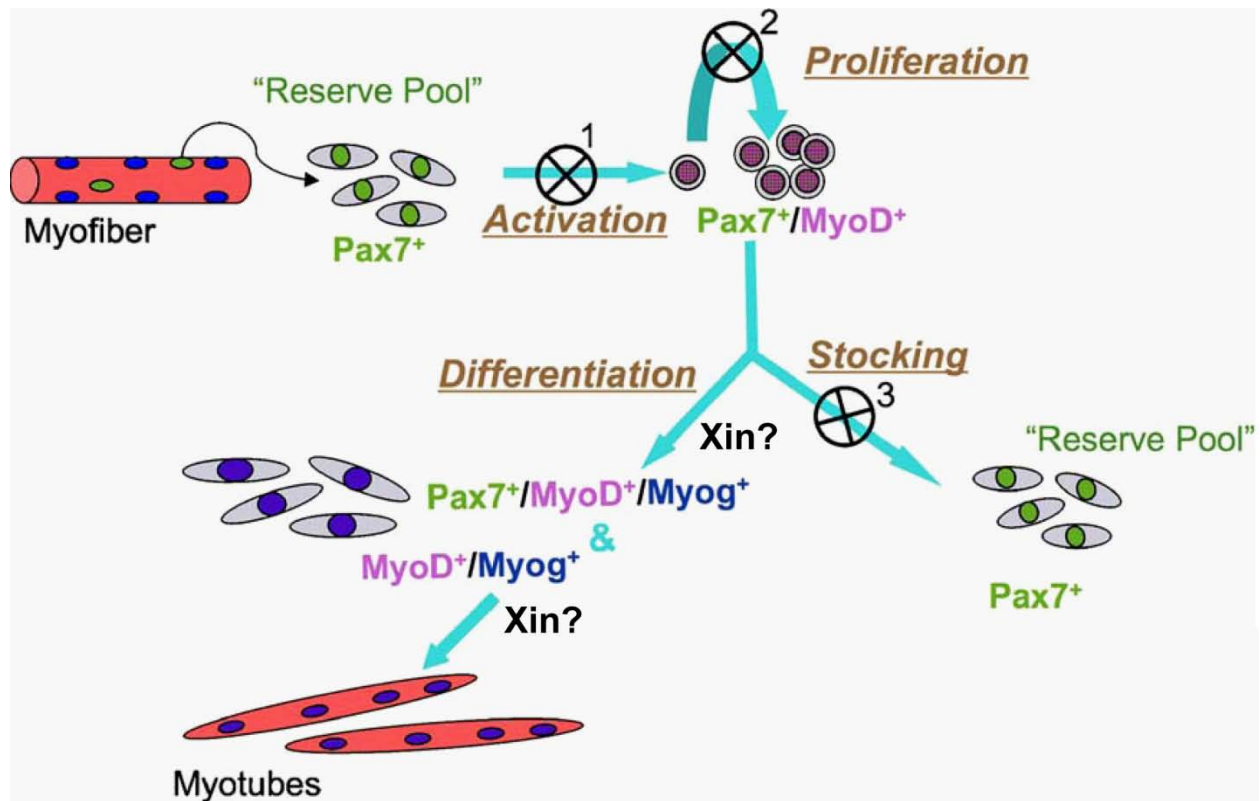


**Figure 5.1. The possible role of Xin in satellite cell differentiation.** Satellite cells are maintained as a reserve pool underneath the basal lamina of skeletal muscle myofibers. These satellite cells are typically characterized by the expression of Pax7, a transcription factor. Activation of satellite cells upon muscle injury is typically characterized by expression of MyoD another muscle specific transcription factor. Activation of satellite cells leads initial proliferation and after attaining sufficient number they can either downregulate MyoD and become 'reserve pool' and useful for future expansion or they can upregulate another muscle specific transcription factor Myogenin (Myog) and proceed along the differentiation pathway ultimately differentiating to myotubes and fusing with existing myofibers. Since Xin is robustly upregulated within 12 hours of muscle injury, where typically satellite cells initially proliferate and then differentiate to repair the damaged tissue, Xin could either influence satellite cell commitment to differentiation or might help in further downstream events necessary for differentiation and myofibril formation ( Figure was modified from (Shefer et al., 2006))

## 5.5. The rationale behind the design of the modular vectors

RNA interference (RNAi) has emerged as a powerful tool to analyze gene function both on the cellular level and the organismic level (by way of creating a knockdown animal) (Hannon et al., 2004). However, key challenges such as the off-target effects, finding the effective sequences which can efficiently knockdown the gene of interest, delivery to the desired tissue or transfectability in cell culture still remain. At least, some of the problems have been solved by recent work. Off-target effects have been minimized by advent of rational design principles

(Khvorova et al., 2003; Reynolds et al., 2004), algorithms predicting effective siRNA sequences, principles for preferential loading of antisense strand in RISC complex, avoiding seed region sequence complementarity to unintended targets (Anderson et al., 2008; Birmingham et al., 2006; Jackson et al., 2006a) utilizing naturally occurring miRNA based hairpin design rules (Chang et al., 2006; McBride et al., 2008; Zeng et al., 2002) and often a combination of several principles. Delivery issues have been solved mainly by adapting viral based systems. Lentiviral based systems in particular, have attracted vast interest primarily for their ability to transduce both dividing and non-dividing cells including primary cells and embryonic stem cells and the consequent ability to generate transgenic animals (Tiscornia et al., 2003). Lentiviruses also offer a very high integration frequency into the host genome allowing for the creation of stable cell lines and transmission of integrated transgenic cassettes to the progeny. Plasmid based shRNA design principles have been used for RNAi with varying degrees of success. Both Pol II (Dickins et al., 2005; Stegmeier et al., 2005; Zeng et al., 2005) and Pol III promoter based strategies have also been developed and several suppliers have commercialized their systems. But each of the systems suffers from a few disadvantages and the systems are very rigid in that a researcher is faced with numerous constraints with regard to selecting system of the choice and the ability to alter the system to suit their changing needs, the primary reason being incompatibility of sequences between different types of vectors. The function of a gene is dynamically regulated in an organism depending on several internal and external conditions. In such a scenario, spatial and temporal control over gene function i.e. the ability to switch ‘‘on’’ and ‘‘off’’ the function of a gene under study at desired time points and in desired tissues would equip the researcher with an excellent tool to do reverse genetics studies. Several of such inducible systems have also been described. Recently a novel lentiviral system was described which attracted the attention of the scientific community (Szulc et al., 2006). Among the many advantages described in this system, very little leakiness, full reversibility and tight regulation of both pol II and pol III promoter expression cassettes are of utmost importance. This novel inducible vector system is based on a single lentiviral vector and relied on the promiscuous activity of tTRKRAB, a fusion protein between the Krüppel-associated box (KRAB) domain and the tetracycline repressor (tetR) of *Escherichia coli* (Szulc et al., 2006). The tTRKRAB-mediated epigenetic repression of cellular Pol II and Pol III promoters juxtaposed to tet operator (TetO) sequences was shown to be reversibly controlled by doxycycline (Szulc et al., 2006). The flexibility of this system was

extended in this work by including multiple expression cassettes and silencing triggers thus creating a systematic and simple method for its modular use.

The main disadvantage of the epigenetic repression based lentiviral plasmids (pLVET-tTRKRAB, pLVCT-tTRKRAB), is that although, the tight regulation is independent of promoter choice, in the current format they offer only a H1-shRNA cassette. Additionally, they have no unique XhoI and EcoRI sites that would facilitate direct transfer of the large collection of sequence-verified miR30 based shRNAmirs from retro- and lentiviral library clones of Open Biosystems. Although the latter libraries are available in an inducible format (TRIPZ lentiviral inducible system), this system is restricted to a limited set of Pol II promoters (such as the CMV minimal promoter) and is based on a leaky transactivation system (Wiznerowicz et al., 2006). We decided to marry these systems to enable the expression of the shRNAmirs under control of the inducible promoters of the former system. A major drawback however, is the necessity of an extremely error-prone PCR-based amplification of the GC rich shRNAmir-sequences and subsequent sequencing of each transferred sequence. To circumvent this impediment, we aimed for the development of a PCR-free method. The resultant vector system introduced in this work (Kesireddy et al., 2010) combines the ease and safety of restriction enzyme-based shuttling of shRNAmir sequences with the flexibility and versatility of a modular system. Thus, this novel vector system combines the advantages of shRNAmirs with an inducible system that is less leaky and enables fine-tuning of the level of silencing. In addition, this work, also presents a modular design to show the flexibility and versatility of the system to achieve constitutive and conditional expression and for synergistic effect and simultaneous knockdown.

## 5.6. Advantages of the modular vectors

The modular nature of the vectors constructed in this work offers more flexibility and versatility as shown in the schematic drawing of the modules (Figure 4.9). These vectors harbor two different expression cassettes for expression of shRNAs and shRNAmirs viz. a Pol II based expression of shRNAmir (similar to pGIPZ vector) and a Pol III based expression of either shRNAs (a range of vectors with both U6 and H1 promoters, see Table 4.1 for compatible vectors for cloning into modular vectors) or shRNAmirs (similar to pSM2 vector). Moreover these expression cassettes can be either constitutive or conditional (depending on the module

chosen) and both expression cassettes can be used alone or in combination additionally in each case it is still possible to achieve constitutive or conditional expression.

In case a simultaneous knockdown of genes is required, e.g. in order to avoid potential compensatory effects that may arise due to upregulation or downregulation of closely related genes, with known systems, independent viruses to target two genes are required, and cells have to be transduced with both viral constructs. Usually, this means that analysis of two different reporters (eg. GFP and RFP) or a reporter plus an antibiotic selection marker is necessary. Often coordinated external control of expression cassettes is difficult to achieve. The two autonomous expression cassettes in the vectors fashioned here can be coordinately controlled externally, ensuring the simultaneous delivery of both cassettes with a single reporter.

### 5.6.1. Advantages of miRNA design over shRNA design

The silencing triggers (siRNAs) are not amplified and transported in mammalian species as opposed to what happens in *C. elegans* or plants. The silencing triggers in mammalian species have half-lives and must be supplied continuously to the RNAi machinery to maintain silencing (Paddison et al., 2004a). Stable RNAi requires stable expression of silencing triggers (dsRNA) which is achieved via retroviral constructs. The design of the hairpin cassettes used in this study, incorporates the sequences of human miR-30-RNA (Stegmeier et al., 2005). First adding a miR-30 loop and a 125 nt of miR-30 flanking sequence on either side of the hairpin results in a more than tenfold greater Droscha and Dicer processing of the expressed hairpins as compared to shRNA based designs (Silva et al., 2005). Increased Droscha and Dicer processing translates into greater siRNA production and greater potency for expressed hairpins (Silva et al., 2005). Finally, the miR-30 design offers more flexibility as miRNAs can be expressed from both Pol II and Pol III promoters (Stegmeier et al., 2005). Since miRNAs are endogenously expressed from Pol II promoters, tissue specific knockdown can be achieved with tissue specific (Pol II) promoters, whereas Pol III promoters (H1 and U6) are ubiquitously expressed in all tissues. Expression of hairpins from Pol III promoters also requires a precise transcription start site and hairpins must also include a stop signal of five thymidines ('TTTTT'). Since miRNAs are transcribed from long transcripts and processed by an endogenous miRNA pathway they require neither a precise transcription start site nor a stop signal. siRNAs and shRNAs can over-saturate cellular miRNA

pathways when present in high concentrations (Grimm et al., 2006). One way to avoid this potential pitfall is to use low concentrations of siRNAs and shRNAs (Cullen et al., 2006). However, oversaturation remains a risk in many cases, since it is extremely difficult to control total cellular concentrations of siRNAs or shRNAs especially taking into account the differences in transfection and transduction efficiencies of different cell types. While MOI can give an idea of transduceability of the cell type it remains difficult to precisely control the number of vector copies in individual cells. In situations where more copies of expressed hairpins are present in a cell, this might again lead to oversaturation of endogenous pathways. Under those circumstances an inducible expression system is more favorable as the knockdown can be tuned more precisely according to the special requirement. Utilizing miRNAs instead of shRNAs has also been shown to prevent oversaturation of endogenous miRNA pathways (presumably shRNAs mimic endogenous miRNAs compared to artificial shRNA sequences). Their expression from pol II promoters can be designed to be tissue specific and by using the modular design hairpins can be transferred in a PCR- free method from publicly available libraries.

Many endogenous miRNAs are expressed in clusters of multiple identical or different copies and since endogenous miRNAs are expressed in a polycistronic cassette, this provides an attractive way to express multiple hairpins from a single Pol II transcript (26, 27). While the modular vectors of this study use different expression cassettes for expressing different hairpins their expression from a single polycistronic cassette can also be achieved with our vectors following a previously published protocol (26).

The modular vectors developed here may be used to (i) knockdown two genes simultaneously using the Pol II and the Pol III cassettes targeting different genes, (ii) achieve synergistic effect using the Pol II and the Pol III cassettes expressing different sequences targeting the mRNA of the same gene at different positions, (iii) target different isoforms of the same gene with different sequences expressed from the Pol II and the Pol III cassettes. Unlike the system that is used in this work, many of the conditional vectors described are specific to certain promoters (such as the CMV minimal promoter) severely restricting the capability of the researcher. Also most of these systems can only control Pol II promoter.

### 5.6.2. Proposed uses of the modular lentivectors

Application for Rescue Plasmid: Since the GFP (Figure 4.9, module IA) can be replaced with a GFP fusion protein of the gene of interest (module IC), one can exploit this feature to express mutant form of the cDNA of the gene (harboring silent mutations at the sequence where the shRNAmir sequence binds the mRNA portion by utilizing codon redundancy) that is targeted with the shRNAmir sequence in the module II. Thus one can create a rescue plasmid expressing the mutant cDNA and the shRNAmir sequence targeting the same gene in a single vector with a single reporter (GFP) and thus a single virus. Moreover both mutant cDNA and shRNAmir sequence can be induced to be expressed at any point of time and can be switched “on” and “off”. When the switch is in the “off” position shRNAmir and mutant cDNA are not expressed (as indicated by the absence of GFP) thus the phenotype will be normal wild type. When the switch is in the “on” position both shRNAmir and mutant cDNA are expressed, shRNAmir targets the wild type protein (this action would have produced a phenotype) but the simultaneous expression of the mutant cDNA from the plasmid rescues the phenotype. The rescue plasmid can also be used to study mutant genes (if the mutations are not silent mutations) by knocking down the wild type genes. Thus, the rescue plasmid has far reaching potential for studying mutant genes in a physiological context.

In summary, a highly versatile lentiviral system that offers an unprecedented variability in the choice of modules that can be combined or excluded as desired was introduced in this work.

### 5.6.3. Double copy design and the Cre-Lox strategy with modular vectors

The 3' LTR of the vector pLVTHM contains the TetO sequence, the Pol III expression cassette (H1-shRNA) and the loxP site immediately after the ClaI restriction site. Since the 3' LTR duplicates during viral reverse transcription (see, SIN vectors in 1.2.3.1) the integrated provirus contains two copies each of TetO sequences, Pol III expression cassettes and loxP sites. The presence of two loxP sites in the integrated provirus enables vectors containing this cassette to be used with the Cre-Lox strategy. A ‘Cre’ coding plasmid when simultaneously transfected or transduced to the cells harboring the integrated provirus excises the expression cassette between

the loxP sites and in this case removes the Pol II promoter cassette along with one copy of the shRNA cassette.

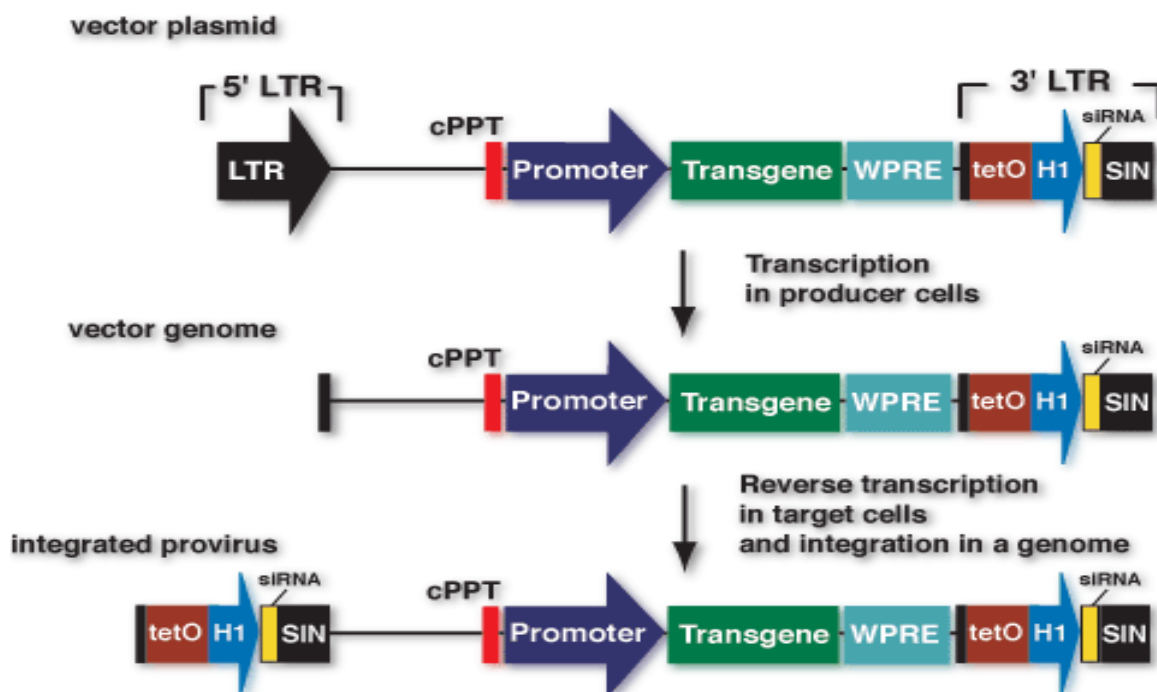


**Figure 5.2. Schematic representation of the double-copy design showing the duplication of 3' LTR during viral replication of pLVTHM.** During reverse transcription, the U3 region of the 5' LTR is synthesized using its 3' homologue as a template, which results in a duplication of the TetO-shRNA cassette in the provirus integrated in the genome of transduced cells. Figure adapted from [http://lentiweb.com/double\\_copy.php](http://lentiweb.com/double_copy.php).

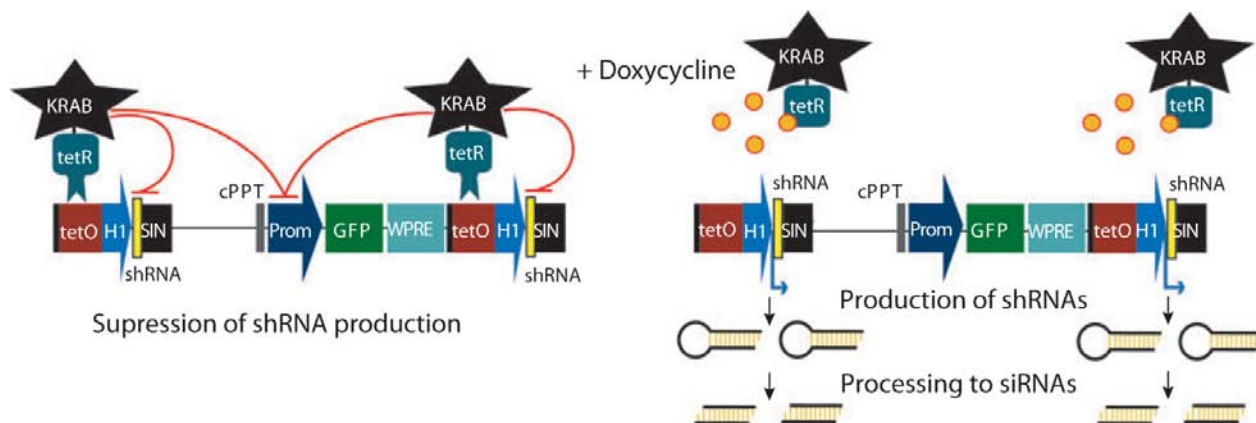


**Figure 5.3. Design and mode of action of the tTRKRAB based reversible, tetracycline controlled systems for conditional knockdown.** In the tTRKRAB based epigenetic repression vectors in the absence of doxycycline (left), the tTRKRAB fusion protein binds to TetO and, by triggering the local formation of heterochromatin, prevents transcription from the H1 promoter. Right, in the presence of the drug, tTRKRAB cannot bind the vector, the repressive epigenetic modification is alleviated, and the

shRNA is produced leading to gene knockdown. The internal transgene (for example, *GFP*) is also subjected to the conditional epigenetic repression providing a monitoring device. Figure adapted from (Wiznerowicz et al., 2006).

---

Although the vectors pLVTHM (H1-shRNA), pLVTHM-mir (H1-shRNAmir), pLVTU6+1 (U6-shRNA) and pLVTU6-mir (U6-shRNAmir) harbor different Pol III expression cassettes, the TetO and the loxP sites are unchanged in all these vectors constructed from pLVTHM backbone in this work. Therefore, the double copy design and the Cre-Lox strategy are applicable to all these vectors in spite of different expression cassettes. By extension, all the modular vectors that include the Pol III module (module IIIA, IIIB, IIIC and IIID) are amenable to Cre-Lox strategy.

## 6. Summary

---

Skeletal muscle differentiation is characterized by a remarkable reorganization of the actin cytoskeleton. In particular actin and actin binding proteins play a vital role in this process. Actin is reorganized from stress fiber like structures to finely organized myofibrillar arrangement. Several proteins have been implicated to function in this complex process. Recently, the striated muscle-specific protein Xin was predicted to play an essential role in early heart formation. This assumption was mainly based on the observation that the treatment of developing chick embryos with antisense oligonucleotides targeting the Xin mRNA resulted in abnormal cardiac morphogenesis (Wang et al., 1999). Therefore, depletion of Xin in mice was also predicted to have identical lethal effects on murine heart development. However, in two different mouse models, the ablation of *Xirp1* (the gene encoding Xin) only resulted in a mild hypertrophic response and knockout mice were found to be viable and fertile (Gustafson-Wagner et al., 2007; Otten et al., 2010). It was suggested that the lack of Xin protein is compensated by the presence of Xirp2, a closely related protein in the mammalian genome encoded by the *Xirp2* gene (Gustafson-Wagner et al., 2007).

In this work, I aimed to analyze the role of both proteins in normal skeletal muscle differentiation and the possible trans-complementation of Xin by Xirp2 in Xin knockout mice. The expression pattern of both Xin and Xirp2 in cultured differentiating murine and human skeletal muscle cells was analyzed by semi quantitative real time PCR and immunofluorescence stainings, respectively. Furthermore, the consequence of the depletion of these proteins (either individual or combined depletion) in skeletal muscle cell differentiation models was studied. Depletion of Xin was achieved making use of satellite cells isolated from *Xin*<sup>-/-</sup> mice previously established in our laboratory (Otten et al., 2010), whereas shRNAmir based *Xirp2* knockdown using lentiviral vectors was applied in muscle cell lines and in primary muscle cells isolated from wild type (SV129 strain) and *Xin*<sup>-/-</sup> mice.

To start with, a multipurpose lentiviral vector system for expressing miRNA 30-based short hairpins (shRNAmirs) for RNAi was created. The core of the resulting vector system, pLVmir, allowed a simple two step cloning procedure for expressing shRNAmirs under the control of a Pol II promoter in both a constitutive and a conditional manner with GFP as a co-

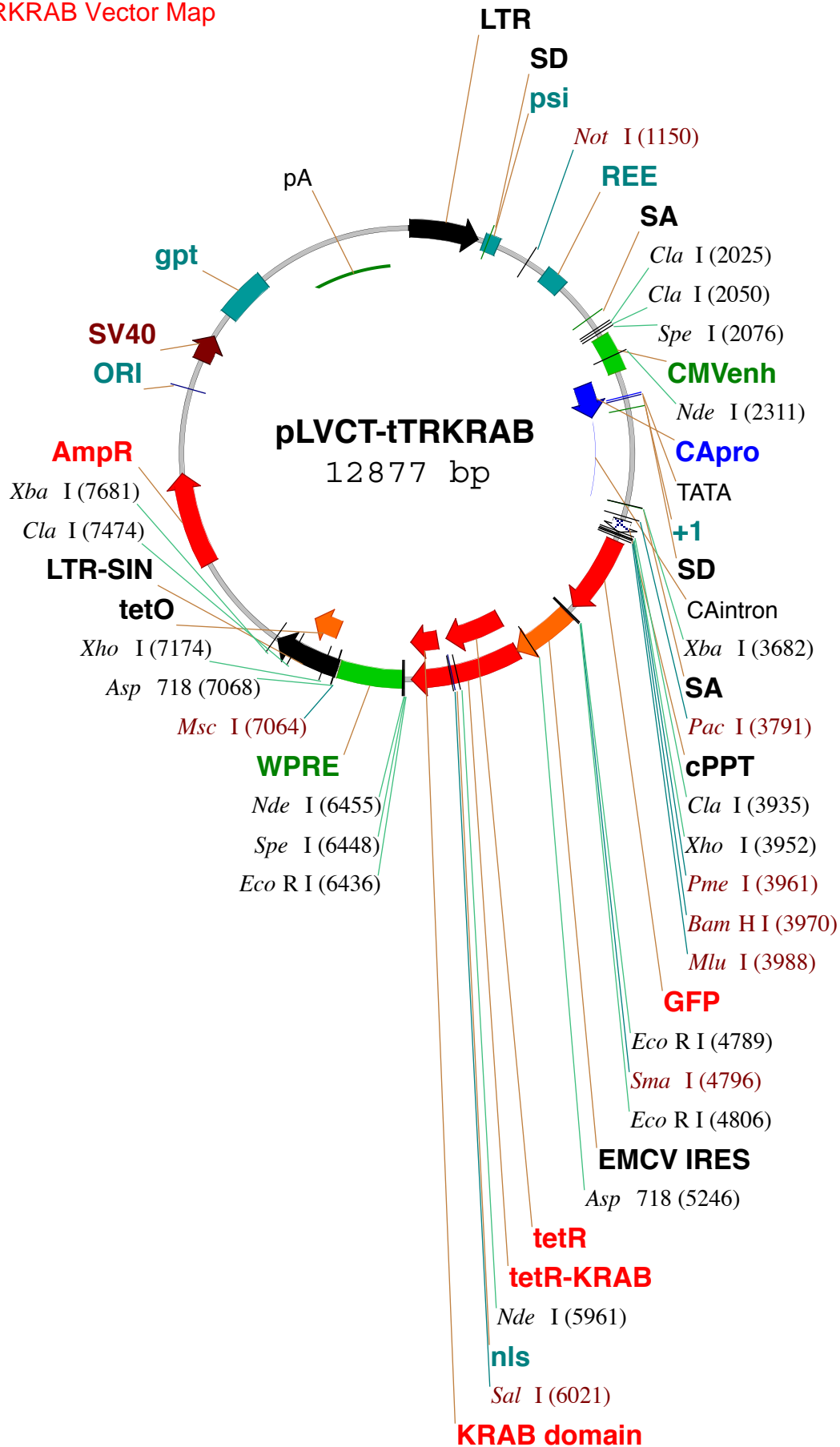
expressing reporter. This novel set of lentiviral vectors was used to knockdown *Xirp2* mRNA expression in five different kinds of cultured myogenic cells. Cell lines stably expressing shRNAmirs were established by selecting GFP positive cells by FACS. Consequences of the lack of *Xirp2* and / or *Xin* on myofibril assembly were analyzed by immunolocalization studies of myofibrillar proteins.

The achieved results indicated that knocking down of *Xirp2* was efficient and specific and had no effect on the expression of the closely related protein *Xin*. In the various cell types tested, *Xirp2* knockdown exhibited variable alterations in myofibril formation. While in H-2K<sup>b</sup>-tsA58 myotubes, *Xirp2* knockdown alone showed no major disruption of myofibril assembly, in *Xin*<sup>-/-</sup> primary murine muscle cells, *Xirp2* knockdown resulted in the development of thinner myotubes that differentiated up to a less advanced degree when compared to wild type cells. In C2C12 and HSKM cells *Xirp2* knockdown was accompanied by a disruption of myofibril development and relatively fewer maturely differentiated cells compared to control cells. Semi quantitative RT-PCR experiments revealed that *Xirp1* was expressed at earlier developmental stages as compared to *Xirp2* in differentiating skeletal muscle cells. Specific antibodies localized human *Xirp2* to mature myofibrils in a striated pattern in human skeletal muscle tissues and HSKM cells, whereas *Xin* was mainly found in the non-striated regions of nascent myofibrils and in structures analogous to the myotendinous junctions of adult muscle. Combined with the finding that *Xirp2* knocked down cells showed no alteration in *Xin* expression levels or localization, these data provided no evidence for a trans-complementation of *Xirp2* by *Xin*. The phenotypes of single and double gene depletions suggested that *Xirp2* plays a more significant role in myofibrillar development compared to *Xin* since primary muscle cells from *Xin*<sup>-/-</sup> mice differentiated without any disorganization in their myofibrillar arrangement.

# 7. Appendix

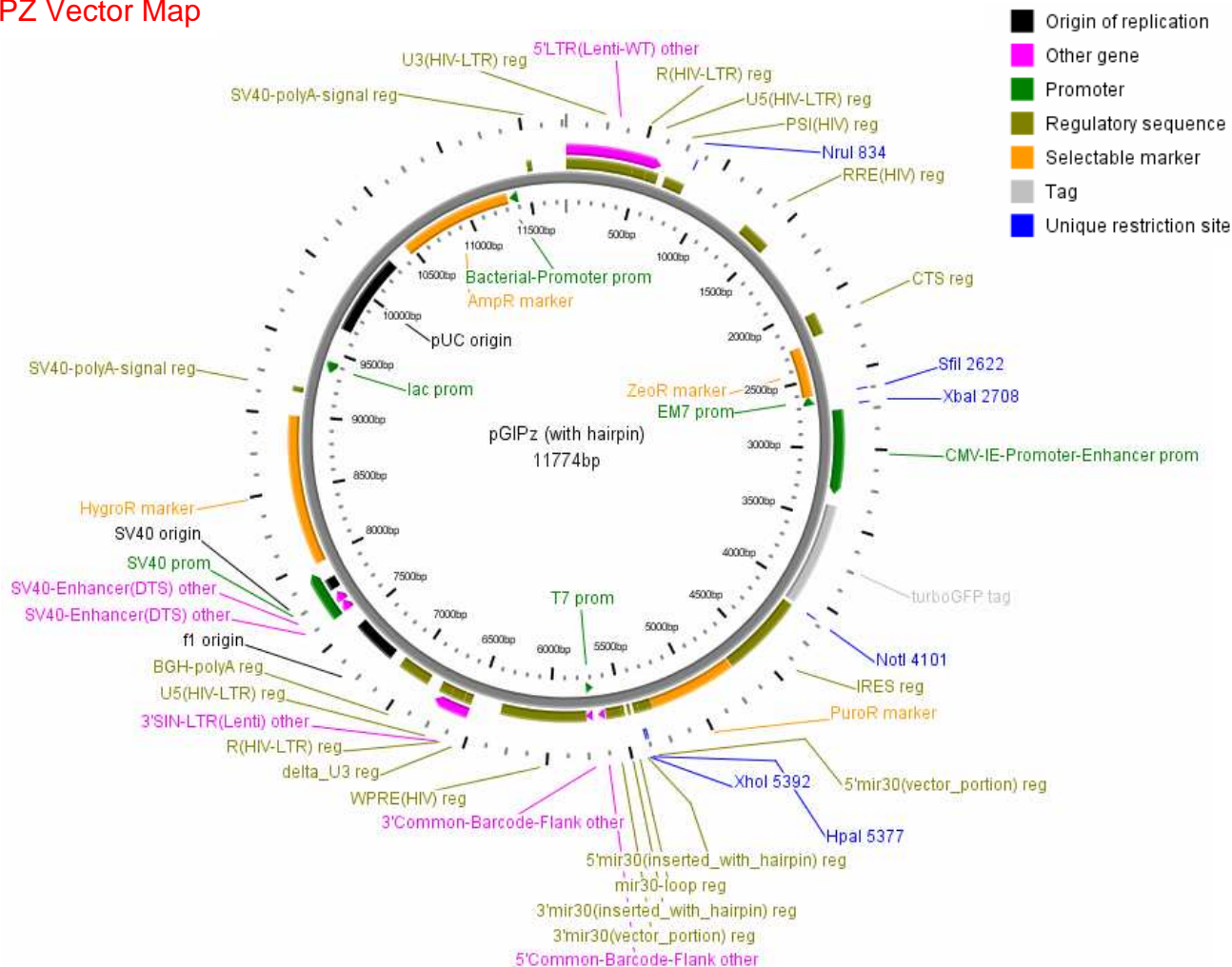
## Appendix Figure 1

### pLVCT-tTRKRAB Vector Map



## Appendix Figure 2

## pGIPZ Vector Map



## Detailed map of pGIPZ lentiviral vector

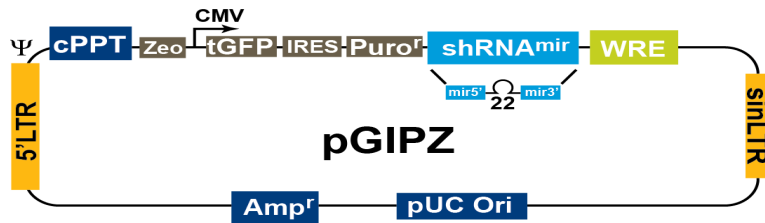
**ANTIBIOTIC RESISTANCE**

pGIPZ contains three antibiotic resistance markers

## Antibiotic resistance markers in pGIPZ

Antibiotic	Concentration	Utility
Ampicillin (carbenicillin)	100µg/ml	Bacterial selection marker (outside LTRs)
Zeocin	25µg/ml	Bacterial selection marker (inside LTRs)
Puromycin	variable	Mammalian selectable marker

## Appendix Figure 2.1



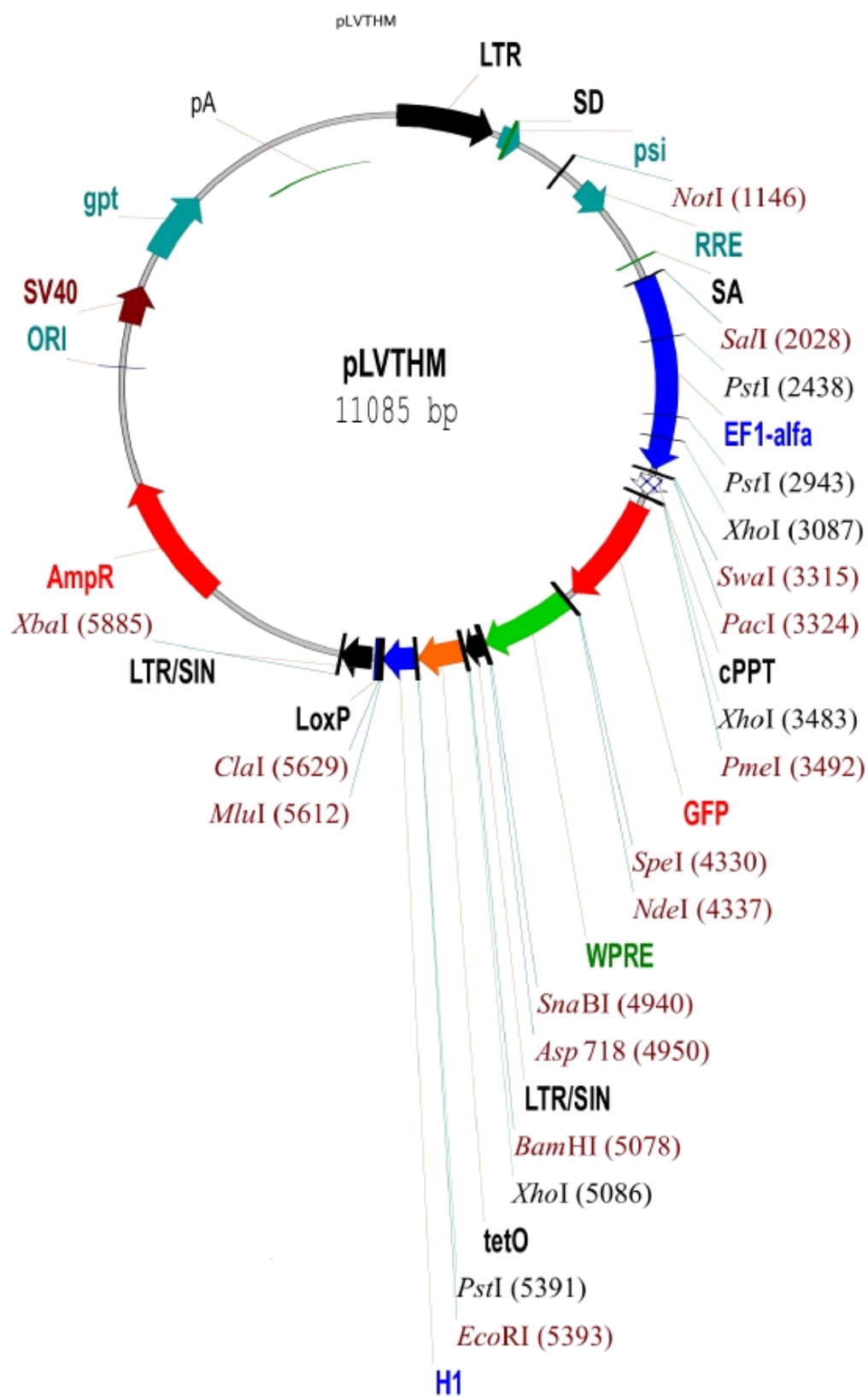
Schematic diagram of the vector pGIPZ

## Features of the pGIPZ vector

Vector Element	Utility
CMV Promoter	RNA Polymerase II promoter
cPPT	Central Polypurine tract helps translocation into the nucleus of non-dividing cells
WRE	Enhances the stability and translation of transcripts
TurboGFP	Marker to track shRNAmir expression
IRES-puro resistance	Mammalian selectable marker
Amp resistance	Ampicillin (carbenicillin) bacterial selectable marker
5'LTR	5' long terminal repeat
pUC ori	High copy replication and maintenance of plasmid in <i>E. coli</i>
SIN-LTR	3' Self inactivating long terminal repeat (Shimada, et al. 1995)
RRE	Rev response element
Zeo resistance	Bacterial selectable marker

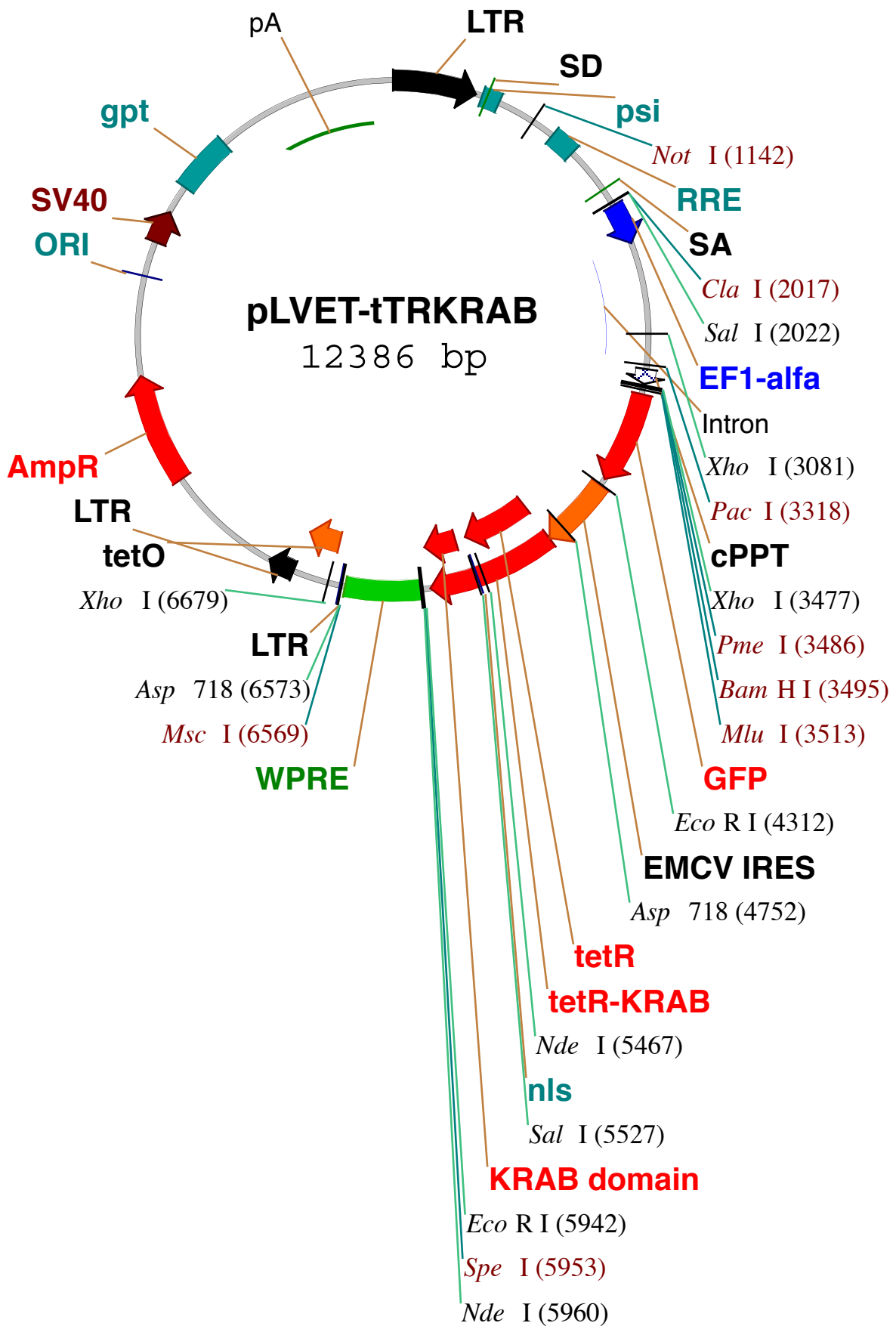
## Appendix Figure 3

## pLVTHM Vector Map



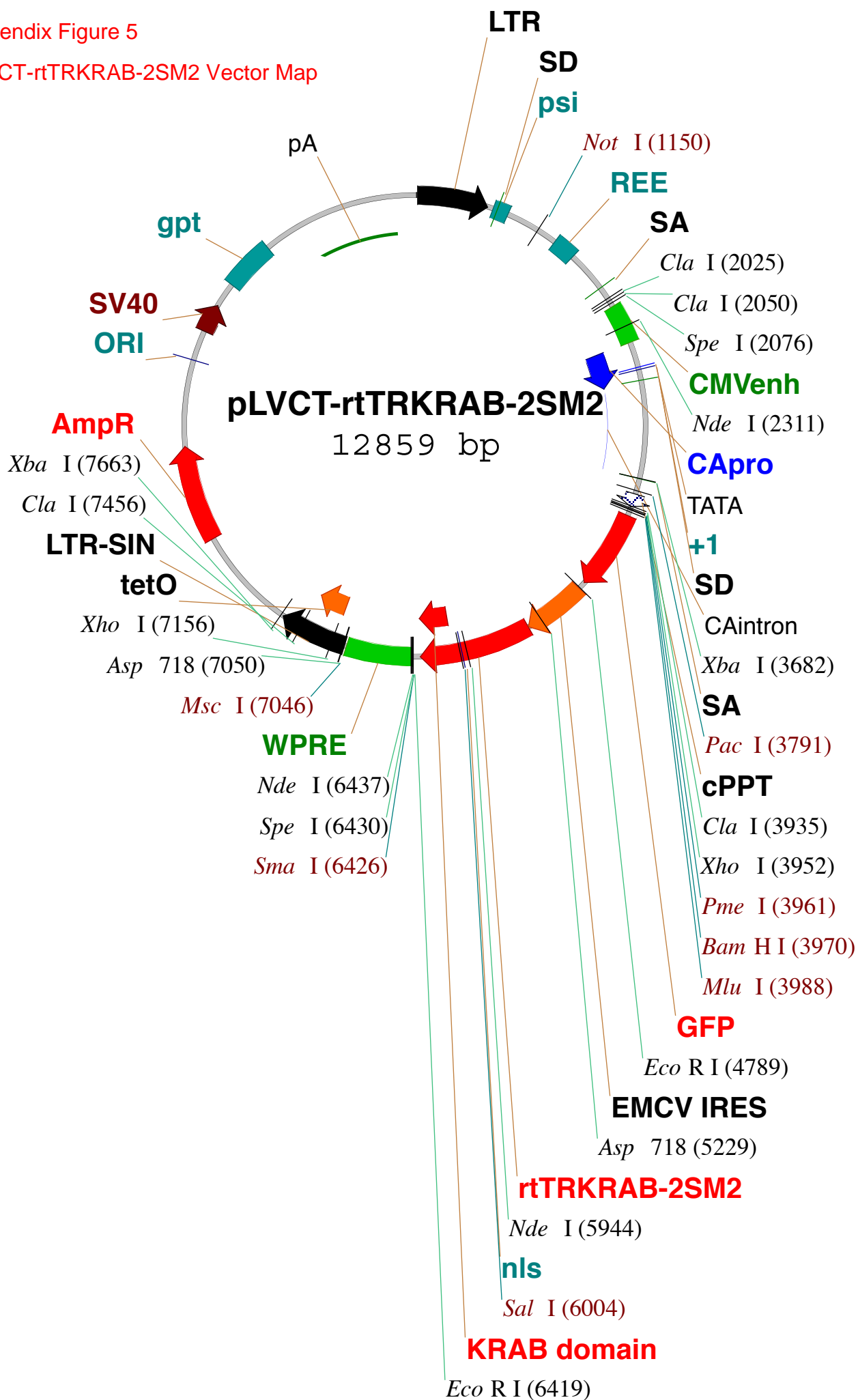
## Appendix Figure 4

## pLVET-tTRKRAB Vector Map



Appendix Figure 5

## pLVCT-rtTRKRAB-2SM2 Vector Map



## Validation of sensitivity of SYBR Green based Real Time PCR method-Melting Curve analysis of primer sets.

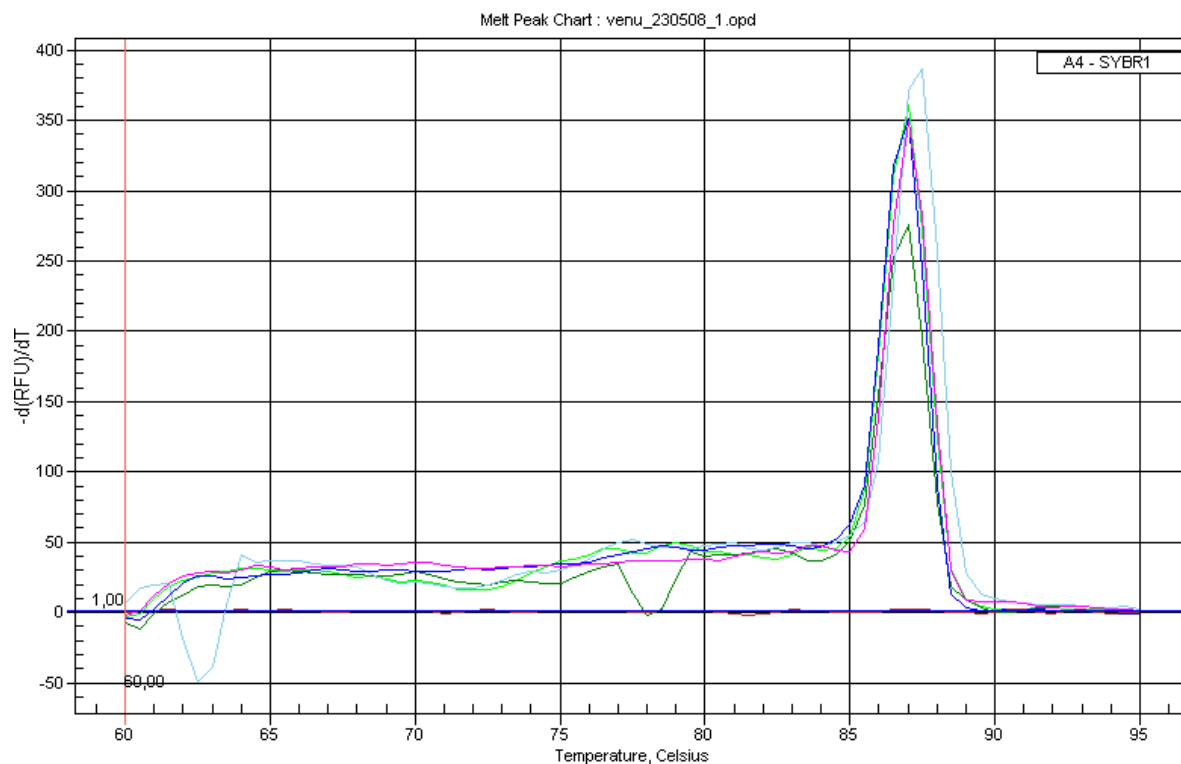


**Figure A1: Melting curve, Primer set 1, Xin.** Single peak was observed in SYBR Green based Real Time PCR validating this method. Sequences of the primers are given in Appendix Table 1.

### Appendix Table 1: Primers used SYBR Green based Real Time PCR

<b>Xin Real Time PCR Primers</b>	
XIN RT1f	5'-GCTCCGGCGTCTCTACAAAC-3'
XIN RT 1r	5'-CCAGCGCATACTGAACATC-3'
<b>Xirp2 Real Time PCR Primers</b>	
XIRP2 RT1f	5'-GCAGCTTCTCGGCTAATGTCA-3'
XIRP2 RT 1r	5'-AGGCGTTGCAGGTTGAAGTC-3'
<b>Gapdh Real Time PCR Primers</b>	
GAPDH RT 1f	5'-AGGTCGGTGTGAACGGATTTG-3'
GAPDH RT 1r	5'-TGTAGACCATGTAGTTGAGGTCA-3'

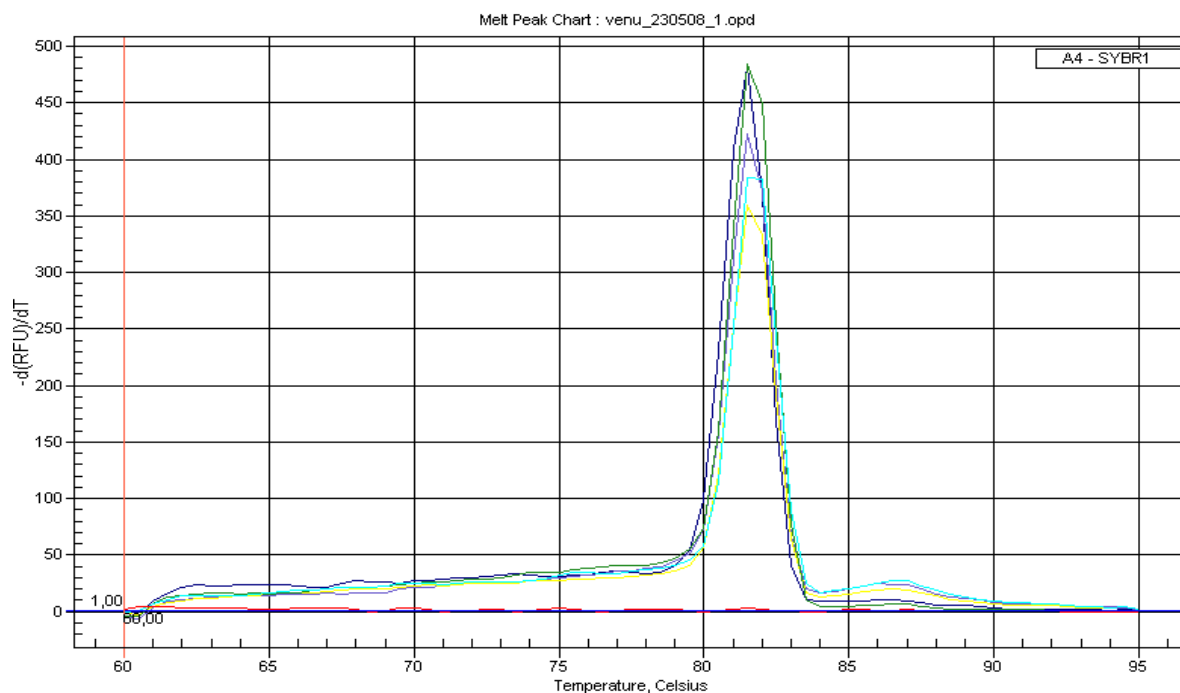


**Figure A2: Melting curve, Primer set 2, Xirp2.** Single peak was observed in SYBR Green based Real Time PCR validating this method. Sequences of the primers are given in Appendix Table 1.

---

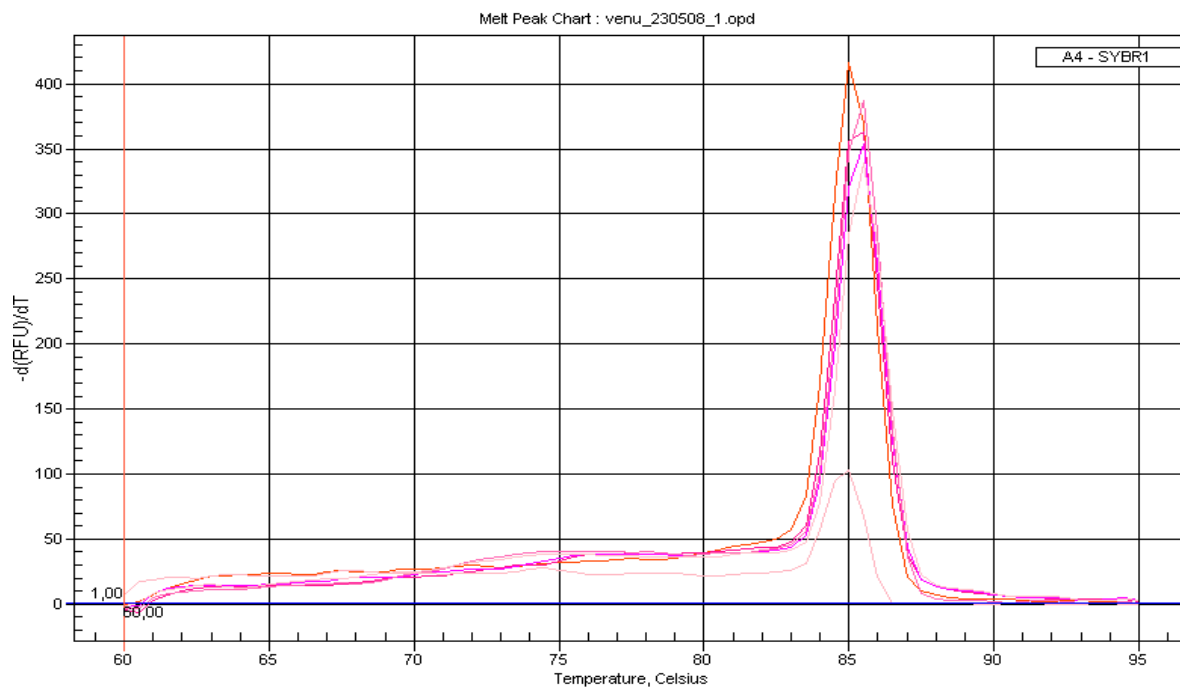


**Figure A3: Melting curve, Primer set 3, Gapdh.** Single peak was observed in SYBR Green based Real Time PCR validating this method. Sequences of the primers are given in Appendix Table 1.

---

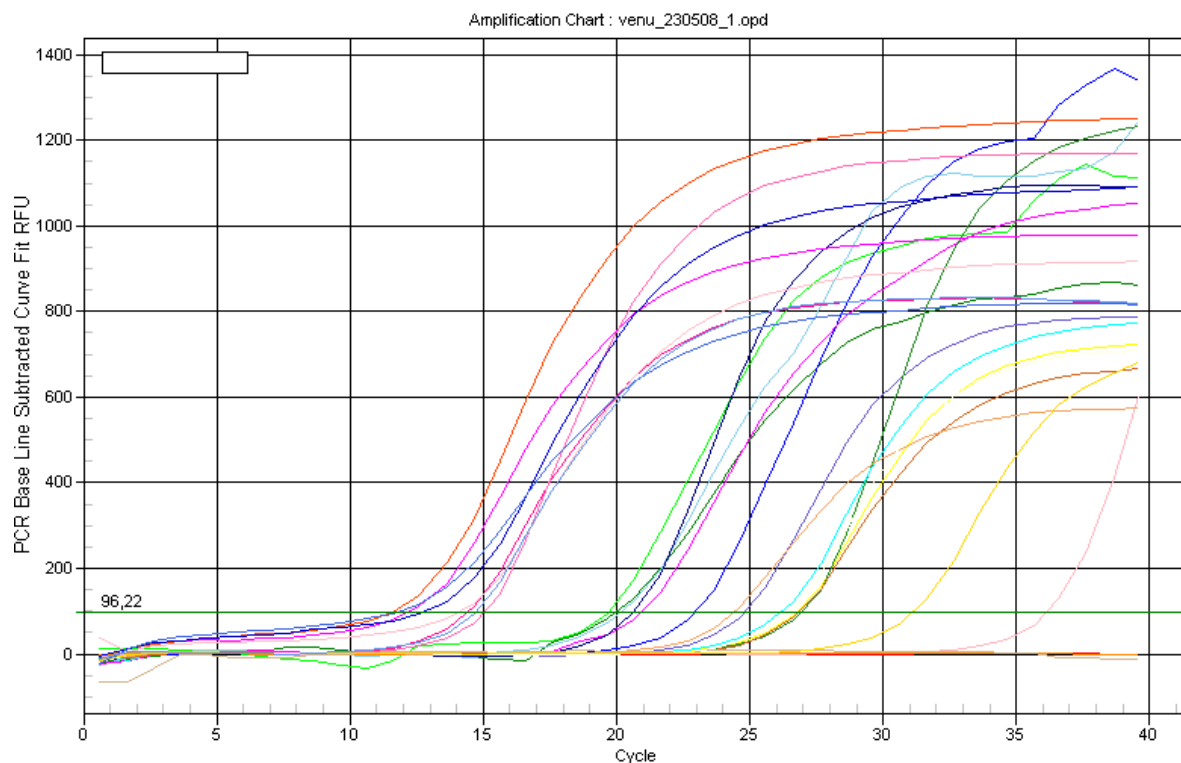


**Figure A4:  $C_T$  Values- first detection in H2k-ts A58 mouse muscle (control) cells. GAPDH was detected after 11.5 cycles, Xin after 19.5 cycles and Xirp2 after 20.7 cycles**

**$\Delta\Delta C_t$  Method for calculation of percentage of remaining mRNA after normalization to GAPDH levels**

$$\Delta\Delta C_t = (C_{t \text{ sample}} - C_{t \text{ control}}) - (C_{t \text{ GAPDHsample}} - C_{t \text{ GAPDHcontrol}})$$

Eg.

$$= (26.76 - 20.63) - (12.09 - 11.49)$$

$$= 6.13 - 0.6$$

$$= 5.53$$

$$\% \text{ Remaining mRNA} = 100 * (1/2)^{5.53} = 2.16\%$$

## 8. References

---

- Almenar-Queralt, A., Gregorio, C.C., and Fowler, V.M. (1999). Tropomodulin assembles early in myofibrillogenesis in chick skeletal muscle: evidence that thin filaments rearrange to form striated myofibrils. *J Cell Sci* 112 ( Pt 8), 1111-1123.
- Amado, R.G., and Y. Chen, I.S. (1999). BIOMEDICINE:Lentiviral Vectors--the Promise of Gene Therapy Within Reach? [10.1126/science.285.5428.674](https://doi.org/10.1126/science.285.5428.674). *Science* 285, 674-676.
- Ambros, V., Bartel, B., Bartel, D.P., Burge, C.B., Carrington, J.C., Chen, X., Dreyfuss, G., Eddy, S.R., Griffiths-Jones, S., Marshall, M., et al. (2003). A uniform system for microRNA annotation [10.1261/rna.2183803](https://doi.org/10.1261/rna.2183803). *RNA* 9, 277-279.
- Anderson, E.M., Birmingham, A., Baskerville, S., Reynolds, A., Maksimova, E., Leake, D., Fedorov, Y., Karpilow, J., and Khvorova, A. (2008). Experimental validation of the importance of seed complement frequency to siRNA specificity. *Rna* 14, 853-861.
- Au, Y. (2004). The muscle ultrastructure: a structural perspective of the sarcomere. *Cell Mol Life Sci* 61, 3016-3033.
- Auerbach, D., Rothen-Ruthishauser, B., Bantle, S., Leu, M., Ehler, E., Helfman, D., and Perriard, J.C. (1997). Molecular mechanisms of myofibril assembly in heart. *Cell Struct Funct* 22, 139-146.
- Ayscough, K.R. (1998). In vivo functions of actin-binding proteins. *Curr Opin Cell Biol* 10, 102-111.
- Bartel, D.P. (2004). MicroRNAs: Genomics, Biogenesis, Mechanism, and Function. 116, 281-297.
- Becher, U.M., Breitbach, M., Sasse, P., Garbe, S., van der Ven, P.F.M., Fürst, D.O., and Fleischmann, B.K. (2009). Enrichment and terminal differentiation of striated muscle progenitors in vitro. *Experimental Cell Research* 315, 2741-2751.
- Berns, K., Hijmans, E.M., Mullenders, J., Brummelkamp, T.R., Velds, A., Heimerikx, M., Kerkhoven, R.M., Madiredjo, M., Nijkamp, W., Weigelt, B., et al. (2004). A large-scale RNAi screen in human cells identifies new components of the p53 pathway. *Nature* 428, 431-437.
- Bindschadler, M., Osborn, E.A., Dewey, C.F., Jr., and McGrath, J.L. (2004). A mechanistic model of the actin cycle. *Biophys J* 86, 2720-2739.

- Birmingham, A., Anderson, E.M., Reynolds, A., Ilsley-Tyree, D., Leake, D., Fedorov, Y., Baskerville, S., Maksimova, E., Robinson, K., Karpilow, J., et al. (2006). 3' UTR seed matches, but not overall identity, are associated with RNAi off-targets. *Nat Methods* 3, 199-204.
- Black, B.L., and Olson, E.N. (1998). Transcriptional control of muscle development by myocyte enhancer factor-2 (MEF2) proteins. *Annu Rev Cell Dev Biol* 14, 167-196.
- Brummelkamp, T.R., Bernards, R., and Agami, R. (2002). A system for stable expression of short interfering RNAs in mammalian cells. *Science* 296, 550-553.
- Bukovsky, A.A., Song, J.-P., and Naldini, L. (1999). Interaction of Human Immunodeficiency Virus-Derived Vectors with Wild-Type Virus in Transduced Cells. *J Virol* 73, 7087-7092.
- Bukrinsky, M.I., Haggerty, S., Dempsey, M.P., Sharova, N., Adzhubel, A., Spitz, L., Lewis, P., Goldfarb, D., Emerman, M., and Stevenson, M. (1993). A nuclear localization signal within HIV-1 matrix protein that governs infection of non-dividing cells. *Nature* 365, 666-669.
- Burns, J.C., Friedmann, T., Driever, W., Burrascano, M., and Yee, J.K. (1993). Vesicular stomatitis virus G glycoprotein pseudotyped retroviral vectors: concentration to very high titer and efficient gene transfer into mammalian and nonmammalian cells. *Proc Natl Acad Sci U S A* 90, 8033-8037.
- Carballido-Lopez, R., and Errington, J. (2003). A dynamic bacterial cytoskeleton. *Trends Cell Biol* 13, 577-583.
- Chang, K., Elledge, S.J., and Hannon, G.J. (2006). Lessons from Nature: microRNA-based shRNA libraries. *Nat Methods* 3, 707-714.
- Chen, Y., Stamatoyannopoulos, G., and Song, C.Z. (2003). Down-regulation of CXCR4 by inducible small interfering RNA inhibits breast cancer cell invasion in vitro. *Cancer Res* 63, 4801-4804.
- Choi, S., Gustafson-Wagner, E.A., Wang, Q., Harlan, S.M., Sinn, H.W., Lin, J.L., and Lin, J.J. (2007). The intercalated disk protein, mXalpha, is capable of interacting with beta-catenin and bundling actin filaments [corrected]. *J Biol Chem* 282, 36024-36036.
- Cooke, R. (1986). The mechanism of muscle contraction. *CRC Crit Rev Biochem* 21, 53-118.
- Cronin, J., Zhang, X.Y., and Reiser, J. (2005). Altering the tropism of lentiviral vectors through pseudotyping. *Curr Gene Ther* 5, 387-398.
- Cullen, B.R. (2005). RNAi the natural way. *Nat Genet* 37, 1163-1165.

- Cullen, B.R. (2006). Enhancing and confirming the specificity of RNAi experiments. *Nat Methods* 3, 677-681.
- Dabiri, G.A., Turnacioglu, K.K., Sanger, J.M., and Sanger, J.W. (1997). Myofibrillogenesis visualized in living embryonic cardiomyocytes. *Proc Natl Acad Sci U S A* 94, 9493-9498.
- DePolo, N.J., Reed, J.D., Sheridan, P.L., Townsend, K., Sauter, S.L., Jolly, D.J., and Dubensky, T.W., Jr. (2000). VSV-G pseudotyped lentiviral vector particles produced in human cells are inactivated by human serum. *Mol Ther* 2, 218-222.
- Dickins, R.A., Hemann, M.T., Zilfou, J.T., Simpson, D.R., Ibarra, I., Hannon, G.J., and Lowe, S.W. (2005). Probing tumor phenotypes using stable and regulated synthetic microRNA precursors. *Nat Genet* 37, 1289-1295.
- Dickins, R.A., McJunkin, K., Hernando, E., Premssirut, P.K., Krizhanovsky, V., Burgess, D.J., Kim, S.Y., Cordon-Cardo, C., Zender, L., Hannon, G.J., et al. (2007). Tissue-specific and reversible RNA interference in transgenic mice. *Nat Genet* 39, 914-921.
- Duka, A., Schwartz, F., Duka, I., Johns, C., Melista, E., Gavras, I., and Gavras, H. (2006). A novel gene (Cmya3) induced in the heart by angiotensin II-dependent but not salt-dependent hypertension in mice. *Am J Hypertens* 19, 275-281.
- Dull, T., Zufferey, R., Kelly, M., Mandel, R.J., Nguyen, M., Trono, D., and Naldini, L. (1998). A third-generation lentivirus vector with a conditional packaging system. *J Virol* 72, 8463-8471.
- Ehler, E., Rothen, B.M., Hammerle, S.P., Komiyama, M., and Perriard, J.C. (1999). Myofibrillogenesis in the developing chicken heart: assembly of Z-disk, M-line and the thick filaments. *J Cell Sci* 112 ( Pt 10), 1529-1539.
- Elbashir, S.M., Harborth, J., Lendeckel, W., Yalcin, A., Weber, K., and Tuschl, T. (2001a). Duplexes of 21-nucleotide RNAs mediate RNA interference in cultured mammalian cells. *Nature* 411, 494-498.
- Elbashir, S.M., Martinez, J., Patkaniowska, A., Lendeckel, W., and Tuschl, T. (2001b). Functional anatomy of siRNAs for mediating efficient RNAi in *Drosophila melanogaster* embryo lysate. *Embo J* 20, 6877-6888.
- Emerman, M., and Malim, M.H. (1998). HIV-1 regulatory/accessory genes: keys to unraveling viral and host cell biology. *Science* 280, 1880-1884.
- Feng, Y., and Walsh, C.A. (2004). The many faces of filamin: a versatile molecular scaffold for cell motility and signalling. *Nat Cell Biol* 6, 1034-1038.

- Fire, A., Xu, S., Montgomery, M.K., Kostas, S.A., Driver, S.E., and Mello, C.C. (1998). Potent and specific genetic interference by double-stranded RNA in *Caenorhabditis elegans*. *Nature* 391, 806-811.
- Frank, D., Kuhn, C., Katus, H.A., and Frey, N. (2006). The sarcomeric Z-disc: a nodal point in signalling and disease. *J Mol Med* 84, 446-468.
- Franke, W.W. (2004). Actin's many actions start at the genes. *Nat Cell Biol* 6, 1013-1014.
- Furst, D.O., Osborn, M., Nave, R., and Weber, K. (1988). The organization of titin filaments in the half-sarcomere revealed by monoclonal antibodies in immunoelectron microscopy: a map of ten nonrepetitive epitopes starting at the Z line extends close to the M line. *J Cell Biol* 106, 1563-1572.
- Furst, D.O., Osborn, M., and Weber, K. (1989). Myogenesis in the mouse embryo: differential onset of expression of myogenic proteins and the involvement of titin in myofibril assembly. *J Cell Biol* 109, 517-527.
- Gregorio, C.C., and Antin, P.B. (2000). To the heart of myofibril assembly. *Trends Cell Biol* 10, 355-362.
- Grimm, D., Streetz, K.L., Jopling, C.L., Storm, T.A., Pandey, K., Davis, C.R., Marion, P., Salazar, F., and Kay, M.A. (2006). Fatality in mice due to oversaturation of cellular microRNA/short hairpin RNA pathways. *Nature* 441, 537-541.
- Grosskurth, S.E., Bhattacharya, D., Wang, Q., and Lin, J.J. (2008). Emergence of Xin demarcates a key innovation in heart evolution. *PLoS ONE* 3, e2857.
- Gupta, S., Schoer, R.A., Egan, J.E., Hannon, G.J., and Mittal, V. (2004). Inducible, reversible, and stable RNA interference in mammalian cells. *Proc Natl Acad Sci U S A* 101, 1927-1932.
- Gustafson-Wagner, E.A., Sinn, H.W., Chen, Y.L., Wang, D.Z., Reiter, R.S., Lin, J.L., Yang, B., Williamson, R.A., Chen, J., Lin, C.I., et al. (2007). Loss of mXin $\alpha$ , an intercalated disk protein, results in cardiac hypertrophy and cardiomyopathy with conduction defects. *Am J Physiol Heart Circ Physiol* 293, H2680-2692.
- Hannon, G.J., and Rossi, J.J. (2004). Unlocking the potential of the human genome with RNA interference. *Nature* 431, 371-378.
- Hawke, T.J., Atkinson, D.J., Kanatous, S.B., Van der Ven, P.F., Goetsch, S.C., and Garry, D.J. (2007). Xin, an actin binding protein, is expressed within muscle satellite cells and newly regenerated skeletal muscle fibers. *Am J Physiol Cell Physiol* 293, C1636-1644.

- Heale, B.S., Soifer, H.S., Bowers, C., and Rossi, J.J. (2005). siRNA target site secondary structure predictions using local stable substructures. *Nucleic Acids Res* 33, e30.
- Heath, J.P. (1981). Arcs: curved microfilament bundles beneath the dorsal surface of the leading lamellae of moving chick embryo fibroblasts. *Cell Biol Int Rep* 5, 975-980.
- Hoeflich, K.P., Gray, D.C., Eby, M.T., Tien, J.Y., Wong, L., Bower, J., Gogineni, A., Zha, J., Cole, M.J., Stern, H.M., et al. (2006). Oncogenic BRAF is required for tumor growth and maintenance in melanoma models. *Cancer Res* 66, 999-1006.
- Holen, T., Moe, S.E., Sorbo, J.G., Meza, T.J., Ottersen, O.P., and Klungland, A. (2005). Tolerated wobble mutations in siRNAs decrease specificity, but can enhance activity in vivo. *Nucleic Acids Res* 33, 4704-4710.
- Huang, H.T., Brand, O.M., Mathew, M., Ignatiou, C., Ewen, E.P., McCalmon, S.A., and Naya, F.J. (2006). Myomaxin is a novel transcriptional target of MEF2A that encodes a Xin-related alpha-actinin-interacting protein. *J Biol Chem* 281, 39370-39379.
- Huxley, H., and Hanson, J. (1954). Changes in the cross-striations of muscle during contraction and stretch and their structural interpretation. *Nature* 173, 973-976.
- Jackson, A.L., Bartz, S.R., Schelter, J., Kobayashi, S.V., Burchard, J., Mao, M., Li, B., Cavet, G., and Linsley, P.S. (2003). Expression profiling reveals off-target gene regulation by RNAi. *Nat Biotechnol* 21, 635-637.
- Jackson, A.L., Burchard, J., Leake, D., Reynolds, A., Schelter, J., Guo, J., Johnson, J.M., Lim, L., Karpilow, J., Nichols, K., et al. (2006a). Position-specific chemical modification of siRNAs reduces "off-target" transcript silencing. *Rna* 12, 1197-1205.
- Jackson, A.L., Burchard, J., Schelter, J., Chau, B.N., Cleary, M., Lim, L., and Linsley, P.S. (2006b). Widespread siRNA "off-target" transcript silencing mediated by seed region sequence complementarity. *Rna* 12, 1179-1187.
- Jung-Ching Lin, J., Gustafson-Wagner, E.A., Sinn, H.W., Choi, S., Jaacks, S.M., Wang, D.Z., Evans, S., and Li-Chun Lin, J. (2005). Structure, Expression, and Function of a Novel Intercalated Disc Protein, Xin. *J Med Sci* 25, 215-222.
- Kesireddy, V., van der Ven, P., and Fürst, D. Multipurpose modular lentiviral vectors for RNA interference and transgene expression. *Molecular Biology Reports* 37, 2863-2870.
- Khvorova, A., Reynolds, A., and Jayasena, S.D. (2003). Functional siRNAs and miRNAs exhibit strand bias. *Cell* 115, 209-216.

- Kim, D.H., and Rossi, J.J. (2007). Strategies for silencing human disease using RNA interference. *Nat Rev Genet* 8, 173-184.
- Korin, Y.D., and Zack, J.A. (1998). Progression to the G1b phase of the cell cycle is required for completion of human immunodeficiency virus type 1 reverse transcription in T cells. *J Virol* 72, 3161-3168.
- Labeit, S., Gautel, M., Lakey, A., and Trinick, J. (1992). Towards a molecular understanding of titin. *Embo J* 11, 1711-1716.
- Lagos-Quintana, M., Rauhut, R., Lendeckel, W., and Tuschl, T. (2001). Identification of Novel Genes Coding for Small Expressed RNAs 10.1126/science.1064921. *Science* 294, 853-858.
- Lange, S., Ehler, E., and Gautel, M. (2006). From A to Z and back? Multicompartment proteins in the sarcomere. *Trends Cell Biol* 16, 11-18.
- Lee, H.Z., Yeh, F.T., and Wu, C.H. (2004). The effect of elevated extracellular glucose on adherens junction proteins in cultured rat heart endothelial cells. *Life Sci* 74, 2085-2096.
- Lee, N.S., Dohjima, T., Bauer, G., Li, H., Li, M.J., Ehsani, A., Salvaterra, P., and Rossi, J. (2002). Expression of small interfering RNAs targeted against HIV-1 rev transcripts in human cells. *Nat Biotechnol* 20, 500-505.
- Lee, R.C., and Ambros, V. (2001). An Extensive Class of Small RNAs in *Caenorhabditis elegans* 10.1126/science.1065329. *Science* 294, 862-864.
- Lewis, B.P., Shih, I.-h., Jones-Rhoades, M.W., Bartel, D.P., and Burge, C.B. (2003). Prediction of Mammalian MicroRNA Targets. 115, 787-798.
- Li, H., Linke, W.A., Oberhauser, A.F., Carrion-Vazquez, M., Kerkvliet, J.G., Lu, H., Marszalek, P.E., and Fernandez, J.M. (2002). Reverse engineering of the giant muscle protein titin. *Nature* 418, 998-1002.
- Lin, X., Ruan, X., Anderson, M.G., McDowell, J.A., Kroeger, P.E., Fesik, S.W., and Shen, Y. (2005). siRNA-mediated off-target gene silencing triggered by a 7 nt complementation. *Nucleic Acids Res* 33, 4527-4535.
- Linke, W.A., Bartoo, M.L., Ivemeyer, M., and Pollack, G.H. (1996). Limits of titin extension in single cardiac myofibrils. *J Muscle Res Cell Motil* 17, 425-438.
- Linke, W.A., and Granzier, H. (1998). A spring tale: new facts on titin elasticity. *Biophys J* 75, 2613-2614.

- Lymn, R.W., and Taylor, E.W. (1971). Mechanism of adenosine triphosphate hydrolysis by actomyosin. *Biochemistry* 10, 4617-4624.
- Marshall, E. (2003). Gene therapy. Second child in French trial is found to have leukemia. *Science* 299, 320.
- Matranga, C., Tomari, Y., Shin, C., Bartel, D.P., and Zamore, P.D. (2005). Passenger-strand cleavage facilitates assembly of siRNA into Ago2-containing RNAi enzyme complexes. *Cell* 123, 607-620.
- McBride, J.L., Boudreau, R.L., Harper, S.Q., Staber, P.D., Monteys, A.M., Martins, I., Gilmore, B.L., Burstein, H., Peluso, R.W., Polisky, B., et al. (2008). Artificial miRNAs mitigate shRNA-mediated toxicity in the brain: implications for the therapeutic development of RNAi. *Proc Natl Acad Sci U S A* 105, 5868-5873.
- Miyoshi, H., Blomer, U., Takahashi, M., Gage, F.H., and Verma, I.M. (1998). Development of a self-inactivating lentivirus vector. *J Virol* 72, 8150-8157.
- Mochizuki, Y., Furukawa, K., Mitaka, T., Yokoi, T., and Kodama, T. (1988). Polygonal networks, "geodomes", of adult rat hepatocytes in primary culture. *Cell Biol Int Rep* 12, 1-7.
- Moffat, J., and Sabatini, D.M. (2006). Building mammalian signalling pathways with RNAi screens. *Nat Rev Mol Cell Biol* 7, 177-187.
- Morgan, J.E., Beauchamp, J.R., Pagel, C.N., Peckham, M., Ataliotis, P., Jat, P.S., Noble, M.D., Farmer, K., and Partridge, T.A. (1994). Myogenic cell lines derived from transgenic mice carrying a thermolabile T antigen: a model system for the derivation of tissue-specific and mutation-specific cell lines. *Dev Biol* 162, 486-498.
- Murchison, E.P., and Hannon, G.J. (2004). miRNAs on the move: miRNA biogenesis and the RNAi machinery. *Current Opinion in Cell Biology* 16, 223-229.
- Naldini, L., and Verma, I.M. (2000). Lentiviral vectors. *Adv Virus Res* 55, 599-609.
- Naya, F.J., and Olson, E. (1999). MEF2: a transcriptional target for signaling pathways controlling skeletal muscle growth and differentiation. *Curr Opin Cell Biol* 11, 683-688.
- Ohkawa, J., and Taira, K. (2000). Control of the functional activity of an antisense RNA by a tetracycline-responsive derivative of the human U6 snRNA promoter. *Hum Gene Ther* 11, 577-585.

- Ojima, K., Lin, Z.X., Zhang, Z.Q., Hijikata, T., Holtzer, S., Labeit, S., Sweeney, H.L., and Holtzer, H. (1999). Initiation and maturation of I-Z-I bodies in the growth tips of transfected myotubes. *J Cell Sci* 112 ( Pt 22), 4101-4112.
- Otten, J., van der Ven, P.F., Vakeel, P., Eulitz, S., Kirfel, G., Brandau, O., Boesl, M., Schrickel, J.W., Linhart, M., Hayess, K., et al. Complete loss of murine Xin results in a mild cardiac phenotype with altered distribution of intercalated discs. *Cardiovasc Res* 85, 739-750.
- Otten, J., van der Ven, P.F., Vakeel, P., Eulitz, S., Kirfel, G., Brandau, O., Boesl, M., Schrickel, J.W., Linhart, M., Hayess, K., et al. (2010). Complete loss of murine Xin results in a mild cardiac phenotype with altered distribution of intercalated discs. *Cardiovasc Res* 85, 739-750.
- Otto, A., Schmidt, C., Luke, G., Allen, S., Valasek, P., Muntoni, F., Lawrence-Watt, D., and Patel, K. (2008). Canonical Wnt signalling induces satellite-cell proliferation during adult skeletal muscle regeneration. *J Cell Sci*.
- Pacholsky, D. (2004). Zell-Zell- und Zell-Matrix-Kontakte während der Muskelentwicklung. In *Math- NaturwissFakultät (Potsdam, Universität Potsdam)*.
- Pacholsky, D., Vakeel, P., Himmel, M., Lowe, T., Stradal, T., Rottner, K., Furst, D.O., and van der Ven, P.F. (2004). Xin repeats define a novel actin-binding motif. *J Cell Sci* 117, 5257-5268.
- Paddison, P.J., Cleary, M., Silva, J.M., Chang, K., Sheth, N., Sachidanandam, R., and Hannon, G.J. (2004a). Cloning of short hairpin RNAs for gene knockdown in mammalian cells. *Nat Methods* 1, 163-167.
- Paddison, P.J., Silva, J.M., Conklin, D.S., Schlabach, M., Li, M., Aruleba, S., Baliya, V., O'Shaughnessy, A., Gnoj, L., Scobie, K., et al. (2004b). A resource for large-scale RNA-interference-based screens in mammals. *Nature* 428, 427-431.
- Patzel, V., Rutz, S., Dietrich, I., Koberle, C., Scheffold, A., and Kaufmann, S.H. (2005). Design of siRNAs producing unstructured guide-RNAs results in improved RNA interference efficiency. *Nat Biotechnol* 23, 1440-1444.
- Pei, Y., and Tuschl, T. (2006). On the art of identifying effective and specific siRNAs. *Nat Methods* 3, 670-676.
- Pfeffer, S., Zavolan, M., Grasser, F.A., Chien, M., Russo, J.J., Ju, J., John, B., Enright, A.J., Marks, D., Sander, C., et al. (2004). Identification of Virus-Encoded MicroRNAs [10.1126/science.1096781](https://doi.org/10.1126/science.1096781). *Science* 304, 734-736.

- Pfeifer, A., Ikawa, M., Dayn, Y., and Verma, I.M. (2002). Transgenesis by lentiviral vectors: lack of gene silencing in mammalian embryonic stem cells and preimplantation embryos. *Proc Natl Acad Sci U S A* 99, 2140-2145.
- Prawitt, D., Brixel, L., Spangenberg, C., Eshkind, L., Heck, R., Oesch, F., Zabel, B., and Bockamp, E. (2004). RNAi knock-down mice: an emerging technology for post-genomic functional genetics. *Cytogenet Genome Res* 105, 412-421.
- Rayment, I., Holden, H.M., Whittaker, M., Yohn, C.B., Lorenz, M., Holmes, K.C., and Milligan, R.A. (1993a). Structure of the actin-myosin complex and its implications for muscle contraction. *Science* 261, 58-65.
- Rayment, I., Rypniewski, W.R., Schmidt-Base, K., Smith, R., Tomchick, D.R., Benning, M.M., Winkelmann, D.A., Wesenberg, G., and Holden, H.M. (1993b). Three-dimensional structure of myosin subfragment-1: a molecular motor. *Science* 261, 50-58.
- Revenu, C., Athman, R., Robine, S., and Louvard, D. (2004). The co-workers of actin filaments: from cell structures to signals. *Nat Rev Mol Cell Biol* 5, 635-646.
- Reynolds, A., Leake, D., Boese, Q., Scaringe, S., Marshall, W.S., and Khvorova, A. (2004). Rational siRNA design for RNA interference. *Nat Biotechnol* 22, 326-330.
- Rhee, D., Sanger, J.M., and Sanger, J.W. (1994). The premyofibril: evidence for its role in myofibrillogenesis. *Cell Motil Cytoskeleton* 28, 1-24.
- Rubinson, D.A., Dillon, C.P., Kwiatkowski, A.V., Sievers, C., Yang, L., Kopinja, J., Rooney, D.L., Zhang, M., Ihrig, M.M., McManus, M.T., et al. (2003). A lentivirus-based system to functionally silence genes in primary mammalian cells, stem cells and transgenic mice by RNA interference. *Nat Genet* 33, 401-406.
- Saiki, R.K., Scharf, S., Faloona, F., Mullis, K.B., Horn, G.T., Erlich, H.A., and Arnheim, N. (1985). Enzymatic amplification of beta-globin genomic sequences and restriction site analysis for diagnosis of sickle cell anemia. *Science* 230, 1350-1354.
- Sandy, P., Ventura, A., and Jacks, T. (2005). Mammalian RNAi: a practical guide. *Biotechniques* 39, 215-224.
- Shefer, G., Van de Mark, D.P., Richardson, J.B., and Yablonka-Reuveni, Z. (2006). Satellite-cell pool size does matter: defining the myogenic potency of aging skeletal muscle. *Dev Biol* 294, 50-66.

- Silva, J.M., Li, M.Z., Chang, K., Ge, W., Golding, M.C., Rickles, R.J., Siolas, D., Hu, G., Paddison, P.J., Schlabach, M.R., et al. (2005). Second-generation shRNA libraries covering the mouse and human genomes. *Nat Genet* 37, 1281-1288.
- Singer, O., Tiscornia, G., Ikawa, M., and Verma, I.M. (2006). Rapid generation of knockdown transgenic mice by silencing lentiviral vectors. *Nat Protoc* 1, 286-292.
- Sinn, P.L., Sauter, S.L., and McCray, P.B., Jr. (2005). Gene therapy progress and prospects: development of improved lentiviral and retroviral vectors--design, biosafety, and production. *Gene Ther* 12, 1089-1098.
- Stegmeier, F., Hu, G., Rickles, R.J., Hannon, G.J., and Elledge, S.J. (2005). A lentiviral microRNA-based system for single-copy polymerase II-regulated RNA interference in mammalian cells. *Proc Natl Acad Sci U S A* 102, 13212-13217.
- Stossel, T.P., Condeelis, J., Cooley, L., Hartwig, J.H., Noegel, A., Schleicher, M., and Shapiro, S.S. (2001). Filamins as integrators of cell mechanics and signalling. *J Cell Biol* 154, 138-145.
- Stryer, L. (1981). Rapid motions in protein molecules. *Biochem Soc Symp*, 39-55.
- Szulc, J., Wiznerowicz, M., Sauvain, M.O., Trono, D., and Aebischer, P. (2006). A versatile tool for conditional gene expression and knockdown. *Nat Methods* 3, 109-116.
- Tiscornia, G., Singer, O., Ikawa, M., and Verma, I.M. (2003). A general method for gene knockdown in mice by using lentiviral vectors expressing small interfering RNA. *Proc Natl Acad Sci U S A* 100, 1844-1848.
- Todarò, G.J., and Green, H. (1963). Quantitative studies of the growth of mouse embryo cells in culture and their development into established lines. *J Cell Biol* 17, 299-313.
- Trotter, J.A., Foerder, B.A., and Keller, J.M. (1978). Intracellular fibres in cultured cells: analysis by scanning and transmission electron microscopy and by SDS-polyacrylamide gel electrophoresis. *J Cell Sci* 31, 369-392.
- van de Wetering, M., Oving, I., Muncan, V., Pon Fong, M.T., Brantjes, H., van Leenen, D., Holstege, F.C., Brummelkamp, T.R., Agami, R., and Clevers, H. (2003). Specific inhibition of gene expression using a stably integrated, inducible small-interfering-RNA vector. *EMBO Rep* 4, 609-615.
- van der Loop, F.T., van der Ven, P.F., Furst, D.O., Gautel, M., van Eys, G.J., and Ramaekers, F.C. (1996). Integration of titin into the sarcomeres of cultured differentiating human skeletal muscle cells. *Eur J Cell Biol* 69, 301-307.

- van der Ven, P.F., Ehler, E., Vakeel, P., Eulitz, S., Schenk, J.A., Milting, H., Micheel, B., and Furst, D.O. (2006). Unusual splicing events result in distinct Xin isoforms that associate differentially with filamin c and Mena/VASP. *Exp Cell Res* 312, 2154-2167.
- van der Ven, P.F., Obermann, W.M., Lemke, B., Gautel, M., Weber, K., and Furst, D.O. (2000). Characterization of muscle filamin isoforms suggests a possible role of gamma-filamin/ABP-L in sarcomeric Z-disc formation. *Cell Motil Cytoskeleton* 45, 149-162.
- Van Der Ven, P.F., Obermann, W.M., Weber, K., and Furst, D.O. (1996). Myomesin, M-protein and the structure of the sarcomeric M-band. *Adv Biophys* 33, 91-99.
- van der Ven, P.F., Schaart, G., Croes, H.J., Jap, P.H., Ginsel, L.A., and Ramaekers, F.C. (1993). Titin aggregates associated with intermediate filaments align along stress fiber-like structures during human skeletal muscle cell differentiation. *J Cell Sci* 106 ( Pt 3), 749-759.
- Ventura, A., Meissner, A., Dillon, C.P., McManus, M., Sharp, P.A., Van Parijs, L., Jaenisch, R., and Jacks, T. (2004). Cre-lox-regulated conditional RNA interference from transgenes. *Proc Natl Acad Sci U S A* 101, 10380-10385.
- Wang, D.Z., Reiter, R.S., Lin, J.L., Wang, Q., Williams, H.S., Krob, S.L., Schultheiss, T.M., Evans, S., and Lin, J.J. (1999). Requirement of a novel gene, Xin, in cardiac morphogenesis. *Development* 126, 1281-1294.
- Wang, Q., Lin, J.L.-C., Reinking, B.E., Feng, H.-Z., Chan, F.-C., Lin, C.-I., Jin, J.-P., Gustafson-Wagner, E.A., Scholz, T.D., Yang, B., et al. Essential Roles of an Intercalated Disc Protein, mXin{beta}, in Postnatal Heart Growth and Survival. *Circ Res* 106, 1468-1478.
- Wang, Y.L. (1984). Reorganization of actin filament bundles in living fibroblasts. *J Cell Biol* 99, 1478-1485.
- White, J.G. (1984). Arrangements of actin filaments in the cytoskeleton of human platelets. *Am J Pathol* 117, 207-217.
- Wiznerowicz, M., Szulc, J., and Trono, D. (2006). Tuning silence: conditional systems for RNA interference. *Nat Methods* 3, 682-688.
- Wiznerowicz, M., and Trono, D. (2003). Conditional suppression of cellular genes: lentivirus vector-mediated drug-inducible RNA interference. *J Virol* 77, 8957-8961.
- Xia, X.G., Zhou, H., Samper, E., Melov, S., and Xu, Z. (2006). Pol II-expressed shRNA knocks down Sod2 gene expression and causes phenotypes of the gene knockout in mice. *PLoS Genet* 2, e10.

- Yaffe, D., and Saxel, O. (1977). Serial passaging and differentiation of myogenic cells isolated from dystrophic mouse muscle. *Nature* 270, 725-727.
- Zack, J.A., Arrigo, S.J., Weitsman, S.R., Go, A.S., Haislip, A., and Chen, I.S. (1990). HIV-1 entry into quiescent primary lymphocytes: molecular analysis reveals a labile, latent viral structure. *Cell* 61, 213-222.
- Zaiss, A.K., Son, S., and Chang, L.J. (2002). RNA 3' readthrough of oncoretrovirus and lentivirus: implications for vector safety and efficacy. *J Virol* 76, 7209-7219.
- Zeng, Y., Cai, X., and Cullen, B.R. (2005). Use of RNA polymerase II to transcribe artificial microRNAs. *Methods Enzymol* 392, 371-380.
- Zeng, Y., Wagner, E.J., and Cullen, B.R. (2002). Both natural and designed micro RNAs can inhibit the expression of cognate mRNAs when expressed in human cells. *Mol Cell* 9, 1327-1333.
- Zufferey, R., Donello, J.E., Trono, D., and Hope, T.J. (1999). Woodchuck hepatitis virus posttranscriptional regulatory element enhances expression of transgenes delivered by retroviral vectors. *J Virol* 73, 2886-2892.

# Erklärung/Declaration

---

An Eides statt versichere ich, dass ich die Arbeit mit dem Titel " **Consequences of Xirp2 knockdown in skeletal muscle cells** " selbst und ohne jede Hilfe angefertigt habe, dass diese oder eine ähnliche Arbeit noch bei keiner anderer Stelle als Dissertation eingereicht wurde. Ich habe früher noch keinen Promotionsversuch unternommen.

This thesis has been written independently and with no other sources and aids other than those stated here. This work has not been submitted to any other university or institute towards the partial fulfillment of any degree.

Bonn, (December) 2010

Venu Kesireddy